DYNAMICS OF RIFTING ALONG THE SOUTHWEST CONTINENTAL MARGIN OF INDIA THROUGH COHERENCE AND PROCESS ORIENTED ANALYSIS OF GRAVITY DATA

THESIS SUBMITTED TO THE

COCHIN UNIVERSITY OF SCIENCE AND TECHNOLOGY

by

SHEENA V. DEV

IN PARTIAL FULFILMENT OF THE REQUIREMENTS

FOR THE DEGREE OF

DOCTOR OF PHILOSOPHY

IN THE FACULTY OF MARINE SCIENCES

DEPARTMENT OF MARINE GEOLOGY AND GEOPHYSICS
SCHOOL OF MARINE SCIENCES
COCHIN UNIVERSITY OF SCIENCE AND TECHNOLOGY
COCHIN-682 016

JUNE 2007

DECLARATION

I, Sheena V. Dev, do hereby declare that the thesis entitled **"DYNAMICS OF RIFTING ALONG THE SOUTHWEST CONTINENTAL MARGIN OF INDIA THROUGH COHERENCE AND PROCESS ORIENTED ANALYSIS OF GRAVITY DATA"** is a genuine record of research work done by me under the supervision of Dr. M. Radhakrishna, Reader, Department of Marine Geology and Geophysics, School of Marine Sciences, Cochin University of Science and Technology, Lake side Campus, Cochin – 682 016. This work has not been previously formed the basis for the award of any degree or diploma of this or any other University or other institute of learning.

(Sheena V. Dev)

Cochin-16
June 2007

CERTIFICATE

I certify that the thesis entitled, **"DYNAMICS OF RIFTING ALONG THE SOUTHWEST CONTINENTAL MARGIN OF INDIA THROUGH COHERENCE AND PROCESS ORIENTED ANALYSIS OF GRAVITY DATA"** *has been prepared by Sheena V. Dev under my supervision and guidance in partial fulfillment of the requirements for the degree of Doctor of Philosophy and no part thereof has been submitted for any other degree.*

M. S B R. Krishna 11|6|07

M. Radhakrishna

(Research Supervisor)
Dept. of Marine Geology and Geophysics
School of Marine Sciences
Cochin University of Science and Technology

Cochin-682 016
June 2007

CONTENTS

CHAPTER 3 METHODOLOGY

CHAPTER 4 COHERENCE ANALYSIS

ACKNOWLEDGEMENTS

This thesis is the end of my long journey in obtaining my PhD degree. I have not traveled in a vacuum in this journey. There are some people who made this journey easier with words of encouragement and more intellectually satisfying by offering different places to look to expand my theories and ideas.

First and foremost I offer my sincerest gratitude to my supervisor, Dr M. Radhakrishna, Reader, Department of Marine Geology and Geophysics, School of Ocean Technology, CUSAT, Cochin 16, who has supported me throughout my thesis with his patience and knowledge, for helping to supervise me, providing resources and subjects, offering direction and penetrating criticism whilst allowing me the room to work in my own way. I attribute this achievement to his encouragement and effort and without him this thesis, too, would not have been completed or written. One simply could not wish for a better or friendlier supervisor. I am indebted to him more than he knows.

My sincere gratitude to Prof. K.T. Damodaran, Director, School of Marine Sciences, Cochin University of Science and Technology, for granting necessary permission to avail of the facilities of the school during the course of my research.

I would like to thank Dr. C.G.Nambiar, Head, Department of Marine Geology and Geophysics, for making the facilities available in the department and for his constant encouragement.

I am extremely grateful to Prof. P Seralathan Doctoral Committee member, for his valuable help and advice during the entire course of this work.

I express my heartfelt gratitude to Dr. A.C. Narayana, Reader, Department of Marine Geology and Geophysics for his critical comments and suggestions during different phases of work.

I wish to record my indebtedness to Dr. C.Subrahmanyam, Emeritus Scientist, National Geophysical Research Institute, Uppal Road, Hyderabad for his valuable advice and directions and critical comments during the various stage of this work.

I wish to express my profound thanks to the faculty members of the Department of Marine Geology and Geophysics, Cochin University of Science and Technology Dr. M. Ravisankar, Prof. K. Sajan, Prof S. Rajendran (Retd. Professor), Dr. A.D. Singh for their blessings and support given to me.

I am also benefited by outstanding work from Dr. Shyam Chand. Many thanks go to him for science discussion and the constant support he has given to me.

I take this opportunity to convey my indebtedness to Shri. T.M. Mahadevan, former Director, Atomic Mineral Division for his motivation and help during the various stages of this work.

I wish to express my whole hearted thanks to all the non-teaching staff, Dept of Marine Geology and Geophysics and staff members of Director's office, especially Mr. Sree Kumar, Cochin University of Science and Technology for their laudable support and help given to me.

I would like to thank those closest to me, whose presence helped make the completion of my graduate work possible, who shared my happiness and made me happy, especially Vinu Prakash, Lasitha S, Shinu N, Subitha Prabhakaran, Anju P.V, Sreela S.R, for their love, patience and understanding. I also wish to thank all other friends in the University, Mr. Babu Nalluswamy, Mr. Nilof S. Pasha, Mr. Mashood, Mr. Subeer Arol, Mr. Sijin Kumar, Dr. Arts K. Purushothaman, Mr. Baiju K.R, Dr. Sanu T.D, Dr. Sunil P.S., Dr. Priju C.P, Mr. Sunil Kumar, Mr. Ajaykumar, Ms. Rekha R, Ms. Subhasree, Mr. Thulasidharan P for their wholehearted help during different stages of my thesis

The Department of Marine Geology and Geophysics has provided the support and equipment I have needed to produce and complete my thesis and the Cochin University of Science and Technology as well as Department of Science and Technology has funded my studies. I specially acknowledge both.

My best thoughts are extended to my parents who taught me that education is the first duty of both parents and children. Most importantly, I wish to thank my parents Mr. K.Vamadevan and Ms. K. Sasikumari and my mother-in law Ms. Sailaja Vijayan who bore me, raised me, supported me, taught me, and loved me. They have waited so long for this moment to come true; I am glad that their waiting has finally been rewarded. I also wish to thank my brother Mr. Sireesh V, brother-in-law Anand V.S and his wife Remya R. Nath for their love and support extended by them during my studies.

Last but not least, I would like to express my special thanks to my life partner Mr. Arun Kumar V.S for his endless love and encouragement throughout this entire journey. Without whom I would have struggled to find the inspiration and motivation needed to complete this thesis. I greatly appreciate for his generous time in proof reading. He is always ready to help me with a smile.

Sheena V. Dev

LIST OF TABLES

LIST OF FIGURES

CHAPTER 1 INTRODUCTION

1.1 INTRODUCTION

Passive margins, which constitute about half of the overall length of the present day continental margins, represent the transition between simple tectonic setting of ocean basins and the more complex continental regions (Figure 1.1) and are considered to be major depocenters of sedimentation (Gallagher and Brown, 1997). Passive margins have been assumed to form by extreme extension and thinning of continental lithosphere (Le Pichon and Sibuet, 1981), ultimately leading to the initiation of seafloor spreading at high stretching factor, where stretching has proceeded to infinity ($\beta=\infty$) as well as shearing and other processes that are acting on

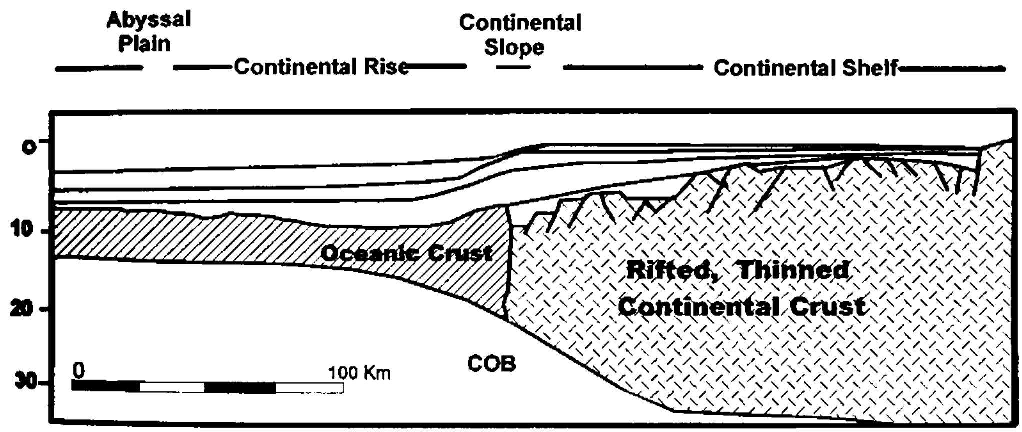

Fig 1.1: Vertical cross section of generic passive continental margin. COB - Continent oceanic boundary

it. Figure 1.2 represents various stages of evolution of the passive continental margin. Most conspicuous feature of a passive continental margin is its thick sediment deposits having an average thickness of about 7-8 km, which may extend up to 22 km. Most of the passive margins exhibit 'edge effect' gravity anomaly, that is, positive free air gravity anomaly along the edge of the shelf and negative free air gravity along the

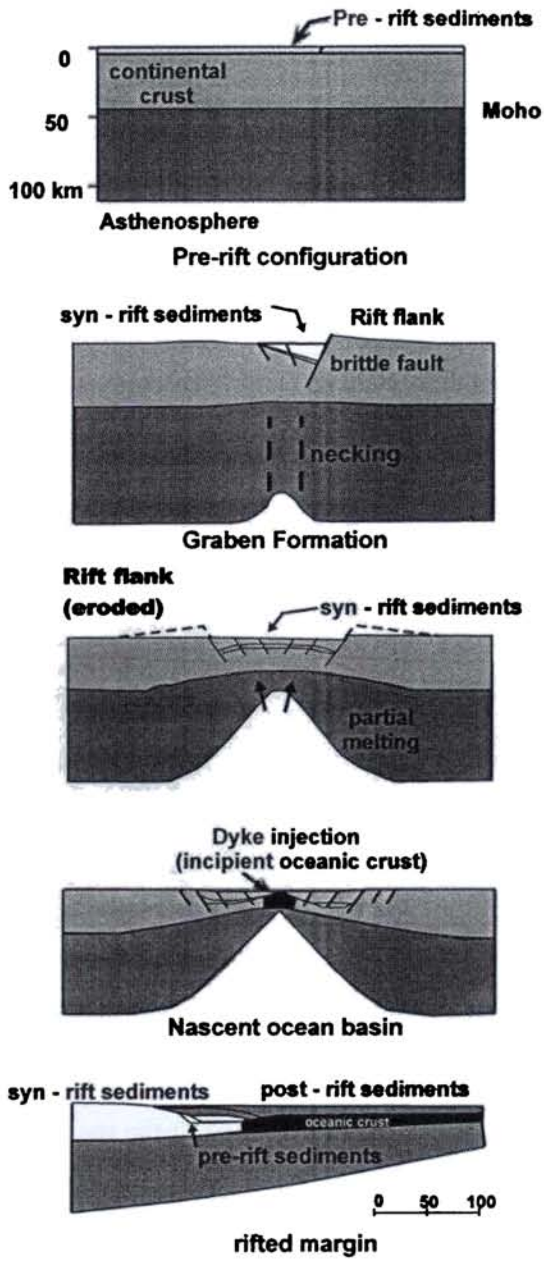

Fig 1.2: Various stages of evolution of passive continental margin

slope. The amplitude of these anomalies and the distance between the positive and negative anomalies are representative of type of margin and sedimentation pattern (Karner and Watts, 1982; Watts, 1988). The evolution of a passive continental margin occurs in two phases:

- Rift phase - which is prior to the breakup of the continent.
- Drift phase or post rift phase – which occurs with the onset of seafloor spreading.

Rifted or passive margins have formerly been classified into non-volcanic and volcanic margins (White, 1992), based on the volume of surficial volcanism or volcanic outpourings imaged in seismic reflection profiles as seaward dipping reflections. A number of recent studies have also addressed the role of upper mantle in the extension process. The difference between volcanic (Fowler et al., 1989; Morgan et al., 1989) and non-volcanic margin (Horsfield et al., 1993) is that (Figure 1.3), huge melt volumes are emplaced during continental breakup within a short time period in the 'volcanic type' margins, whereas, in 'non-volcanic type', only small amount of melt is produced as continental breakup proceeds (White, 1992). In the upper crust of the non-volcanic rifted margins, tilted fault blocks are invariably present, where as, in volcanic margins no such features are noticed because of extensive volcanism which obscures and overprints any tilted fault block and also the volcanic margins behave more ductile (White, 1992). The volcanic margins are formed due to 'active' rifting (Figure 1.4a), which evolve in response to thermal upwelling of the asthenosphere (Dewey and Burke, 1974; Bott and Kusznir, 1979; Spohn and Schubert, 1982). On the other hand, the non - volcanic margins are formed due to passive rifting (Figure 1.4b) formed in response to lithospheric extension developed by far field boundary stresses and frictional forces exerted on the base of the lithosphere by convecting upper mantle (McKenzie, 1978;

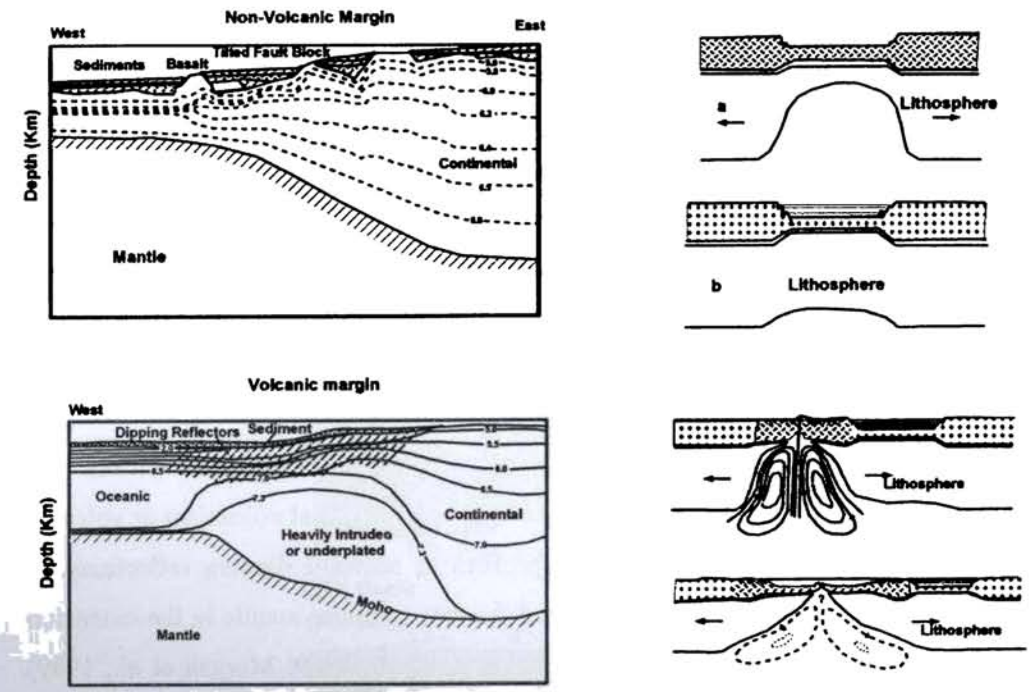

Fig 1.3: Cross sections of typical volcanic (from Morgan et al., 1989) and non-volcanic (from Horsfield et al., 1983) continental margins. The evolutionary model for the development of thicker oceanic crust is depicted in stages I to III (after Hinz et al., 1987). I – pre-breakup tectonism, II- breakup with vigorous convection and melting, III – post - breakup abating convection.

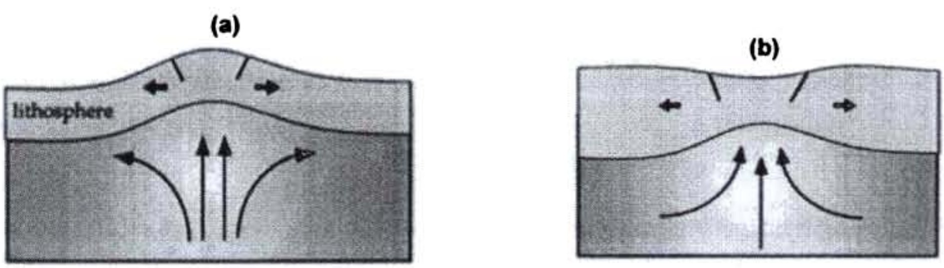

Fig 1.4: Models showing (a) Active rifting and (b)Passive rifting.

McKenzie and Bickle, 1989; Khain, 1992). During early phase, the future zone of crustal separation is affected by tensional stresses, giving rise to development of complex graben system, and in time, the tectonic activity decreases and ultimately the formation of the graben system ceases. Because of progressive lithospheric attenuation and crustal doming, local deviatoric tensional stresses play an important secondary role in the evolution of margin. Upon crustal separation, the divergent continental margin becomes tectonically inactive. However, subsequent tectonic cycles may activate the aborted rifts and again cause volcanism. Mutter (1993) states that seismic studies along the passive margins prove that the distinction between active and passive rifting is not useful, because the magmatic input to the crust during continental rifting is extraordinarily variable, both in time and space and hence is only conditionally justified.

A detailed study of the passive continental margins is of prime importance, as they are the sites of world's largest sedimentary accumulation, where, significant parts of the World's hydrocarbon reserves are found. They are relatively shallow areas, and accessible to offshore exploratory drilling as well as oil and gas production wells. Studies on evolution of the passive margins help us to have a clear picture on generic link between geomorphic, tectonic and sedimentary aspects during its formation. The sedimentation history needs to be studied in the context of entire margin system, including tectonic influences and fluid flow circulation. The sea level fluctuations, climatic changes, isostatic rebound and associated tectonics, sedimentation rate, behaviour of fluids and gas hydrates are some of the dynamic activities that take place along the margins.

The Continental Margins of India, evolved due to rift-drift events of the Indian subcontinent, is an extensive Atlantic type passive continental margin. It extends on either side of the Indian Peninsular shield and is referred as Eastern Continental Margin of India (ECMI) and Western Continental Margin of India (WCMI). The ECMI has evolved during the breakup of India from East Antarctica in Early Cretaceous (Powell et al., 1988). It has a strike length extending to about 2000 km whose shelf width is more in north due to the presence of Bengal fan. The present day continental margin of East Antarctica agrees well with the ECMI and has been strongly supported by magnetic lineations and structural lineaments traced into both continents (Johnson et al., 1976; Lawver et al., 1991). The conjugate nature of these two continents has been further supported by the presence of Mesozoic anomalies (Ramana et al., 2001) and admittance signatures (Chand et al., 2001). The ECMI along the coast is characterised by the presence of five major onshore-offshore sedimentary basins, the Cauvery, Palar, Krishna - Godavari, Mahanadi and Bengal basins (Sastri et al., 1973).

The WCMI has evolved through rifting and subsequent seafloor spreading between India and Madagascar at 88 Ma. The rifting and seafloor spreading history of the WCMI and the adjoining Arabian Sea is known in general terms (McKenzie and Sclater, 1971; Whitmarsh, 1974; Norton and Sclater, 1979; Chaubey et al., 1993). The northern part of the WCMI is characterised by the presence of Deccan Continental Flood Basalt province due to the interaction of ReUnion mantle plume during rifting and breakup of Seychelles from India in Paleocene. The margin comprises of several surface/sub-surface structural features that include the Chagos-Laccadive Ridge (CLR), Laxmi Ridge (LR), Pratap Ridge (PR) and a belt of numerous horst graben structures in the sediment filled basins bordering the West Coast of India. The WCMI comprises of five major sedimentary basins. These are Kutch, Saurashtra, Bombay, Konkan and Kerala basins and are separated by southwesterly trending structures namely, the Saurashtra Arch, Surat depression, Vengurla Arch and Tellicherry Arch respectively.

1.2 DEFINITION OF THE PROBLEM

It is now well known that the passive continental margins of India have formed by processes of lithospheric rifting, stretching and subsequent seafloor spreading. However, we can expect significant variations in terms of varying mechanical properties, sedimentation, flexure and subsidence history in different segments of the margin during their evolution. Previous studies indicate that gravity anomalies at rifted continental margins give valuable information on flexural response to sediment loads, the long-term mechanical properties of the lithosphere and influence of plumes, if they are spatially related to the margin (Karner and Watts, 1982; Watts, 1988; Watts and Stewart, 1998). Estimate of lithospheric strength is also useful in modeling the rift flank topography observed along most of the passive continental margins.

1.3 OBJECTIVES

Lithospheric studies along the WCMI, throw light on the style of rifting, flexural characteristics, role of ReUnion and Marion mantle plumes and their probable interaction with the lithosphere and processes involved in the uplift of the Western Ghats. A detailed and systematic gravity data analysis and interpretation integrated with available seismic data has been carried out along the southern part of the WCMI with the following major objectives:

- Estimation of effective elastic thickness (Te) of the lithosphere in selected segments of the margin, in order to understand the spatial variations in the lithospheric strength based on Coherence analysis.

- To study the segmentation of the margin and geodynamic processes operative in the region by analyzing strength during rifting and flexure due to sedimentation through subsidence analysis.

- To examine the uplifted rift-flank topography of Western Ghats.

- To study the role played by mantle plumes during the rifting and subsequent evolution of the margin.

1.4 PREVIOUS STUDIES

Our present knowledge of the origin and evolution of WCMI is based on investigations carried out for more than three decades. Studies related to magnetic anomaly identifications gave rise to valuable information on the seafloor spreading history of the Arabian Sea and the evolution of the WCMI (Norton and Sclater, 1979; Schlich, 1982; Masson, 1984; Karasik et al., 1986; Royer et al., 1989; Miles and Roest, 1993; Chaubey et al., 1993, 1995 and 1998; Bhattacharya et al., 1994; Malod et al., 1997; Miles et al., 1998; Talwani and Reif, 1998; among others). The crustal structure, tectonics and rifting history of the WCMI was investigated by several workers (Naini and Talwani, 1982; Biswas, 1982, 1987; Biswas and Singh, 1988; Ghosh and Zutshi, 1989; Miles and Roest, 1993; Miles et al., 1998; Radhakrishna et al., 2002; Chaubey et al., 2002; Mishra et al., 2004; Krishna et al., 2006; among many others). Some workers like Bhattacharya and Subrahmanyam (1986), Kolla and Coumes (1990), Subrahmanyam et al. (1995), Mishra et al. (2004) proposed the extension of several onshore structural features in to the offshore areas.

Detailed studies were made in the Arabian Sea, which is the oceanic extension of the sediment filled WCMI. The Chagos – Laccadive ridge together with Laxmi Ridge act as a barrier that separates the Arabian Sea into Eastern and Western basins

(Naini and Talwani, 1982). The geophysical characteristics of the Western basin suggest that the crust below the basin is oceanic in nature (McKenzie and Sclater, 1971; Whitmarsh, 1974; Naini and Talwani, 1982), while, the Eastern basin is underlain by transitional rift stage crust (Harbinson and Bassinger, 1973; Naini and Talwani, 1982; Kolla and Coumes, 1990; Subba Raju et al., 1990).

The sediment thickness and nature of the basement of Indus Fan and the adjacent Indian Continental margin (Neprochnov, 1961; Narain et al., 1968; Ewing et al., 1969; Closs et al., 1969; Rao, 1970; Harbinson and Bassinger,1973; Babenko et al., 1980; Bachman and Hamilton, 1980; Biswas and Singh, 1988; Ghosh and Zutshi, 1989; Ramaswamy and Rai, 2000; Chaubey et al., 2002; Krishna et al., 2006) were discussed based on seismic data. Again a detailed picture of the nature of sediment acoustics, sediment thickness distribution and sedimentary processes in the Arabian Sea is given by Naini and Kolla (1982) and Kolla and Coumes (1987). Through sonobuoy refraction data, a detailed discussion on crustal structure variations and nature of the crust below the WCMI was made by Naini and Talwani (1982).

The volcanic episode that occurred at the Cretaceous and Teritiary transition plays an important role in the evolution of WCMI (Venkatesan et al., 1993; Pande et al., 1988; Duncan and Pyle, 1988; Courtillot et al., 1988). The interaction between continental rifting and ReUnion plume generated huge volume of lava and gave rise to sub aerial Deccan volcanism. The influence of plume and the related thermal aspects have been studied by several workers (Morgan, 1981; Cox 1989; Richards et al., 1989; White and McKenzie, 1989, 1995; Hooper, 1990; Kent et al., 1992). Gravity field of the WCMI and the eastern Arabian Sea has been analysed and interpreted by many workers to delineate the crustal structure and rifting history (Naini and Talwani, 1982; Subba Raju et al., 1990; Miles and Roest, 1993; Subrahmanyam et al., 1995; Pandey et al., 1995, 1996; Miles et al., 1998; Talwani and Reif, 1998; Todal and Eldholm, 1998; Singh, 1999; Radhakrishna et al., 2002; Chaubey et al., 2002, Mishra et al., 2004; Krishna et al., 2006). The flank uplift topography and the evolution of the Western Ghats has been studied through, lithospheric modeling (Gunnell and Fleitout, 2000; Chand and Subrahmanyam, 2003), Apatite Fission Track data (Brown, 1991; Kalaswad et al., 1993; Gallagher et al., 1998) and denudation isostasy (Gallagher et al., 1994; Widdowson and Cox, 1996). Whiting et al. (1994) studied the 3D-flexural loading and subsidence history of the northern part of the WCMI and adjoining Indus Fan.

1.5 STUDY AREA

In the present study, the southern part of WCMI outside the Deccan Volcanic Province (DVP) has been considered for detailed geophysical data analysis. The margin consists of Konkan and Kerala offshore basins and the study area include, the deep oceanic parts of the Arabian Sea covering the Chagos Laccadive Ridge. South of the WCMI and Southwest of Sri Lanka, the distinct topographic expression of the Comorin Ridge can be seen aligned along the margin. Kahle et al. (1981) interpreted this ridge to be a structural boundary between the continental and oceanic crust. Evolution or mode of formation of this ridge is not yet known and therefore attains significance in terms of understanding the reconstruction history and breakup of eastern Gondwanaland. In view of its significance, the Comorin Ridge is also considered in the present study. The study area lies between 63° E to 80° E longitude, 0 to 16° N latitude as shown in Figure 1.5.

1.6 SCOPE OF THE PRESENT STUDY

The main objective of the present study is to estimate the Effective Elastic thickness (Te) of the lithosphere below different segments of the southwest continental margin and the adjoining areas, to understand the dynamics of rifting and the attendant tectonics. This is achieved by following two different approaches: one is through the process - oriented approach of gravity modeling, a method by which different components such as rifting, sedimentation and flexure, and erosion can be separately

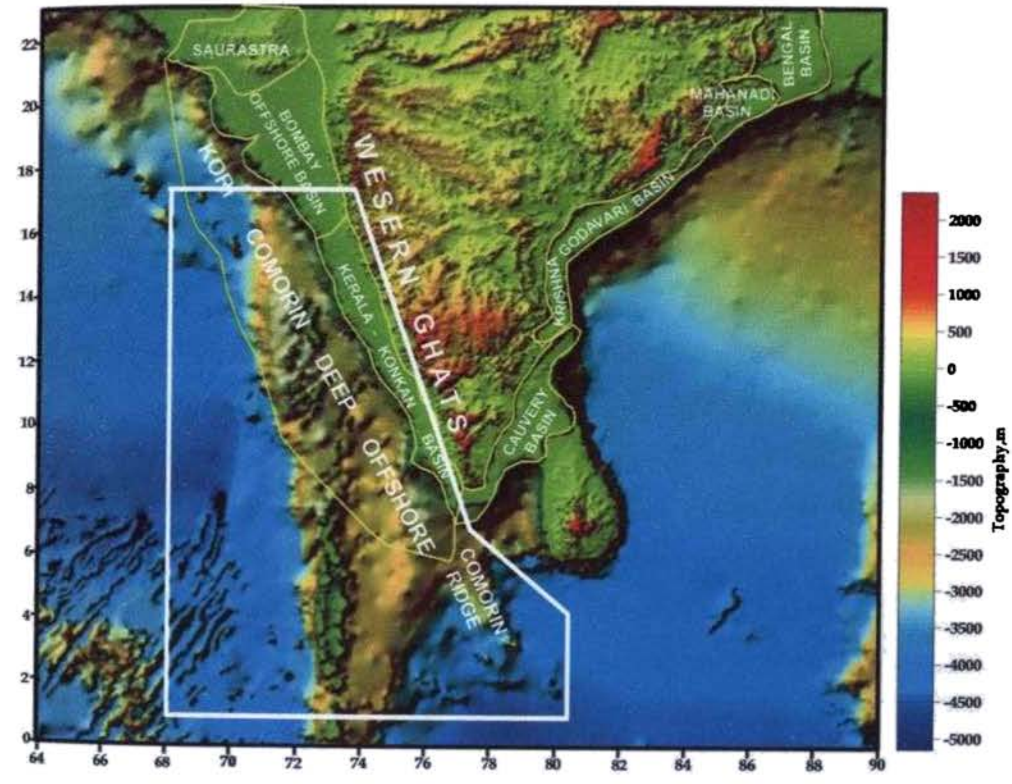

Fig 1.5: Map showing continental margins of peninsular India and the adjoining oceanic areas. White line marks the area considered in the present study. The major onshore-offshore sedimentary basins at the continental margin are demarcated (after Zutshi et al., 1995).

modeled that lead to the present day configuration of the margin. The other approach is through estimation of Coherence function, which can be modeled to obtain an integrated estimate of the lithospheric strength at the margin. In order to present these studies, results and interpretations in a concise way, the thesis has been organized into seven chapters. A brief description of each of these chapters is given below.

Chapter 1 gives a brief introduction to the evolution of passive continental margins. The significance of continental margins in general and a brief account on the evolution of the Indian margins have been presented. A brief description of the method of analysis is provided.

In Chapter 2, a detailed account of the geotectonics, rifting history and tectono stratigraphic evolution of major sedimentary basins along the WCMI is given. The nature of plume lithosphere interactions during rifting history (India – Madagascar at ~ 88 Ma and India-Seychelles at ~ 65 Ma) and formation of the WCMI have been discussed. The development of major onshore and offshore sedimentary basins such as the Kutch, Cambay, Saurashtra, Bombay and Konkan - Kerala basins during the India's northward flight which led to the deposition of thick pile of sediments in the margin. The structure and stratigraphic history of these basins in the light of rift tectonics has been discussed. The major topographic features in the eastern Arabian Sea mainly include the Chagos-Laccadive Ridge, the Pratap ridge and the Laxmi ridge. The nature of crust and their formation during the evolution of the eastern Arabian Sea is still enigmatic. The nature of crust below the Laxmi basin in the NW part of the margin is debatable. In order to highlight some of these problems, a detailed review on kinematic history of evolution for the eastern Arabian Sea has been presented in this chapter.

In Chapter 3, a detailed description on the methodology adopted in the present study has been provided. The significance of Coherence analysis particularly the use of Maximum Entropy Spectral Estimation (MESE) has been highlighted. The chapter also includes a discussion on the importance of subsidence and sediment loading studies and provides description of various methods such as Airy and flexural backstripping and the lithospheric models such as Necking and Magmatic underplating.

Chapter 4 gives the details on estimation of Te based on Coherence analysis in the Southwestern Continental Margin and adjoining areas. A description of the gravity anomalies along the WCMI, calculation of Complete Bouguer Anomaly through application of terrain correction has been provided. The results obtained from the Coherence analysis are also discussed.

The sediment loading and flexural characteristics of the lithosphere have been carried out along two seismo-geologic sections compiled from the available seismic data in the Konkan and Kerala basins. Based on the process-oriented approach, two lithospheric models (Necking and Magmatic underplating) of evolution of the margin were tested. The results of this analysis are given in chapter 5.

Chapter 6 presents a detailed discussion and geological implications of the results obtained in the above analysis. A discussion on India and Madagascar breakup – role of Marion mantle plume , isostasy at the Konkan and Kerala basins, lithospheric strength and evolution of the Western Ghats, Geophysical characteristics and probable mode of emplacement of Comorin Ridge in relation to the evolution of the Western Continental Margin are included in this chapter.

Chapter 7 provides summary of the work and major conclusions drawn from the present study.

****

CHAPTER 2 REGIONAL GEOTECTONIC SETTING

2.1 INTRODUCTION

Amalgamation of Gondwanaland has generally been recognized sometime around 500-550 Ma (McWilliams, 1981; Unrug, 1996). At various times in the Jurassic and Cretaceous, that is, around 160-70 Ma, extensional plate margins formed within Gondwanaland. Due to major plate reorganization in the Mesozoic period, India got separated from East Antarctica (Powell et al., 1988). In the wake of northward drift of India, the Bay of Bengal, the Arabian Sea and the Central Indian Ocean have evolved. Further drift of the India towards north resulted in the collision with Eurasia which brought forth the closure of the Tethys Ocean and uplift of Himalaya. Rifting and subsequent breakup of India with east Antarctica, Madagascar and Seychelles at different times during early to mid Cretaceous led to the formation of passive continental margins of India. Geologic as well as geophysical characteristics of the passive continental margins bring out different stages in the evolution of lithosphere of any region. The WCMI is one such passive continental margin created by the drifting of India, Madagascar and the Seychelles. Around 66 Ma, the Deccan volcanism took place along the developing continental boundary. Many of the structural features such as, Chagos Laccadive Ridge, Laxmi Ridge and Laxmi Basin were evolved during the margin development.

2.2 INDIA, MADAGASCAR AND SEYCHELLES IN EASTERN GONDWANALAND, BREAKUP HISTORY AND PLUME LITHOSPHERE INTERACTIONS ALONG WCMI

The position of India in the Eastern Gondwanaland reconstruction has been studied by many authors (Johnson et al., 1976; Besse and Courtillot, 1988; Powell et al., 1988; Storey et al., 1995). The ECMI fits well with the East Antarctica Continental Margin (EACM) along the 2000 m bathymetry. The conjugate nature of ECMI and

EACM has been supported by Mesozoic magnetic anomalies (Ramana et al., 2001), admittance signatures (Chand et al., 2001) and structural lineaments (Johnson et al., 1976; Lawver et al., 1991). Similarly, the juxtaposition of WCMI and Eastern Continental Margin of Madagascar (ECMM) is consistent with Precambrian trends, lithologies and age provinces (Figure 2.1). The Precambrian geology of Madagascar and India are well comparable (Agarwal et al, 1992). Paleomagnetic data also gives ample evidence on general fit of Madagascar against India and suggests the trace of the reassembly to Proterozoic times. Most of the plate reconstructions of Eastern Gondwanaland show Madagascar sandwiched between the west coast of India and Africa, but its position during Gondwana times has been a topic of debate (Green, 1972; Embleton and McElhinny, 1975). The major reconstructions are mainly with Madagascar:

- Adjacent to the coast of Somalia, Kenya and Tanzania (Mc Elhinny et al., 1976; Coffin and Rabinowitz,1987)
- Against the coast of Mozambique (Green, 1972; Coffin and Rabinowitz, 1987)
- Close to the West Coast of India (Katz and Premoli, 1979; Yoshida et al., 1999)

The age of the Southern Granulite Terrain (SGT) of India (2.5 ~ 2.6 Ga) corresponds well with Madagascar Granulite Terrain. The shallow water Cretaceous fossils along the west coast are reported to be closely akin to specimens from Madagascar (Stokes, 1965). The Axial Shear Zone of Madagascar can be compared with dextral Moyar - Bhavani shear zone of India and the most noticeable feature is that both comprise of extensive alkaline mafic intrusions (Windley et al., 1994; Yoshida et al., 1987). The dextral Palghat-Cauvery Shear Zone which trends E-W can be correlated either to western edge of Axial Shear Zone or Ranotsara Shear zone (Katz

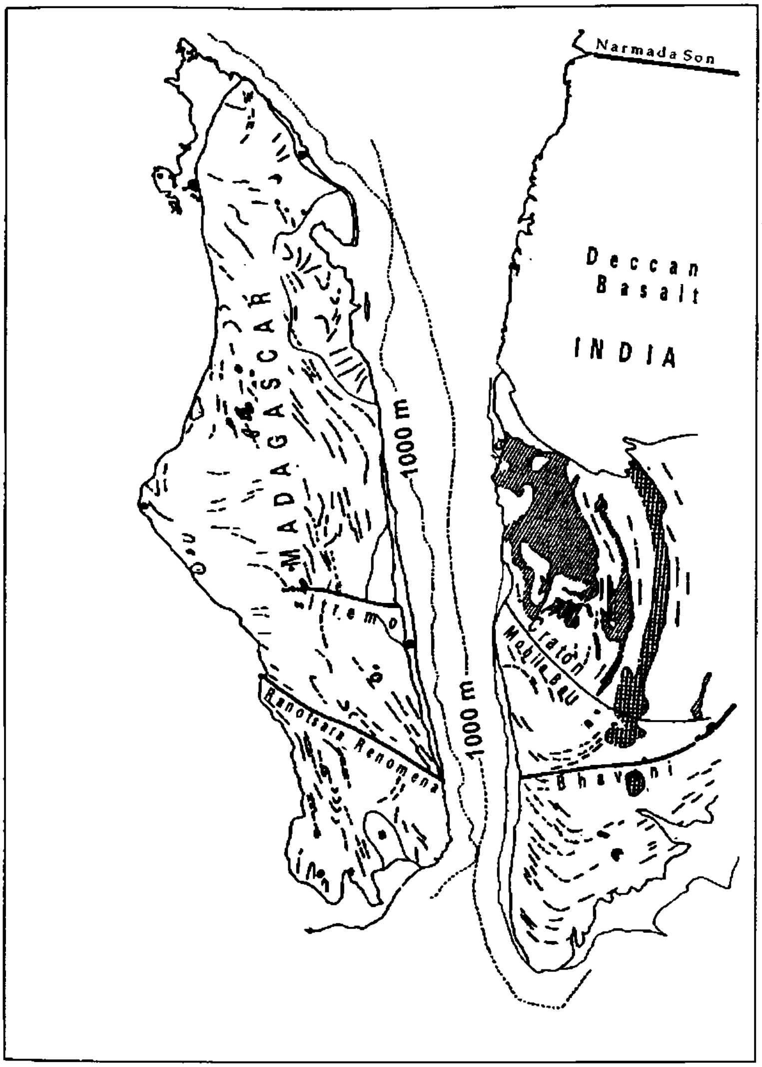

Fig 2.1: Reconstruction of India and Madagascar at 1000 m isobath and matching of Precambrian structural trends (after Katz and Premoli, 1979)

and Premoli,1979). The lineaments such as Narmada-Son Lineament (Fig. 2.1) are traced along the northern part of Madagascar by Crawford (1978). The presence of Upper Cretaceous volcanic rocks, mafic dykes, the escarpment structure on the eastern side of Madagascar and western side of India and nature of long wavelength gravity anomalies (Agarwal et al., 1992) on the two sides all point towards the conjugate nature of India and Madagascar.

The continental breakup in Gondwanaland is believed to have resulted from the interaction of series of hotspots or mantle plumes (Courtillot, 1999). Approximately around 88 Ma, the combined India - Madagascar - Seychelles block came over the location of the Marion mantle plume (Figure 2.2a). As a result, the separation of Madagascar from Seychelles-India block occurred (Besse and Courtillot, 1988; Storey et al., 1995). The separation of Seychelles and India took place during the Paleocene (Figure 2.2b). The widespread volcanism over the Indian landmass due to Re Union mantle plume at K-T boundary (~65 Ma) led to the formation of Deccan Continental Flood Basalt Province (Subba Rao and Sukheswala, 1981; Courtillot et al., 1986). The separation of Seychelles and India during Paleocene also indicate a causal link between plumes and margin formation (Courtillot et al., 1986). As India moved further north, the influence of the hotspot created Chagos-Laccadive Ridge and reorganization of nearby spreading centers in the oceanic areas.

2.3 MORPHOTECTONIC FEATURES IN THE ARABIAN SEA AND THE ADJOINING AREAS

The Arabian Sea forms the deep oceanic part of WCMI. It exhibits a triangular shape bounded by different morphological features. To the west of Arabian Sea, the Owen Fracture zone (Whitmarsh, 1974; Naini and Talwani, 1982) offsets the Carlsberg

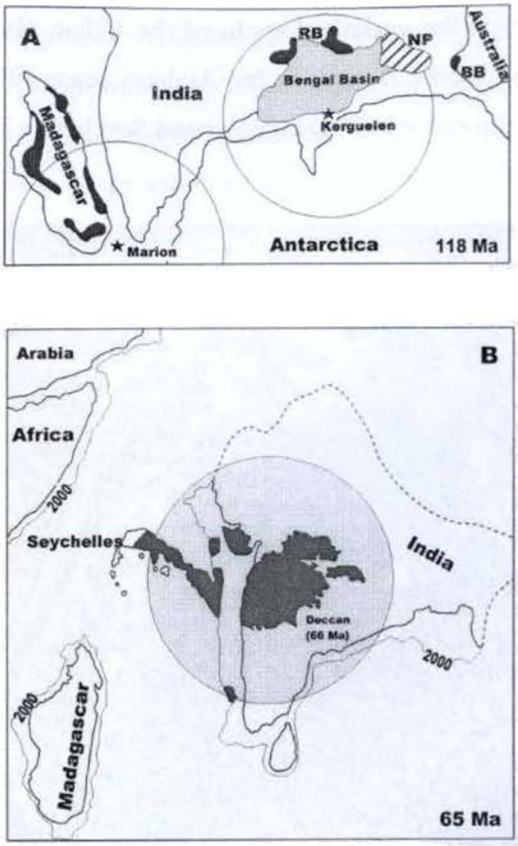

Fig 2.2: Rifting and breakup of the eastern and western continental margins of India and association of major plumes. The possible extent of the the Kergulean Plume (around 118 Ma) , Marion plume (around 88 Ma) and Re Union Plume (66Ma) is shown as circle (adopted from White and McKenzie, 1989; Storey, 1995).

and Sheba Ridges with a sinistral motion along the active part of the transform fault (Gordon and DeMets, 1989). The Owen Fracture zone continues northward up to the Murray Ridge off Pakistan shelf (Figure 2.3) and is considered as a boundary separating Indian and Arabian Plates (Gordon and DeMets, 1989). Towards the south, the Arabian basin is bounded by the slow spreading Carlsberg Ridge. To the east, the Chagos Laccadive Ridge forms a 2000 km long linear feature and strikes almost north-south.

The Arabian basin is thus the oceanic domain of the Indian plate in the NW Indian Ocean. Major morpho-tectonic features in the Arabian Sea are believed to have been inherited from the breakup history of Madagascar and Seychelles from India.

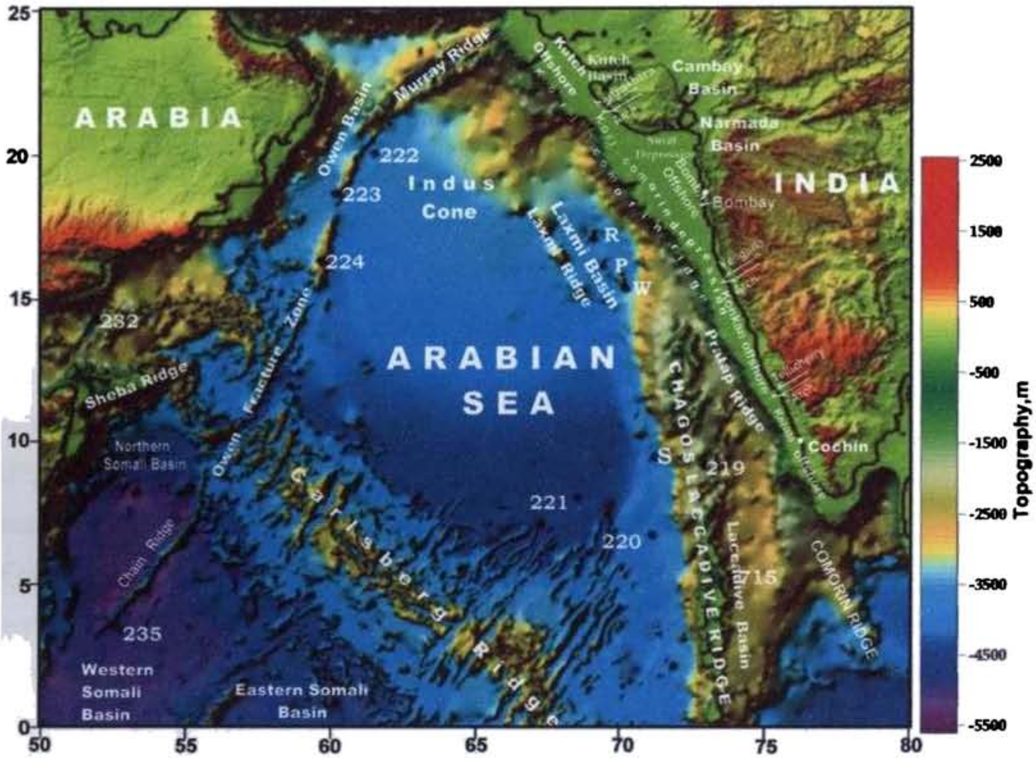

Fig 2.3: Physiographic map of the Arabian Sea and adjoining areas showing major structural features. The dots with number indicate the locations of deep drilling (DSDP and ODP) sites. The various sub-basins and basement arches along the WCMI are shown from Biswas (2001). Solid triangles indicate seamounts. (Bhattacharya et al., 1994.b)

Numerous regional structures and sedimentary basins are located along the WCMI and contiguous Arabian Sea. In the northern part of the Arabian Sea, the Indus deep-sea fan is well developed. The fan is characterized by the presence of several valleys and channels through which the turbidity currents transport primarily the Indus river sediments into areas as far south as the Carlsberg Ridge. Laxmi Ridge, which overlies the Indus cone and extends from 16°N to 18°N, separates the Arabian basin and Laxmi basin (Bhattacharya et al., 1994). Seismic refraction studies brought out the crustal configuration below the Laxmi basin (Naini and Talwani, 1982). The Western basin is oceanic; while the Laxmi Ridge based on the velocity structure is a continental ridge. The Laxmi basin exhibits linear magnetic anomalies which have been interpreted as oceanic magnetic anomalies (Bhattacharya et al., 1994). Geophysically, the Laxmi Ridge is an enigma. It differs from the other oceanic features and continental plateaus by being associated with negative free air gravity anomaly (Miles et al., 1998).

The region between the Chagos Laccadive Ridge and the west coast, south of about 16°N has a complex bathymetry with numerous topographic highs and lows. The shelf break occurs at an average depth of 200 m along the margin with the width of shelf varying from 150 km near Karachi, 350 km off Bombay to 60 km towards south of Cochin (Naini and Kolla, 1982). Between Goa and Kathiawar, the continental slope-rise is normal where as, north of Kathiawar, margin morphology is modified by Indus cone. However, between Goa and Cochin several topographic highs complicate the nature of continental rise. Major topographic feature is Pratap Ridge, which extends from 7°N to 15°N latitude and runs parallel to the WCMI. Another important feature in this region is the Chagos – Laccadive Ridge which extends from about 10°S to 15°N latitude. The relief of the ridge is about 1000 m and demarcated by volcanic islands such as Laccadive Islands and ornamented occasionally with coral atolls.

Along the west coast, several basement highs (Arches) trending perpendicular to the coast divide the shelf region into various thick sedimentary basins. They include Kutch basin, Saurashtra basin, Bombay basin, Konkan basin and Kerala basin.

Northern most basins of Western continental margin, Kutch and Saurashtra, are separated by a southwesterly plunging basement high called Saurashtra Arch. The separation of Bombay and Konkan basins is by southwesterly plunging Vengurla Arch and the southern most Kerala–Konkan basins are demarcated by Tellicherry Arch (Fig. 2.3).

Biswas and Singh (1988) present six contiguous NW-SE trending morpho-tectonic features such as shelfal horst-graben complex, Kori-Comorin ridge, the Laxmi-Laccadive depression, Laxmi-Laccadive Ridge and Arabian abyssal plain. The West Coast Fault and its northward extension, the East-Cambay Fault and the Nagar-Parkar Fault mark approximately landward limit of the WCMI (Figure 2.4). The shelfal horst-graben complex off Saurashtra and Bombay consist of three Precambrian orogenic trends namely the NNW-SSE Dharwar trend, the NE-SW Aravalli trend and ENE-WSW Satpura trend (Biswas and Singh, 1988). Re-activation of these trends during and after rifting, determined the shape, extend and subsidence history of the shelfal horst graben complex.

The Kori-Comorin ridge is a very prominent NW-SE trending structural feature traversing the entire WCMI. South of Vengurla Arch, the ridge becomes a part of continental slope. The northern extent of the ridge is Kori high and southern one is Pratap Ridge. The Kori-Comorin Ridge is separated from the shelfal horst-graben complex by a linear shelf margin depression named Kori-Comorin depression. The northern part of the Kori-Comorin depression extends up to 200 m isobath and the southern part is up to the water depth greater than 200 m isobath (Biswas and Singh, 1988). Morphologically, the Laxmi Ridge appears as the northwestern extension of Chagos Laccadive Ridge. The Laxmi-Laccadive ridge is separated from the Kori-Comorin Ridge by a vast depression called Laxmi-Laccadive depression. It is about 300 km wide in the north and narrows down abruptly south of 16°N lattitude to an average width of 150 km. Further west of Laxmi-Laccadive Ridge is the Arabian abyssal plain, which lies between the isobaths 4000 m and 4500 m.

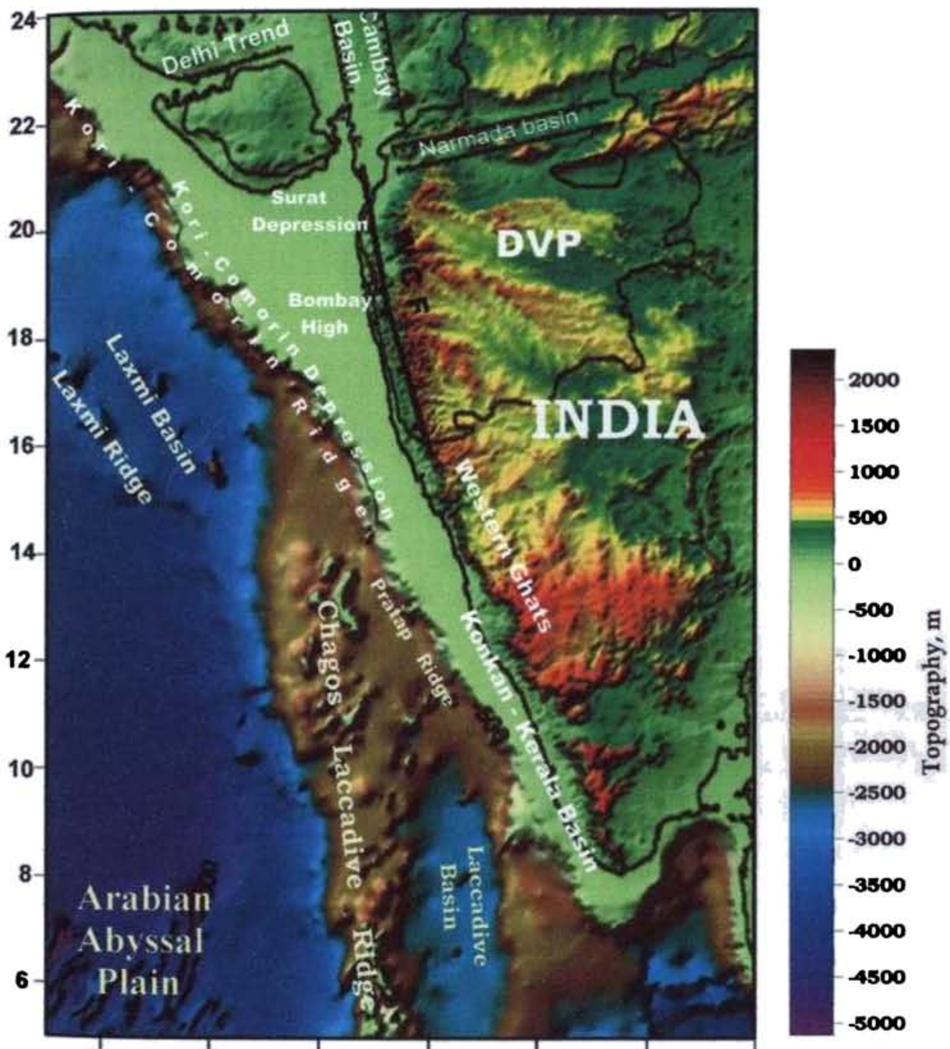

Fig 2.4: Major tectonic elements in the WCMI (after Biswas, 1987; Biswas and Singh, 1988). WCF- West Coast Fault, DVP- Deccan Volcanic Province.

2.4 STRUCTURE AND STRATIGRAPHY OF SEDIMENTARY BASINS ALONG THE WCMI

The WCMI is divided into five major sedimentary basins. These are

- The Kutch basin
- The Saurashtra basin
- The Bombay basin
- The Konkan basin
- The Kerala basin

Along the northern part of the WCMI, very thick shelf sedimentary column is deposited by the major rivers such as Indus, Narmada and Tapti. Further, the longitudinal extensional faults, promote widening of shelf and horst-graben structures and act as favourable habitat of hydrocarbon accumulation. The style of faulting is controlled by three major orogenic trends in the western part of the Indian shield margin, namely NE-SW Aravalli, ENE-WSW Satpura and NNW-SSE Dharwar trends (Biswas, 1982). These trends have a bearing on the north to south sequential rifting of Indian subcontinent during the breakup of Gondwanaland (Biswas, 1982). Two major conjugate rift systems, Narmada and Cambay which locate south of Saurashtra peninsula in the Surat offshore region form a deep depression and cross each other. The Surat depression is considered by many as a triple junction (Thomson, 1976; Powar, 1987). The onshore Mesozoic rift basins such as Kutch, Narmada and Cambay basins are created on the northwest coast. The structural styles of the shelf in Kerala-Konkan basins are similar to north.

Six contiguous tectonic elements running north-south in the shelf and deep oceanic areas of the Arabian Sea have been identified by Biswas and Singh (1988) along the WCMI. These are horst-graben complex, Kori-Comorin ridge, Laxmi-Laccadive depression, Laxmi-Laccadive ridge and Arabian abyssal plain. The syn-rift phase during WCMI evolution is dominated by terrigenous clastics that include conglomerates and red beds of variable thickness (Gopala Rao, 1990). The process of rifting gradually advanced towards south and by Cretaceous almost all the rift related horst and graben structures came into existence. This is evidenced by the presence of vast amount of sediments beneath the Deccan traps along the wells drilled in the Cochin, Kutch, Saurashtra and Narmada offshore (Biswas, 1988). Towards the end of Cretaceous, voluminous continental flood basalts were emplaced (Courtillot et al., 1986; Jaeger et al., 1989; Vandamme et al., 1991,Venkatesan et al., 1993) through a series of eruptions in a very short span of time and covering an area estimated to be greater than 1,000,000 km^2 (Duncan, 1990; Devey and Stephens, 1991). Soon after the Deccan volcanism, in the northern Arabian Sea, the sea floor spreading began and Seychelles separated from India (Norton and Sclater, 1979; Besse and Courtillot, 1988; Molnar et al., 1988).

The rifting and drifting of India since the breakup of Madagascar around 85-90 Ma gave rise to Peri-cratonic offshore rift basins such as Kutch, Saurashtra, Bombay (Ratnagiri), Konkan and Kerala basin. The lithostratgraphic structure of Bombay, Konkan and Kerala basins is shown in Table 2.1 - Table 2.3. A brief description of structure, stratigraphy and tectonics of these basins is presented below.

2.4.1 Offshore basins

The Western offshore contains several deep water sedimentary basins extending from Kutch in the north to Cape-Comorin in the south which encompasses a vast sedimentary track of 4,71,000 km^2 up to the Exclusive Economic Zone (EEZ) (Thakur et al., 1999). The formation of these basins occurred because of the thermo-mechanical evolution of the continental margin since the breakup of Madagascar around 88 Ma (Storey et al., 1995)

2.4.1.1 Bombay Offshore basin

The Bombay offshore basin is the most important among the five offshore basins along the WCMI. It is considered as the most petroliferous basin so far discovered in the sedimentary province in India, which is covering an area of 1,20,000 km^2 up to 200 m isobath. Along the north, the basin is separated from the Kutch basin by Saurashtra Arch and along the south; it is separated from Konkan basin by Vengurla Arch (Rao and Talukdar, 1980; Mathur and Nair, 1993). The basin consists of six major structural units each having well marked sub units. The structure and sedimentation history of the basin are:

- The Surat depression is one of the major basinal areas with more than 3 km of clastic fill of Paleocene-Eocene.
- The N-S trending Diu Arch separates the Surat depression from the Saurashtra basin.
- The Saurashtra and shelf margin basins, although formed in the Paleocene, experienced maximum subsidence during late Oligocene.
- The NE trending Ratnagiri Arch separates the Murud depression from the Rajapur depression and is traceable from the shelfal area to the deep sea.
- The Kori-Arch separates the shelf margin.

<table>
<tr><th rowspan="2">Age</th><th rowspan="2">Saurashtra Baisn</th><th rowspan="2">Surat Depression</th><th rowspan="2">Shelf Margin Basin</th><th rowspan="2">Shelf Margin Banks/Reefs</th><th colspan="2">Bombay Platform</th><th rowspan="2">Heera-Bassein Comp-Block</th><th rowspan="2">Ratnagiri Block</th><th rowspan="2">Transgession (T) Regression (R)</th></tr>
<tr><th>DCS Area</th><th>Bombay HIgh</th></tr>
<tr><td>Middle Miocene-Holocene</td><td colspan="4">Tarapur Formation</td><td colspan="4">Tarapur Formation</td><td>T R</td></tr>
<tr><td>Early-Middle Miocene</td><td rowspan="3">Shale with Limestone bodies</td><td>Tapti Fm.</td><td rowspan="5">Shelf Margin Group</td><td rowspan="6">Angaria Bank Group (includes many unnconformities)</td><td rowspan="5">DCS Group</td><td colspan="2">Saurashtra Fm</td><td rowspan="2">Ratnagiri Formation.</td><td>T</td></tr>
<tr><td>Early Miocene</td><td>Mahim Fm.</td><td colspan="2">Bombay Formation.</td><td>R T</td></tr>
<tr><td>Late Oligocene - Early Miocene</td><td>Daman Fm.</td><td colspan="2">Alibag Formation</td><td></td><td>R T</td></tr>
<tr><td>Early Oligocene</td><td rowspan="2">Shale with Limestone Interbed</td><td rowspan="2">Dahahanu Formation</td><td rowspan="2"></td><td rowspan="2">Bassein Fm.</td><td rowspan="2">Bassein Fm.</td><td>R T</td></tr>
<tr><td>Middle - Late Eocene</td><td>R T</td></tr>
<tr><td>Paleocene-Late Eocene</td><td colspan="2">Panna Fm</td><td>Vashi Formation.</td><td>Panna Fm</td><td></td><td colspan="2"></td><td>R</td></tr>
<tr><td rowspan="3"></td><td colspan="3">Deccan trap</td><td colspan="3">Deccan Trap</td><td colspan="2">Deccan Trap</td><td>T</td></tr>
<tr><td colspan="3">Mesozoic Rocks</td><td colspan="2">?</td><td>Absent</td><td>?</td><td>Mesozoic rocks</td><td></td></tr>
<tr><td colspan="8">Precambrian Rocks</td><td></td></tr>
</table>

Table 2.1: Generalised stratigraphy of various tectonic elements in the Bombay Offshore basin (modified after Mathur and Nair, 1993).

2.4.1.2 Konkan Offshore basin

The offshore area between the Vengurla Arch in the north and Tellicherry Arch in the south along the central part of the west cost of India is known as the Konkan basin. The continental slope off Konkan has a gentle dip of about 2 to 5 degrees and drops off moderately to form a linear feature at a water depth of 1000 m (Thakur et al., 1999). The ocean floor is having a relatively rugged topography along the southern part with a number of submarine topographic features aligned parallel to the present day coast (Subba Raju et al., 1990). Several structural features such as the Pratap Ridge complex, the shelf-margin basin, the mid shelf basement ridge and inner shelf graben are delineated in the Konkan Offshore by Subrahmanyam et al. (1993, 1994). Three sedimentary units belonging to pre-rift, syn-rift (Paleocene-Eocene) and post rift (Middle Eocene to Recent) stages have been identified. The basin contains nearly 3 km of sediments. The generalised stratigraphy of the basin showing various litho units is shown in Table 2.2.

2.4.1.3 Kerala Offshore Basin

The Kerala offshore basin was formed during Middle to late Cretaceous as a result of an early phase of rifting between India and Madagascar. The basin lies between the Tellicherry Arch in the north and Cape - Comorin in the south. Alleppey platform is the major tectono-morphological element in the shelfal horst - graben complex. The shelfal horst-graben complex consists of two major depressions called Cochin depression and Cape - Comorin depression (Singh and Lal, 1993). Two wells Off -Cochin revealed marginal to shallow marine clastic fill having an age of late

<table>
<tr><th colspan="2">AGE</th><th>KARWAR -I</th><th>KASARGODE -I</th></tr>
<tr><td colspan="2">Pleistocene
to
Recent</td><td>Clay: Grey to Dark Grey., soft plastic with shale fragments
299-334 (35m)</td><td rowspan="3">Clay/Claystone,Pyritic,silty
Slightly calcareous
242-940 (690 m)</td></tr>
<tr><td colspan="2">Pliocene</td><td rowspan="2">Claystone: Grey., Pyritic, pebbly calcareous, fossiliferous
334-599 (265m)</td></tr>
<tr><td rowspan="4">Miocene</td><td>Late</td></tr>
<tr><td rowspan="2">Middle</td><td>Lime stone, Light Grey.,micritic,chalky dolomitic,yellow minor shale
599-889 (90 m)</td><td rowspan="3">Lst:
Micritic to Biomicritic
White,corals and shell fragments
940-1336 (396 m)</td></tr>
<tr><td>Limestone, Light Grey.,micritic,chalky dolomitic,yellow minor shale
889-997 (308m)</td></tr>
<tr><td>Early</td><td>Limestone, Light Grey.,micritic,chalky yellow , minor shale
997-1187(190 m)</td></tr>
<tr><td colspan="2">Basal Miocene</td><td rowspan="2">Limestone, Light Grey., Micritic,chalky dolomitic, yellow minor shale
1187-1318 (131 m)</td><td rowspan="2">Lst:
Chalky,micritic
1336-1470 (134 m)</td></tr>
<tr><td rowspan="3">Oligocene</td><td>Late</td></tr>
<tr><td>Middle</td><td rowspan="2">Dolomitic Limestone with minor shale
1318-1408 (90 m)</td><td rowspan="2">Chalky micritic Limestone
1470-1540 (70 m)</td></tr>
<tr><td>Early</td></tr>
<tr><td rowspan="3">Eocene</td><td>Late</td><td></td><td></td></tr>
<tr><td>Middle</td><td rowspan="2">Dolomitic Limestone with minor shale
1408-1504 (96 m)</td><td rowspan="3">Micritic, biomecritic Marl and Silt
1540-2380 (840 m)</td></tr>
<tr><td>Early</td></tr>
<tr><td colspan="2">Paleocene</td><td rowspan="2"></td></tr>
<tr><td colspan="2">Mesozoic
Paleozoic</td><td>Sand : quartzose, poorly sorted Br,Grey., Clay, Limestone towards bottom
2380-3970 (590 m)</td></tr>
<tr><td colspan="2">Achaean</td><td></td><td></td></tr>
</table>

Table 2.2: Generalised stratigraphy of the Konkan offshore basin obtained from two offshore wells (after Singh and Lal, 1993)

Cretaceous (Dirghangi et al., 2000). Detailed stratigraphy of the offshore Kerala basin is shown in Table 2.3. Two dominant fault trends are traced along the base of the formation, one, NNW - SSE trend parallel to the margin representing the rift trend and the other, younger shear fault trending NNE-SSW (Dirghangi et al., 2000).

The early rift phase ended in Pre Santonian time (Singh and Lal., 1993). The oldest marine sediments traced along the Kerala-Konkan basin are of Santonian age. The Kerala-Konkan basin is limited by Miocene Pliocene shelf edge to the west. Some of the salient features associated with the basins are:

- Basin margin fault zone restricting the deposition of the thicker sediments towards the West.
- Miocene shelf edge, which creates a thick wedge of Neogene sediments showing a prograding sequence across the basin. This paleo high gives rise to the formation of reefs.

2.5 GEOTECTONIC FRAMEWORK OF WCMI AND ADJOINING AREAS.

The basic framework of WCMI was established by the end of Cretaceous (Biswas, 1987). The development of structural features along the margin is related to breakup of Gondwanaland and northward movement of the Indian plate and its ultimate collision with Eurasia (Norton and Sclater, 1979; Veevers et. al., 1980; Subrahmanya, 1998; among others). The Peninsular India mainly consists of Archean gneisses, schists, charnockites and metamorphosed sedimentary rocks. The rest of the peninsula

<table>
<tr><th colspan="2" rowspan="2">Age</th><th colspan="3">Offshore</th></tr>
<tr><th colspan="2">K-1-1</th><th>CH-1-1</th></tr>
<tr><td colspan="2">Pleistocene to Recent</td><td colspan="2">Dominantly Coarse Sandstone</td><td rowspan="3">Clay/Claystone</td></tr>
<tr><td colspan="2">Pliocene</td><td rowspan="3">Shallow Marginal Marine</td><td rowspan="2">Dominantly fine to medium grained Sandstone</td></tr>
<tr><td rowspan="5">Miocene</td><td>Late</td></tr>
<tr><td>Middle</td><td>Coarse grained, pebbly Sandstone, clayey in lower part</td><td>Limestone</td></tr>
<tr><td rowspan="3">Early</td><td rowspan="3">Shallow Marine</td><td>Clay/Sand stone alternations with occasional carbonaceous bands</td><td rowspan="3">Limestone</td></tr>
<tr><td>Carbonates with thin Sandstone and sandy Clay bands</td></tr>
<tr><td>Sandstone with Clay bands and carbonaceous band in lower part</td></tr>
<tr><td colspan="2">Basal Miocene</td><td>Shallow Marginal Marine</td><td>Sandstone/Clay alternations with Lignitic Coal bands</td><td>Limestone with Claystone</td></tr>
<tr><td colspan="2">Oligocene</td><td>Shallow Marine</td><td>Sandy Clays with thin carbonate bands</td><td>Limestone with Claystone</td></tr>
<tr><td colspan="2" rowspan="2">Eocene</td><td rowspan="3">Continental</td><td>Sandstone with Lignitic Coal bands</td><td>Limestone/ Dolomitic</td></tr>
<tr><td>Sandy Clay</td><td rowspan="3">Sandstone/ Siltstone Limestone/Shale Siltstone/ Claystone Sandstone/ siltstone/Shale</td></tr>
<tr><td colspan="2">Paleocene</td><td>Clay/Shale, Trap derivatives</td></tr>
<tr><td colspan="2">Mesozoic</td><td>Dominantly Fresh Water</td><td>Sandstone with Clay and weathered Trap</td></tr>
<tr><td colspan="2">Archean</td><td></td><td></td><td></td></tr>
</table>

Table 2.3: Generalised stratigraphy of the Kerala basin as obtained from well data (after Singh and Lal, 1993)

is dominated by the Deccan Traps. The NW-SE to NNW-SSE Dharwar trend, NE-SW Aravalli and ENE - WSE to E - W Satpura trend are the predominant structural grain, which has a bearing on the north to south sequential rifting of the Indian subcontinent during the breakup of Gondwanaland. The western margin of India has a long coastline bordered by coastal region of low elevation with an average width of 50 km. The coastal region rises in small steps and there is a drastic change in altitude, which reaches even up to 1500 m that runs parallel to the coast along its entire length. This precipitous terrain which is well known as Western Ghats is having highly varied lithologies like peninsular gneisses, granulites and Deccan basalts. This feature has been considered to be formed as a result of differential denudation and flexural isostasy (Gilchrist and Summerfield, 1991). Apatite Fission Track Analysis (AFTA) (Gallagher et. al., 1998) indicates that the escarpments formed due to uplift during rifting followed by a lateral scarp retreat.

The Arabian Sea evolved as a result of seafloor spreading following the breakup of Madagascar and Seychelles (McKenzie and Sclater, 1971; Whitmarsh, 1974; Norton and Sclater, 1979; Naini and Talwani, 1982; Chaubey et. al., 1993). The Arabian Sea is divided into several deep ocean basins by submarine plateaus, aseismic Laxmi and Laccadive ridges, the active spreading Carlsberg and Sheba ridges and regionally extending Owen fracture zone. The western Arabian basin and the Somali basin are considered to be underlain by oceanic crust (Naini and Talwani, 1982) as they have crustal structure similar to a known oceanic crust and identifiable magnetic anomalies.

The actual timing of opening of the Arabian Sea is under debate. Considerable ambiguity on the oldest identifiable magnetic anomaly still exists. The oldest sea floor spreading magnetic anomaly and the location of Ocean Continent Transition (OCT) along the margin are the two most important aspects while considering the tectonic history of Arabian Sea. Another factor that should be given considerable importance is the role of Deccan plume activity during the breakup of Gondwanaland and further rifting. However, in the case of western continental margin, the separation of Seychelles from India and the initial opening history of the Arabian Sea and eastern Somali basin are poorly known. Some recent works made in the Arabian Sea mainly focused on these aspects (Bhattacharya et al., 1994; Malod et al., 1997; Miles et al., 1998; Talwani and Reif, 1998; Todal and Eldholm, 1998; Chaubey et al., 2002; Krishna et al., 2006). The identification of sea floor spreading magnetic anomalies in the Laxmi basin by Bhattacharya et al. (1994) is the most significant aspect that has wider implications on plate tectonic reconstruction of the Arabian Sea. Based on this observation, Talwani and Reif (1998) proposed a reconstruction history shown in Figure 2.5 which moves Seychelles original location closer to India and a new rotation pole between anomaly 28 and 34. They further interpreted that >7.0 km/sec velocities observed in the Laxmi basin represents the initial oceanic crust. On the other hand, Todal and Eldholm (1998), Miles et al. (1998) and Krishna et al. (2006) support continental type of crust below the Laxmi basin. Miles et al (1998) believe that some of the basement features in the Laxmi basin originated from large scale intrusions and also the crustal models derived by them do not support pre-anomaly 28 phase of sea floor spreading in the basin. On the basis of magnetic anomaly identifications, Todal and Eldholm (1998) proposed a plate reconstruction history (Figure 2.6) of the Seychelles microplate with reference to Indian plate. According to the model, during A29-27 time, the continental extension followed by fan shaped spreading between Seychelles and India, cessation of the fan shaped spreading just after A27 time followed by spreading between India and Seychelles, and margin subsidence modified south of Goa due to the effect of plume trail.

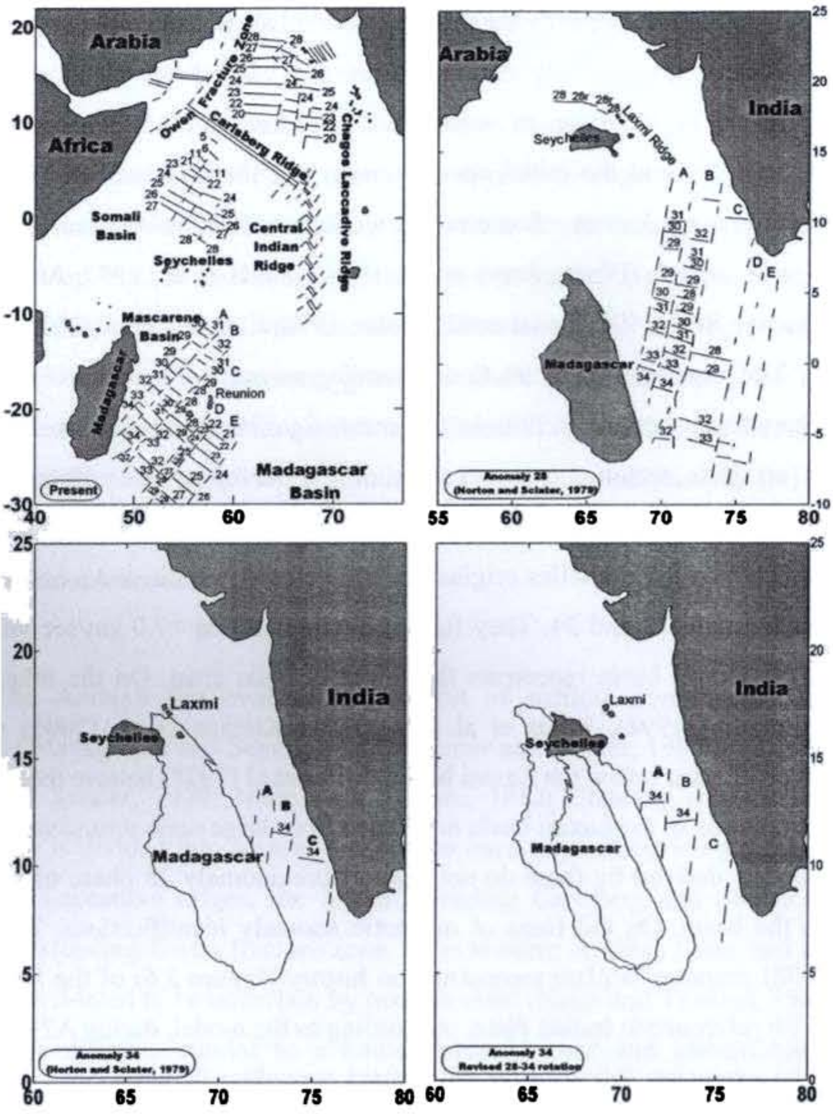

Fig 2.5: Reconstruction of India and Madagascar (after Talwani and Reif, 1998). The sea floor spreading anomalies in the Laxmi basin (Bhattacharya et al., 1994) and a new rotation pole between anomaly 28 and 34 have been used in the reconstruction.

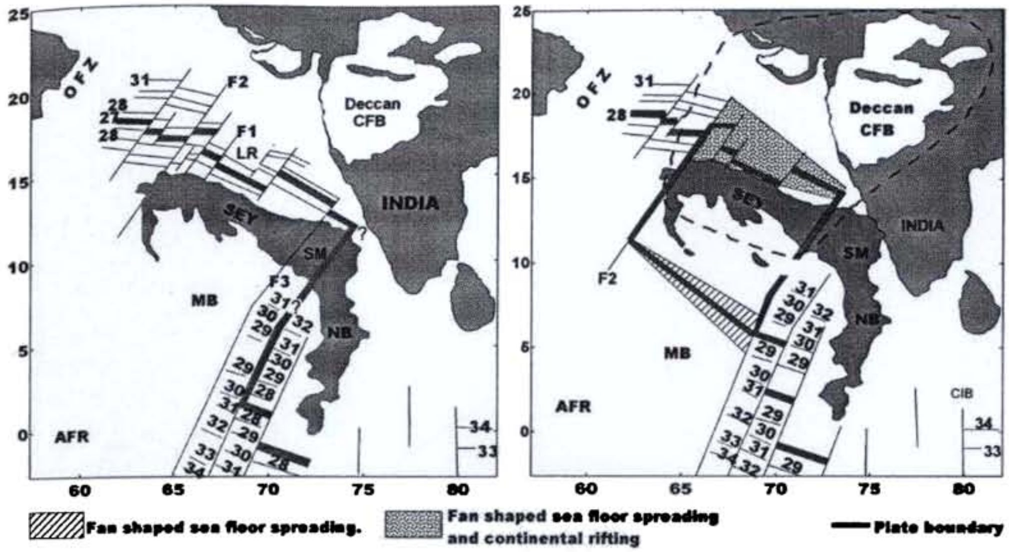

Fig 2.6: Plate reconstruction of Seychelles microplate (SEY) with reference to the Indian plate (IND) (after Todal and Eldholm, 1998). AFR- African plate, OFZ - Owen fracture zone, MB- Mascarene basin, CIB- central Indian basin, NB- Nazareth bank, SM- Saya de Malha Bank. LR – Laxmi ridge. Thick dashed line in the right diagram encircles the Deccan Large Igneous Province.

****

CHAPTER 3 METHODOLOGY

3.1 INTRODUCTION

It is well established that lithospheric flexure has played an important role in the evolution of the Earth's surface features. Flexure and deformation it causes contributes directly to the crustal structure, subsidence, uplift history and the gravity anomaly at the passive continental margins. The accumulation of sediments at the margin represents loads over long geological periods. The stratigraphic architecture of the major deltaic basins such as offlap, downdip, thickening and uplift can be explained on a smaller scale through flexure. It is observed that flexural effects extend onshore as evidenced by raised onshore regions. Also, it is important to understand, how the Earth's crust and upper mantle adjust to the geological loads. It is known that isostasy is operative over timescales range from a few thousands to a few million years and the main factor that determines the degree to which the particular surface feature is compensated is its size. The strength of the lithosphere is an important factor that determines the amount of bending and the degree to which the compensation approaches the prediction of local models. It is well known that the lithosphere responds to long term geological loads not locally, as Airy and Pratt models would predict, but regionally by flexure. Significant information has been derived from the studies on elastic thickness of the lithosphere regarding the long-term mechanical properties of the lithosphere and the relationship to plate and load age.

The amplitude and wavelength of the gravity anomalies at the continental margin are sensitive to the value of effective elastic thickness (Te) (Walcott, 1972; Cochran 1973). The gravity anomaly at the continental margins can be considered as a result of several processes that include rifting, sedimentation, erosion and magmatic underplating operating through time. This distinctive gravity field at the margin called 'edge effect anomaly', a gravity high over the outer shelf, and low associated with the slope and rise regions, has been modeled by several workers to understand the crustal processes and geodynamics of the passive continental margins.

Two different approaches are available to model this edge effect gravity anomaly of the margin, one, is through isostatic response estimates to model the isostasy in terms of local and flexural isostatic compensation mechanisms, the other is through process oriented approach in which detail crustal seismic information on initial crustal structure (from seismic reflection and refraction data) is incorporated to model the gravity edge effect anomaly by clubbing the gravity contributions from different processes such as rifting, sedimentation, erosion and underplating. While the former approach gives rise to the effective elastic thickness (Te) as an integrated mechanical strength of the lithosphere since rifting, the latter approach yields strength of the lithosphere at the time of rifting as well as its temporal variation since rifting.

In the present thesis, these two approaches are dealt in detail along the southwest continental margin of India to understand the geodynamic evolution of the margin. A detailed description on the methodology followed for both isostatic response estimates as well as process-oriented approach have been presented in the subsequent part of this chapter.

3.2 ISOSTATIC RESPONSE FUNCTION

Through the statistical relationship between the gravity and bathymetry in the wave number domain using either, the Admittance function (Dorman and Lewis; 1970), or Coherence function (Forsyth; 1985), the measure of correlation between them can be estimated and helps to estimate the Te and hence the rigidity of the lithosphere. In the estimation of admittance function, the contribution from loading is ignored and the gravity effect due to this loads are considered to be noise. In the oceanic settings, this approach gave excellent results (McKenzie and Bowin, 1976; Watts, 1978; Karner and Watts, 1982). However, Forsyth (1985) pointed out that the admittance function is weighted by topography to varying degrees and if subsurface loads are included in the model, then the admittance can be modeled arbitrarily. Therefore, the estimation of Te using admittance function is valuable only when reasonable constraints are induced on the distribution of loads. However, Forsyth (1985) argued that the best assumption about the load distribution is that the subsurface loads are present and uncorrelated with the surface loads. He developed a linear model with multiple inputs consisting of various loads at surface and internal interfaces (Figure 3.1), which gives multiple

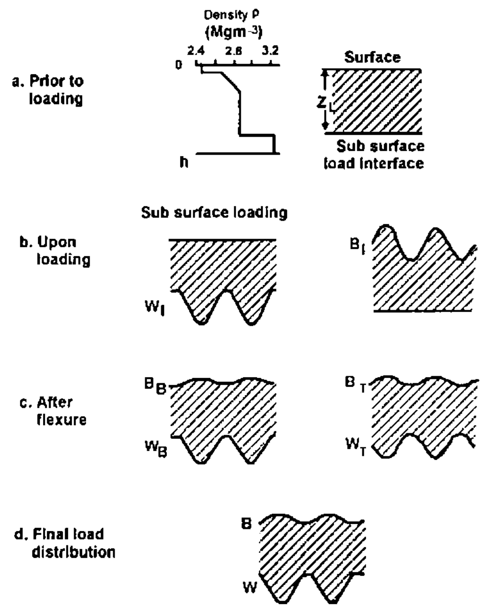

Fig 3.1: Fourier isostatic model (after Forsyth, 1985). (a) an elastic layer of thickness h, having an arbitrary density variation with depth. (b) Sinusoidal loading with Fourier amplitude B_I is applied at the top; loading with W_I occurs at depth Z_L. (c) Flexural results in topographic amplitudes B_T due to surface loading and B_B due to subsurface loading. Deflections of the subsurface load interface have amplitude W_T and W_B, respectively. (d) Observed topography B and internal deflection W sum the surface and subsurface responses.

outputs of gravity and topography at the surface of elastic plate Unfortunately, due to interference of multiple input loads, this model implies loss of coherence between predicted Bouguer gravity and topography. Assuming that the surface and subsurface loads are uncorrelated, Bechtel et al (1987) modified this coherence method and estimated the Te as well as the ratio of surface to subsurface load that matches the topography and gravity and best predicts the coherence. In the investigation of continental flexural rigidity, variation of Forsyth's method has been generally used.

3.2.1 Coherence analysis

Through coherence analysis, an integrated approach is made to estimate the effective elastic thickness of the lithosphere through which we can estimate the variation in Te along the margin. This will help to analyse segmentation across the margin, understand the origin of various structural features along the margin and hence to understand the evolutionary history of the margin. .The coherence function is the square of correlation coefficient between the Bouguer gravity and bathymetry. Since coherence has a strong dependence on flexural rigidity of the lithosphere, it is used for the estimation of Te (Figure3.1). The coherence function measures the consistency of phase relationship between the two fields regardless of their amplitude and is a positive number ranging between zero and one. Theoretically, coherence function $\hat{\gamma}^2_{bg}(k)$ can be estimated from the auto power spectra of bathymetry $P_{bb}(k)$ and gravity $P_{gg}(k)$ and the cross power spectrum of bathymetry and gravity, $P_{bg}(k)$ using the formula

$$\hat{\gamma}^2_{bg}(k) = \frac{\left|P_{bg}(k)\right|^2}{P_{bb}(k)P_{gg}(k)^{\bullet}} \qquad \text{.........(3.1)}$$

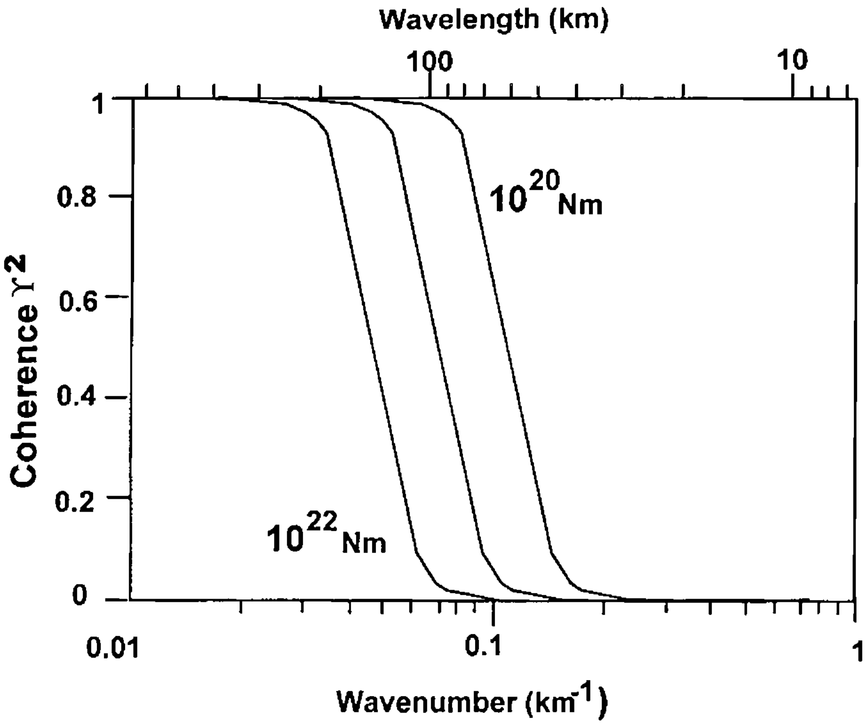

Fig 3.2: Coherence of gravity and topography vs. wavelength. The transition from low – to – high coherence strongly depends on flexural rigidity (after Forsyth, 1985)

Usually in order to reduce the bias introduced by correlated processes, two dimensional power spectra are averaged and is performed within the annular wave number bins based on the assumption that flexural response is isotropic. Hence the coherence is one dimensional and is expressed as

$$\hat{\gamma}^2_{bg}(k) = \frac{\left|\left\langle P_{bg}(k)\right\rangle\right|^2}{\left\langle P_{bb}(k)\right\rangle\left\langle P_{gg}(k)\right\rangle^{\bullet}} \qquad \text{..........(3.2)}$$

where **k** is the modulus of the two dimensional wave number given as

$$k = |k| = \left(k_x^2 + k_y^2\right)^{-\frac{1}{2}} \quad \text{..........(3.3)}$$

The 2D-Coherence analysis between the Bouguer gravity and topography can be carried out using different approaches such as conventional Fourier periodogram, maximum entropy, Multitaper or Wavelet analysis methods (Lowry and Smith 1994; McKenzie and Fairhead 1997; Simons et al. 2000; Daly et al. 2004; among others). Some salient aspects of each of these methods are presented below:

3.2.1.1 Periodogram Spectral Estimation

Periodogram spectral estimation is a classical Fourier transform technique to estimate power spectra and is considered as conventional method of calculating the coherence function. The periodogram, which is considered as the square of magnitude of the Fourier coefficient of the signal is a first order spectral estimator (Tukey, 1967; Kay and Marple, 1981; Percival and Walden, 1993). The coherence function is approximated with periodogram (Bendat and Piersol, 1986; 1993; Touzi et al., 1996; 1999) is expressed as

$$\gamma^2(k) = \frac{\left|E\{B(k)G^*(k)\}\right|^2}{E\{G(k)G^*(k)\}E\{B(k)B^*(k)\}} \quad \text{..........(3.4)}$$

where B and G denote the Fourier transforms of the random variable b and g (bathymetry and gravity), E denotes the expectation or averaging operator and the asterisk denotes the complex conjugation (Simons et al., 2000).

But according to Kay (1988), this method unfortunately is contaminated by spectral bias as well as leakage due to the implicit windowing of finite data. The data sequence should be selected in such a way that it might be large relative to the wavelengths of interest (Bechtel, 1989) and hence modifying the periodogram with mirrored data is used in order to improve the estimation properties of Periodogram (Tukey, 1967; Welch, 1967; Percival and Walden, 1993). The choice of the data windows primarily controls the bias, while smoothing and averaging reduces the estimation variance (Chave et al., 1987). In the periodogram method, spectral properties should be computed for very large geographic areas in the order of $10^5\,km^2$ to $10^6\,km^2$ and assumes a uniform flexural rigidity for the sampled region. This is an inherent draw back in the method as the flexural rigidity varies significantly over very short distances. The periodogram method yields a poor approximation to the true coherence function at transitional wavelengths.

3.2.1.2 Multitaper Spectral Estimation

The multitaper spectral analysis technique, originally introduced by Thomson (1982) using functions developed by Slepian (1978), reduces the estimation variance of the spectrum in the calculation of power spectral density. To minimize the spectral leakage, it is required to find data windows whose spectral responses have the narrowest central lobe and smallest possible sidelobe level. The resolution of this estimate depends on the width of the central lobe. As the width of the central lobe in the spectral domain broadens and their side lobe level increases, the resolution progressively degrades and causes leakage. Estimation variance is reduced by incorporating different tapers into the spectral estimation. Slepian (1978) found out that the ideal data windows are given by discrete prolate spheroidal sequence (dpss). The half-width of their central lobe is usually an integer multiple of the fundamental frequency, commonly quoted as NW. For every such choice of resolution bandwidth, there are 2NW-1 useful tapers, where 2NW is referred as Shannon number in the information theory (Simons et al., 2000), which extracts information evenly from the entire signal.

The direct spectral estimates using multitaper U_t^k is defined as $S_k^{mt}(f)$, where k is the order of the taper. Simply multitaper spectral estimator, $S^{mt}(f)$, is the average over K direct spectral estimates and hence can be reproduced by the simplest formulation

$$S^{mt}(f) = \frac{1}{K}\sum_{K=0}^{K-1} S_k^{mt}(f) \qquad \text{.............(3.5)}$$

for

$$S_k^{mt}(f) = X(f) \otimes U_k(f) \qquad \text{..............(3.6)}$$

where U_k are the tapers, X(f) is the data function and $\otimes$ represents the convolution. In Thomson (1982), the estimator $S_k^{mt}(f)$ is called k[th] Eigen vector. The corresponding spectral window $U_k(f)$ controls the extent to which the direct spectral estimate is free of leakage. The estimated variance of $S^{mt}(\bullet)$ is much smaller than the individual $S_k^{mt}(\bullet)$ as it has been reduced by factor of 1/K. The multitaper coherence function of two signals **b** and **g** are defined as

$$\hat{\gamma}_{bg}^{2} = \frac{\left|S_{bg}^{mt}(\bullet)\right|^2}{S_{bb}^{mt}(\bullet)S_{gg}^{mt}(\bullet)^{\bullet}} \qquad \text{......................(3.7)}$$

where S_{bg}^{mt}, S_{bb}^{mt}, S_{gg}^{mt} is the cross correlation of bathymetry and gravity, auto correlation of bathymetry and autocorrelation of gravity respectively.

In this method, tapers are applied in both rows and columns of the gravity and topography data. These are then Fourier transformed and the observed coherence function is calculated. The coherence estimation using MTM method yields more accurate Elastic thickness estimate than the conventional periodogram method (McKenzie and Fairhead, 1997; Simons et al., 2000).

3.2.1.3 Maximum Entropy Spectral Estimate

The maximum entropy spectral estimation (MESE) method gives rise to a power spectrum exhibiting minimum bias, corresponding to the Fourier transform of the extrapolated correlation function having maximum entropy. Burg (1967) formulated this method for one dimensional signals and is equivalent to autoregressive spectral estimates (Kay and Marple, 1981). The "extrapolation" of the correlation function to larger lags is implicit rather than explicit. The two dimensional extension of this method for estimating auto and cross power spectra was possible after the development of an iterative MESE algorithm by Lim and Malik (1981). Through reasonable extrapolation of the known correlation function having maximum entropy within a windowed area A, is formulated as

$$\hat{r}_{hh}[m,n] = F^{-1}\left\{\hat{P}_{hh}(k_1,k_2)\right\} = r_{hh}[m,n] \text{ for } [m,n] \in A \quad \ldots\ldots\ldots(3.8)$$

where $F^{1}\{\bullet\}$ represents the inverse Fourier transform operator and $\hat{r}_{hh}[m,n]$ is the extrapolated correlation function.

By averaging with the annular wave number bins, the coherence function was reduced to one dimension and is defined as

$$\hat{\gamma}^{2}_{hb} = \left| \left\langle \frac{\left(P_{hb}\right)^{2}}{P_{hh} P_{bb}} \right\rangle \right| \qquad \text{...........(3.9)}$$

The resulting coherence function exhibit a positive bias at wavelengths for which true coherence approaches zero. The MESE can be used in very short number of data sets that is, even data windows over small-scale features can be analysed due to high spectral resolution.

3.2.1.4 Wavelet analysis

The wavelet multiresolution technique has been developed over a decade or so. Its aim is to achieve good spatial resolution over long length scales (wide analysis regions) and good wave number resolution over short length scales (narrow analysis region). The local wavelet cross-spectral power is defined as the product of the wavelet transforms of each signal averaged over some scaling window (Stark et al., 2003). The wavelet cross spectral power of two signal , i.e., bathymetry b and Bouguer gravity anomaly g at a point x is given by

$$P_{\psi}\{b,g\}(a,x,s) = \int W_{\psi}^{*}\{h\}(a,r) W_{\psi}\{b\}.(a,r)\phi(sa,x-r)dr \qquad \text{...........(3.10)}$$

where ϕ is the averaging window. This window is centered at the specified location x and has a width factor s. As a result, the window s scales with the relative length scale of the wavelet. In order to obtain the global wavelet power spectra the precision of the local cross-spectral power is adjusted as $s \to \infty$. The wavelet cross spectral power can be used to derive both wavelet admittance and wavelet coherence of the topography and gravity anomaly. The wavelet admittance function between bathymetry and Bouguer gravity signals b and g respectively in spatial domain is defined as

$$Q_W(b,g) = \frac{P_W(b,g)}{P_W(b,b)} \qquad \text{.............(3.11)}$$

where P_w represents the local wavelet power spectra. In the spectral domain, the above equation is defined as

$$Q(k) = \frac{\langle BG^* \rangle_k}{\langle HH^* \rangle_k} \qquad \text{...........(3.12)}$$

with annular averaging $\langle \ \rangle_k$ at radial wavenumber k. Writing the above equation in terms of bottom B and top T loading gives

$$Q_k = \frac{B_T G_T + B_B G_B}{|B_T|^2 + |G_B|^2} \qquad \text{...........(3.13)}$$

only if initial surface and subsurface loads are uncorrelated (Forsyth, 1985) and an inverse admittance can also be defined

$$Q'(k) = \frac{\langle GB^* \rangle_k}{\langle GG^* \rangle_k} \qquad \text{..........(3.14)}$$

When this inverse is combined with standard admittance function, a wavelet coherence function may be defined. This function is called pseudo-coherence (Stark, 2003) and in the spectral domain is written as

$$\gamma^2(k) = Q(k)Q'(k) = \frac{\langle BG^* \rangle_k^2}{\langle BB^* \rangle_k \langle GG^* \rangle_k} \qquad \text{............(3.15)}$$

3.2.2 Method adopted in the present study

In order to study the spatial variations in the effective elastic thickness Te along the southwest continental margin of India and adjoining oceanic areas, coherence analysis has been undertaken in the present study. For this purpose, the Maximum Entropy Spectral Estimation (MESE) method has been used. As the region contains smaller scale morphological or structural features, it is expected that the MESE method would give rise to better coherence estimates.

3.2.3 Estimation of theoretical coherence

In the coherence analysis of isostatic response introduced by Forsyth (1985), the observed admittance and an assumed flexural rigidity were used to solve for the load structure in the Earth. Prior to the flexural compensation, the Fourier amplitudes of topography B and Bouguer gravity G are considered to algebraically solve for the amplitudes of topography B_I and a subsurface load horizon W_I (Fig. 3.1). After determining the initial loads, the amplitudes of topography and gravity load is deconvolved into their respective components B_T and G_T due to surface loads and B_B and G_B due to internal loading or subsurface loading of the elastic plate (Fig 3.1c). The coherence of the deconvolved signals has some random difference in phase and is estimated by assuming the surface and subsurface load which are statistically uncorrelated. Hence, the predictive coherence is calculated using the formula given below:

$$\gamma_{bg}^{-2} = \frac{\left|\left\langle P_{bg}^{tt}(k) + P_{bg}^{bb}(k)\right\rangle\right|^2}{\left\langle P_{bb}^{tt}(k) + P_{bb}^{bb}(k)\right\rangle\left\langle P_{gg}^{tt}(k) + P_{gg}^{bb}(k)\right\rangle} \quad \text{..................(3.16)}$$

where, superscripts t and b denote top and interior loading respectively. In order to determine the best fitting model for the load response of the layer, a Te value is assumed for calculating the predictive coherence function and comparing with the observed coherence.

3.3 PROCESS ORIENTED APPROACH TO GRAVITY MODELING

Sleep (1971) demonstrated that the subsidence in rift type basins is exponential in form and enable us to track the cumulative sediment accumulation in the basin through geologic time. Watts and Ryan (1976) developed a method to correct the stratigraphic record for disturbing effects of water and sediment loading, and to isolate the form of the unknown tectonic driving forces that were responsible for rift basin subsidence. These workers referred the term 'backstripping', a technique to remove loads from the basement by restoring the sediment thickness at the time of deposition taking into account compaction and water depth changes and isostatically unload it. This technique has been proved very useful to analyse the stratigraphic data in the form of lithology, seismic reflection profile or seismo-geological cross section. The main objective in subsidence analysis is to separate various components causing subsidence, so as to examine the roles played by each of these forces. The backstripping method can be used to calculate and remove the effects of compaction, sediment loading, Paleobathymetry and eustatic sea level changes. Hence, the tectonic related subsidence at the margin, such as cooling of lithosphere and compressive stresses can be estimated. There are two main types of backstripping that differ in the way that sediment load is treated; 1-D backstripping and 2-D backstripping. Brief descriptions of these two approaches are given below:

3.3.1 1-D backstripping

The backstripping applied to a well is usually termed as l-D backstripping (Airy backstripping). In 1-D backstripping, the concept of Airy local loading isostasy is applied assuming continuity of sedimentary sequences for a long distance, though it is not the case. In this method, each layer is removed one by one; while the remaining layers are decompacted to the datum, obtained from the paleo bathymetry and the eustatic sea level changes .The process involved in Airy backstripping is shown in Figure 3.3 and consists of following steps.

- A sediment loaded basement subsidence curve is constructed from the initial stratigraphic data by removing each layer in the sequence.
- The remaining underlying sediment units are then decompacted
- As each layer is removed, the new sediment surface is set to the prescribed datum but assuming a depth of deposition for each stratigraphic interval and if derived, correcting sea level for long term eustatic changes
- The sediment loaded subsidence curve is corrected to an equivalent water loaded subsidence curve. The loading correction from sediment to water is performed assuming Airy isostasy.

The various steps in the Airy 1D backstripping are listed below:

- Sediment decompaction.
- Corrections for Paleo bathymetric effects
- Correction for eustatic sea level changes.
- Sediment load correction

3.3.1.1 Sediment decompaction

The present day stratigraphic thickness is the product of cumulative compaction through time. The first step in backstripping is to reconstruct the original sediment thickness of the stratigraphic sequence obtained from the well data (Figure 3.3). By knowing the variations in porosity with depth of a particular stratigraphic unit, we can estimate the decompaction. According to Steckler and Watts (1978), the pressured sediments exhibit an exponential relationship as follows

$$\phi = \phi_0 e^{-cy} \qquad \text{................(3.17)}$$

ϕ = porosity at any depth , y
ϕ_0 = surface porosity
c = compaction parameter

In over pressured units there will be strong deviation from the porosity - depth curve and as the amount of compaction increases there will be an increase in effective stress also. In order to calculate the thickness of the sedimentary layer formed in the past, we have to move the layer along the appropriate porosity-depth curve. This is equivalent to sequentially removing the overlying sediment layers and allowing the layer of interest to decompact. The new thickness of the underlying layer after decompaction can be found out using the relation

$$y'_2 - y'_1 = y_2 - y_1 - \frac{\phi_0}{c}\left[e^{-cy_1} - e^{-cy_2} + e^{(-cy'_1 - cy'_2)}\right] \qquad \text{............(3.18)}$$

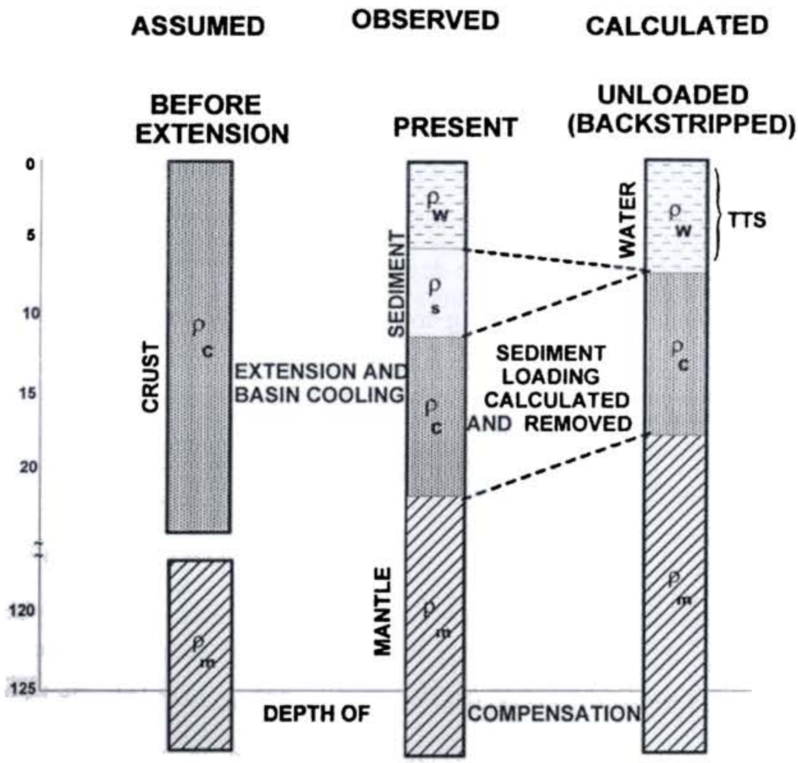

Fig 3.3: Process involved in 1-D backstripping (Sawyer, 1985). Three stages of backstripping analysis is shown in the figure. The first column shows the initial assumed lithospheric configuration. The second column shows the present day lithospheric configuration and the third column shows the backstripped crustal/lithospheric configuration.

3.3.1.2 Correction for paleobathymetry

For estimating the difference in height between the depositional and the regional data, paleobathymetric correction is done. Obtaining paleobathymetry is possible through certain "depth indicators" such as benthic micro fossil, sedimentary facies, sedimentary facies and distinctive geochemical signatures. However, the water depths are still difficult to resolve, especially in lower slope and rise environments and in Mesozoic and older sediments.

3.3.1.3 Correction for effects of eustatic sea level changes

The variations that occur in the sea level that occur through time are contributing first, to the reference surface for paleo bathymetry, second, its loading effect (Figure 3.4). For tectonic subsidence calculation, the changes in sea level with respect to present day are required, in order to provide a reference surface. But it should be kept in mind that the calculation of sea level also has some uncertainties.

3.3.1.4 Sediment load corrections

The true tectonic subsidence is obtained after the removal of subsidence due to sediment load and after corrections fro variation in water depth and eustatic sea level fluctuations. In 1-D backstripping, the loading effect of sediment is treated using (Airy) local isostatic phenomena, where sediment is replacing a column of water. The response to the load is just below it. The sediment load correction (Steckler and Watts,1978), y is given as

$$y = S\frac{\rho_m - \rho_s}{\rho_m - \rho_w} \qquad \text{..........(3.19)}$$

By considering all the above factors the 1-D (Airy) backstripping equation is as follows

$$Y = W_d + S^* \left[\frac{\left(\rho_m - \bar{\rho}_s\right)}{\left(\rho_m - \rho_w\right)} \right] - \Delta SL \frac{\rho_m}{\left(\rho_m - \rho_w\right)} \qquad \text{...........(3.20)}$$

$\because$ W_d = the water depth

S^* = de-compacted sediment thickness

Y = tectonic subsidence

ρ_m, ρ_s, ρ_w = densities of mantle, sediment and water respectively.

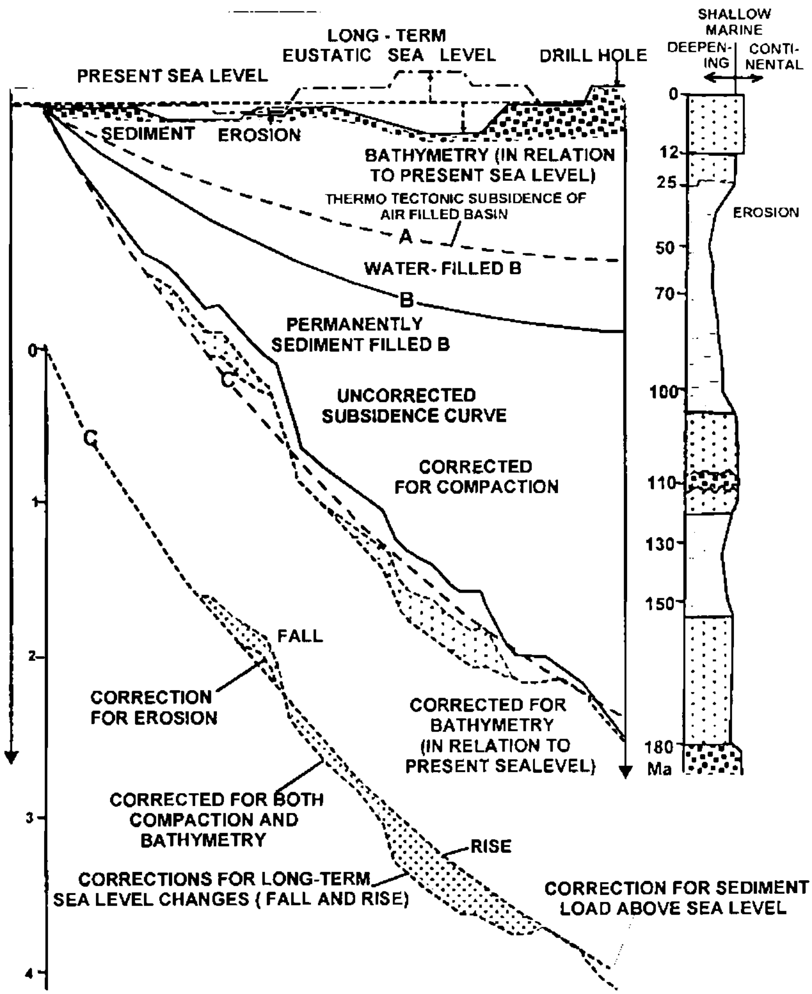

Fig 3.4: Various factors involved in 1-D backstripping and their contribution to the subsidence at the location (Einsele,1992).

The backstripping technique described above can be is applied to commercial borehole litholog data. Though this method provides valuable information on sediment loading characteristics, subsidence history and lithospheric stretching factor (β) at that particular location of the margin, no information can be obtained on the tectonic subsidence or uplift on either side of a well. For this purpose, the 2-D backstripping (flexural backstripping) method is applied along seismo-geologic or lithostratigraphic sections obtained from seismic reflection profiles.

3.3.2 2-D flexural backstripping

In this method, the flexural isostasy is used with a certain flexural rigidity for the lithosphere, instead of local isostasy. It differs from the Airy isostasy in that the response of a given sediment load not only affects the point below but also its nearby points. The lithostratigraphic data is obtained by tying well data with the seismic section. Since the load is not a simple analytic function of time and space, it is approximated as a set of prismatic loads for each time interval. The loading effect of each prism is calculated by equations for the response of loading of a thin plate on elastic foundation. The loading effect, w(x, t), for a prism of width 2a, thickness h, at a distance x from the well, with age t, and effective elastic thickness (Te) (Sawyer et al., 1982) is

If $|x| < a$

$$W(x,t) = \frac{h}{2}\frac{\rho_s - \rho_w}{\rho_m - \rho_s}\left[2 - e^{\frac{-x-a}{D}}\cos\left(\frac{x-a}{D}\right) - e^{\frac{-x+a}{D}}\cos\left(\frac{x+a}{D}\right)\right] \qquad \text{..........(3.21)}$$

if $|x| > a$

$$w(x,t) = \frac{h}{2}\frac{\rho_s - \rho_w}{\rho_m - \rho_s}\left[2 - e^{\frac{-x-a}{D}}\cos\left(\frac{x-a}{D}\right) - e^{\frac{-x+a}{D}}\cos\left(\frac{x+a}{D}\right)\right] \qquad \text{........(3.}$$

where

$$D^4(t) = \frac{ETe^3(t)}{3(1-\sigma^2)(\rho_m - \rho_w)g} \qquad \text{........(}$$

Young's modulus $E = 6.5 \times 10^{11}$ dyne/cm^2
Poisson's ratio $\sigma = 0.25$
$g = 980.621$ cm/sec^2

The total unloading correction. U_f is obtained by summing the contribution of each prism

$$U_f(t) \approx \underbrace{\Sigma_{n=0}^{t}}_{time}\ \underbrace{\Sigma_{m=1}^{n}}_{sediment\ prisms}\ w(x(m), n) \qquad \text{........(3.2}$$

This loading correction is made on the basement along with the usual corrections such as corrections for paleobathymetric effects, correction for the eustatic sea level changes, sediment load. Apart from the limitations in sediment decompaction parameters, the main error comes from the variations in flexural rigidity through space and time. For simplicity, we assumed a uniform flexural rigidity for the lithosphere and an airy type of compensation during rifting. In practice, flexural backstripping is carried out layer by layer with the option of assigning each layer a different density and Te.

Due to strength of the lithosphere, a region around the load will also deform by flexural downwarping. Hence, subsidence beneath the load will decrease. Flexural backstripping requires knowledge about both loading history of the margin and flexural rigidity as a function of time. If stratigraphy of the medium is known, then the loading history can be estimated once the flexural rigidity is determined iteratively. The main problem is to estimate the flexural rigidity as a function of time. After water loaded subsidence curve is obtained, it can be modeled with various rifting models such as Airy isostatic model, necking model and underplating model. According to Airy model, the backstripped basement is compensated locally by changes in the thickness of the crust. This is a good approximation to McKenzie's uniform stretching model and do not take into account the finite strength of lithosphere.

Braun and Beaumont (1989) pointed out that the strong zones in the lithosphere might significantly modify the crustal structure of the extended lithosphere. In the lithosphere that makes up the crust and the upper part of the mantle, the strength initially increases and then decreases with depth. There will therefore be strength *maxima* in the lithosphere. The depth of the strength maxima, which is called Z_{neck} acts as a resistant zone that vertically partitions the strain into shallower and deeper levels within the crust and mantle. Depth of basin depression,S_t, depends on depth of Necking (Z_{neck}) and represented by the equation

$$S_t = \left(1 - \frac{1}{\beta_s}\right) Z_{neck} \qquad \text{.....................(3.25)}$$

This relationship suggests that for a particular streaching factor, β_S, the depth of basin increases with level of necking. For shallow level of necking, there is only a shallow basin and deep level of necking there is a deep basin (Figure 3.5). If the lithosphere has no strength then the forces will return the depression to the state of

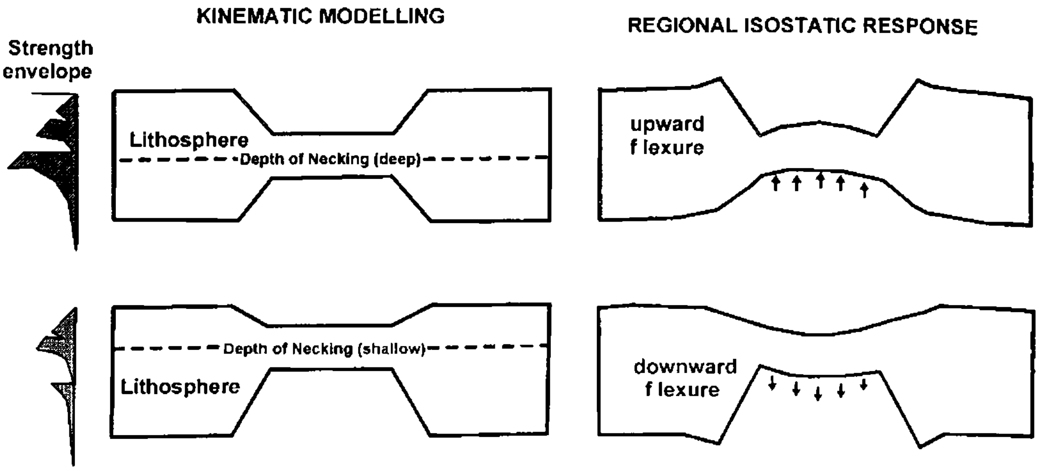

Fig 3.5: Model showing Lithosphere necking (after Braun and Beaumont, 1989)

Airy type isostatic equilibrium. With strength during rifting, the basin shape will be modified by flexure as it returns to state of equilibrium. The initial basin depression depends critically on Zneck. For shallow Zneck, the basin is small in comparison to the magnitude of Moho up warp and downward state of flexure results. For deep depths, an upward state of flexure prevails, predicting an upwarp in the basin center and uplift at the basin flanks. If the upward and downward forces exactly balance, the final basin shape is same as that predicted by an Airy model. Hence, by modeling with different level of necking depths and different Te values, various crustal models can be generated. The gravity anomaly for each crustal model is calculated and compared with the observed gravity anomaly. The best fitting model is calculated and compared with the observed gravity anomaly. The best fitting model gives the depth of necking and Te at the margin.

Magmatic underplating implies a re-distribution of mass that should be associated with gravity anomalies and it disturbs the state of isostasy of the region (Figure 3.6). Hence, one can estimate the amount of uplift occurred by balancing the column of crust that has been underplated. Underplating the continental slope with

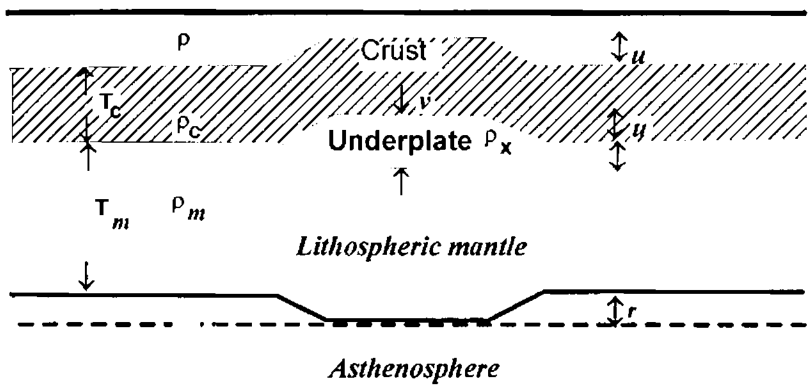

Fig 3.6: Simple model of magmatic underplating of crust of uniform thickness (after Watts, 2001)

no flexural strength widens the edge effect low. If the crust has flexural strength, then the low narrows and increases in amplitude. Hence with different amount of underplating and different effective elastic thickness values, we obtain gravity anomalies which can be matched with the observed anomaly. The best fitting model gives the extent of underplated crust required to explain the flank uplift topography at the margin.

The gravity anomaly at the margin is integrated effect of crustal structure and later processes such as sedimentation, magmatic underplating, lithospheric necking and erosion that may have modified the crust since rifting. This approach termed as "process oriented approach to gravity modeling" has been used by Watts (1988) to model spatial variations in lithospheric strength across the margin. According to this method, the margin is first restored to the initial rifting through backstripping and from the initial crustal structure, the rifting anomaly is computed. The gravity anomaly due to sediment load and its compensation are computed that give rise to sedimentation anomaly. The gravity anomaly due to erosion that took place later to rifting in the flank region is computed and called as erosion anomaly. The observed anomaly at the margin is the sum effect of all these anomalies. During this process, other aspects like lithospheric necking during rifting or magmatic underplating can also be tested.

****

CHAPTER 4 COHERENCE ANALYSIS

4.1 INTRODUCTION

The WCMI, which is a passive continental margin evolved as a consequence of rifting and seafloor spreading between India and eastern continental margin of Madagascar during Cretaceous (Besse and Courtillot, 1988). By the end of Cretaceous several surface/subsurface structural features such as Chagos Laccadive Ridge, Laxmi Ridge, Pratap Ridge and belt of numerous rift related horst- graben structures in the sediment filled basins which are believed to have been controlled by the Precambrian structural grain of the Indian shield were formed at the margin (Biswas, 1987; Kolla and Coumes, 1990; Subrahmanyam et al., 1995). Three major crustal provinces such as the Deccan Volcanic Province (DVP), Archean Dharwar Craton Province (DCP) and Archean/Proterozoic high grade Southern Granulite Terrain (SGT) characterise the western Indian shield margin (Figure 4.1). The Western Ghats with its remarkable west facing scrap can be seen following all along the west coast regardless of the structure and lithology. The morphological evolution of the Western Ghats is related to the rifting and sedimentation history of the WCMI. The massive influence of the Re Union plume in the northern part of WCMI consisting of the DVP as well as variations in the nature of shield crust along the west coast might have influenced the rifting style and lithospheric structure from north to south along the WCMI (Radhakrishna et al., 2002). In the southwestern part, Kolla and Coumes (1990) inferred extension of onshore structural trends into the offshore areas as far as the CLR by which they proposed extension of continental crust up to at least east of CLR. In the southern most part, the Comorin Ridge aligned along the margin, is another topographic feature believed to be related to the earliest phase of margin evolution. The detailed integrated geological and geophysical study of the margin should be made in order to understand the regional geodynamic processes and lithospheric strength. Reliable estimation of effective elastic

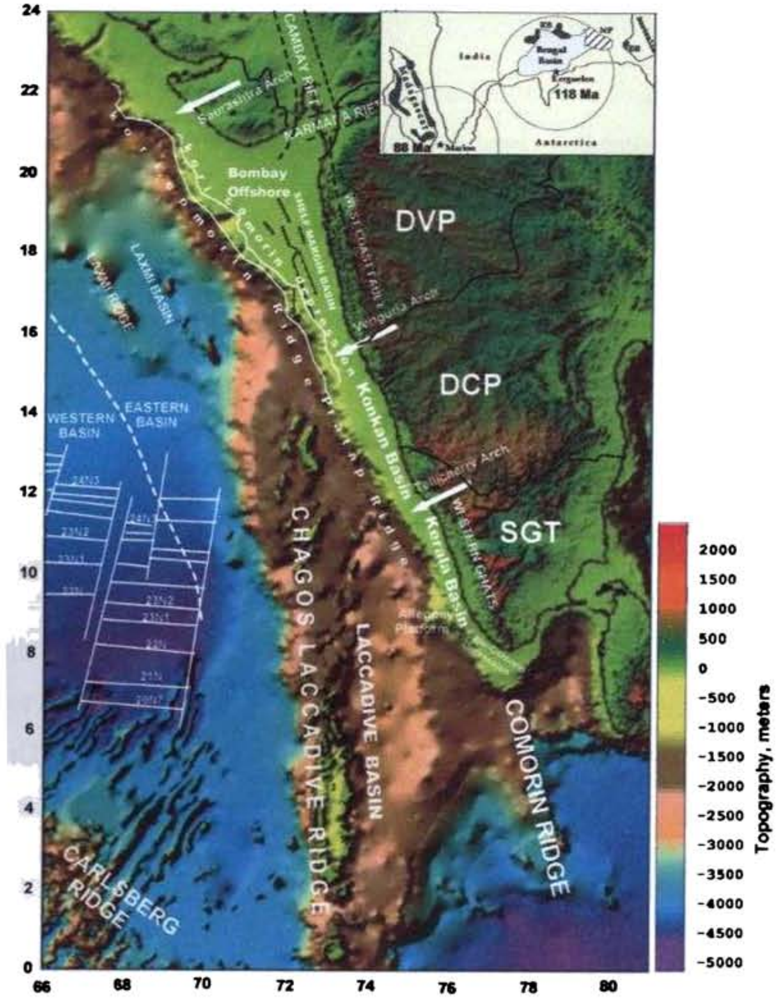

Fig 4.1: Map showing the tectonic and morphological features along the Western Continental Margin of India (WCMI) and the adjoining Arabian Sea. The structural details of the Indian shield are adopted from Biswas (1982, 1987) and magnetic anomaly identifications from Chaubey et al. (1993) and Miles et al. (1998). Inset shows the reconstruction of India, east Antarctica and Madagascar in the Gondwana period (Kent, 1991), the location of the Kergulean plume (~118Ma) and the position of Marion plume (~ 88Ma) adopted from Storey (1995).

thickness (Te) of the lithosphere and its lateral variations along the continental margin would be helpful in understanding the regional tectonic processes and the flexure that controls basin evolution at the margin. Knowledge of lithosphere strength will also help in modeling the flank uplift topography observed along the margin. Estimation of lithospheric strength along passive margins elsewhere have been made by earlier workers through coherence analysis using different approaches such as periodogram, multitaper, maximum entropy and wavelet methods (Lowry and Smith, 1994; McKenzie and Fairhead, 1997; Simons et al., 2000; Daly et al., 2004; among others). In this chapter, the results obtained on lithospheric strength based on Coherence analysis for different regions of the WCMI and the adjoining eastern Arabian Sea are presented. For this purpose, the Maximum Entropy Spectral Estimation method (MESE) (Lowry and Smith, 1994) is used for Coherence analysis between Bouguer gravity and bathymetry. This method reduces the effect of data windowing via a reasonable extrapolation of information. Using a two dimensional spectral estimator based on maximum entropy method, the spatial resolution of flexural properties can be enhanced by a factor of 4 or more, enabling more detailed analysis of individual tectonic features with very short number of data sets, that is, even data windows over small-scale features can be analysed due to high spectral resolution.

4.2 DATA

The basic geophysical data required for such a study is the gravity and topographic data in the margin. As the available ship-borne bathymetry data is sparse in the region, the 1- minute grid digital GEBCO bathymetry in the offshore areas has been used throughout the study. The measurements of gravity include three methods – ship-borne measurements, satellite measurements and satellite borne altimeter measurement. Of these three, the most accurate one is ship-borne gravity measurement, but it is slow and coverage is not always uniform. The satellite measurements are made by measuring the gravity field using the satellites CHAMP and GRACE, but they give accurate measurements of long wavelength field at the satellite altitude (~800 km) and unable to recover wavelengths shorter than about 160 km (Tapley and Kim, 2001). The satellite borne altimeter measurements monitor sea surface height variations using radar. The gravity response at the sea level instead of satellite altitude can be made, thus the resolution can be directly compared to ship-borne gravity. Though vast amount of ship-borne gravity data have been acquired by several national and international agencies along the WCMI and the adjoining oceanic areas, still large data gaps exists and the coverage was not uniform. The satellite derived GEOSAT free air gravity data of Sandwell and Smith (1997) gives a uniform coverage of 2-minute interval in the offshore areas. A comparison of the satellite derived GEOSAT gravity and GEBCO bathymetry with the shipboard gravity and bathymetry reveal that both data sets match well along the Indian offshore regions as demonstrated by Chand and Subrahmanyam (2003) and Subrahmanyam et al (2005). However, minor discrepancies between the two data sets at shorter wavelengths (< 25 km) will not affect the analysis carried out here. These two data sets were essentially used to carry out coherence analysis of gravity and topography at the southwest margin of India.

4.3 GRAVITY ANOMALY MAP OF THE WCMI

Interpretation of free air gravity map in the offshore areas help to understand the crustal mass anomalies and dynamic processes related to the formation of sedimentary basins and tectonics operative during the evolution of continental margins. The gravity field of the WCMI and the adjoining areas have been studied in the past by various investigators (Naini and Talwani, 1982; Subba Raju et al., 1990; Miles and Roest, 1993; Subrahmanyam et al., 1995; Pandey et al., 1995, 1996; Malod et al., 1997; Miles et al. 1998; Talwani and Reif, 1998; Todal and Eldholm, 1998; Singh, 1999; Radhakrishna et al., 2002; Mishra et al., 2004). In the present study, the satellite derived GEOSAT free-air gravity data has been used to prepare the gravity anomaly map of the WCMI and the adjoining oceanic areas (Figure 4.2). Some of the salient observations made from this map are given below:

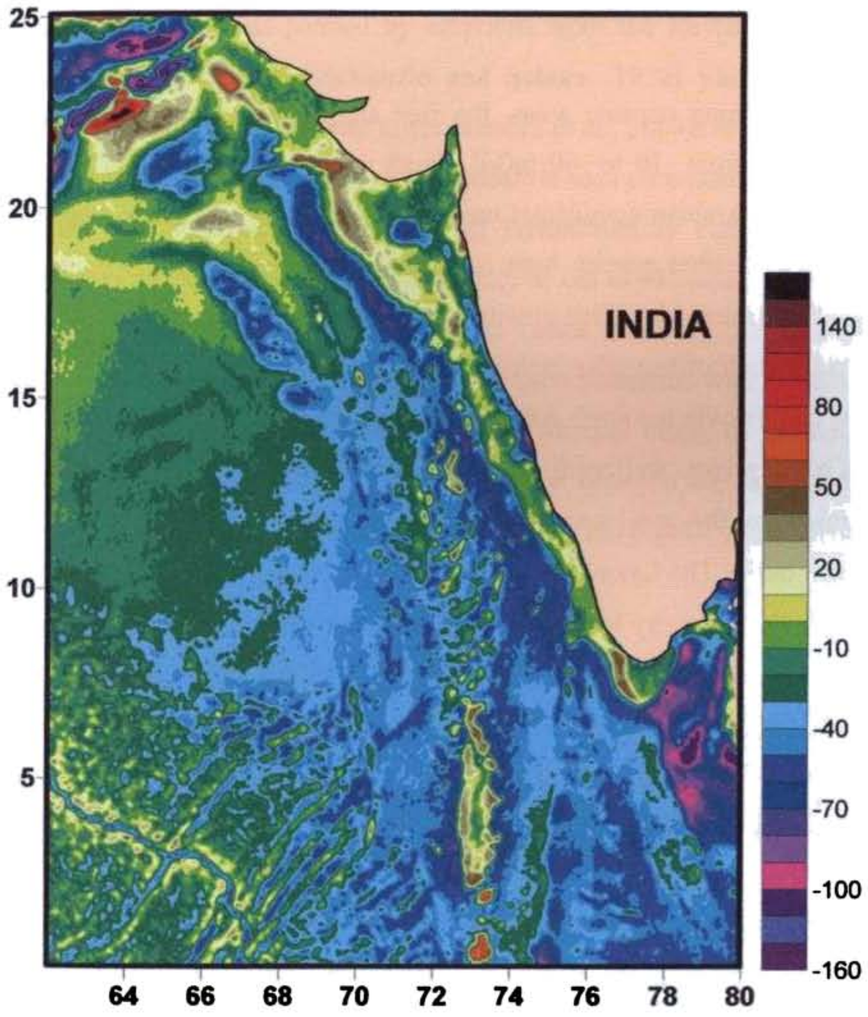

Fig 4.2: Satellite derived (GEOSAT) free air gravity anomaly map of the WCMI and adjoining oceanic areas

The WCMI in general shows a bipolar edge effect anomaly, that is gravity high of +10 to +60 mGal in the inner shelf region and a low of as much as -80 mGal in the slope. However, between 12° - 16°N, this anomaly pattern seems to have disturbed due to basement highs and isolated bathymetric features as also observed by Subba Raju et al. (1990) based on ship-borne measurements.

In the adjoining oceanic areas, the free air gravity anomalies are generally negative and range from -10 to -60 mGal. South of the bipolar edge effect anomaly observed along the Arabian continental margin lies a gravity high over Murray ridge. Further southeast, another gravity high runs sub-parallel to the Murray ridge and is related to the Saurashtra ridge. This gravity high starts from the Owen fracture zone and extends up to the shelf offshore Saurashtra. Between the Murray and Saurashtra ridges, a gravity low occurs over the north Arabian basin. A characteristic gravity low of more than –60 mGal correlates well with the Laxmi ridge which trends in NW-SE. To the east of Laxmi ridge, the gravity anomalies increase in amplitude from south to north over the Laxmi basin. The Laxmi Basin as a whole is characterised by a broad gravity high with a prominent gravity low within it. The gravity highs seen in the Laxmi basin correlate with Panikkar ridge which is a continuous structure running for about 600 km (Krishna et al., 2006) in the middle of the basin and parallels the Laxmi Ridge in the west. To the west of the Laxmi Ridge, free-air gravity anomaly swiftly rises and continues seaward without prominent anomalies.

In the southwestern part, the Arabian basin is characterised by subdued and broadly varying gravity field of –20 to –40 mGal. The presence of several gravity lows and highs mark criss-cross fractures and transform faults related to the flank part of Carlsberg ridge.. The median rift valley of the Carlsberg ridge is clearly seen on the gravity field as a gravity low of about -40 to -70 mGal surrounded by gravity highs of around +10 to +50 mGal.. The low and subdued gravity field of the Arabian Sea sharply rises towards east to as much as +70 mGal over the CLR. The N-S trend of the gravity field of CLR is seen highly dissected and fragmented towards north and the trend becomes curvilinear sub-parallel to west coast of India. Along its eastern boundary, a prominent gravity low correlates with the Chagos fracture zone. The CLR consists of volcanic islands formed by eruptions from the Re Union mantle plume during the Late Cretaceous (McKenzie and Sclater, 1971) yielding high density volcanic rocks giving rise to gravity highs (Mishra et al., 2004). At the southern tip of India, a prominent gravity high (+10 to +50 mGal) is seen correlated with a terrace like feature in the shelf referred as the Terrace off Trivandrum by Yatheesh et al. (2006). The Alleppey Platform exhibits a gravity anomaly of -20 to +10 mGal. Further south of peninsular India and the region southwest of Sri Lanka, a relative gravity high ranging in values between -10 mGal to -50 mGal can be seen correlated with NE-SW trending Comorin ridge. The gravity anomalies fall more sharply along its eastern side and indicate the presence of a fracture zone. The region between the ridge and the west coast of Sri Lanka, the gravity anomaly pattern shows the bipolar edge effect anomaly related to the margin.

4.4 DATA PREPARATION

Gravity and topography in any region provide important insights regarding the degree and mechanism of isostatic compensation as well as mechanical properties of the lithosphere. The effective elastic thickness (Te) is a parameter that characterises the integrated mechanical strength of the lithosphere (Watts and Burov, 2003). Te can be estimated through the statistical relationship between gravity and topography (McKenzie and Bowin, 1976). The free air anomaly is in general smaller and approaches to zero at longer wavelengths. On the other hand, the Bouguer anomaly strongly correlates with the topography at longer wavelengths. In general, the correlation of the Bouguer anomaly to topography is wavelength dependent. This wavelength dependency is useful in evaluating the isostatic compensation over topographic features. In addition, the wavelength range at which the transition from compensated to uncompensated topography occurs is diagnostic of the lithospheric rigidity. As the simple Bouguer anomaly contains errors due to strong lateral topographic variations, terrain correction was applied to the data to obtain Complete Bouguer anomaly. The terrain correction was calculated using the algorithm of Ballina (1990) as described below.

4.4.1 Complete Bouguer anomaly through terrain correction

Calculation of the terrain correction is tedious and potentially important task and has to be done efficiently as well as accurately by using different approximations of topography depending on the distance from the gravity station. The method of computation is based on the model (Figure 4.3) proposed by Kane (1962). The model

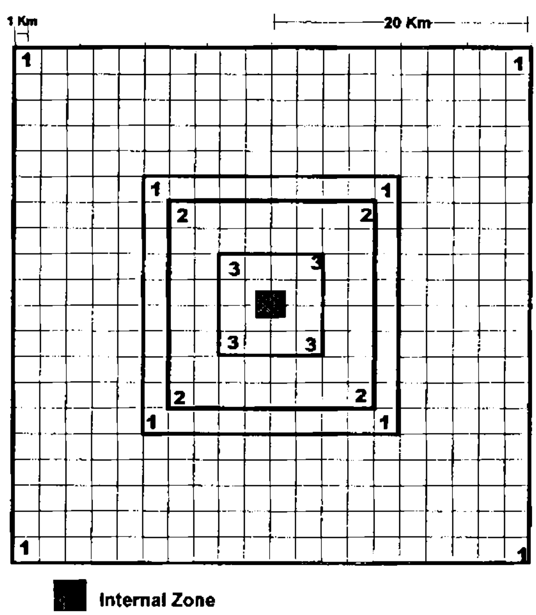

Fig 4.3: Model used in the computation of terrain correction (after Ballina, 1990)

selects a 40 × 40 km grid with the gravity station in the center and it is divided into two computational areas: an external and inner zone. The computation in the external zone is based on the gravitational attraction of prisms, which can be approximated to that of an annular ring with the same height (the difference in the attraction of two vertical cylinders with same height but different radii) times the ratio of the horizontal section of the prism to that of the horizontal section of the ring 1 (Figure 4.4).

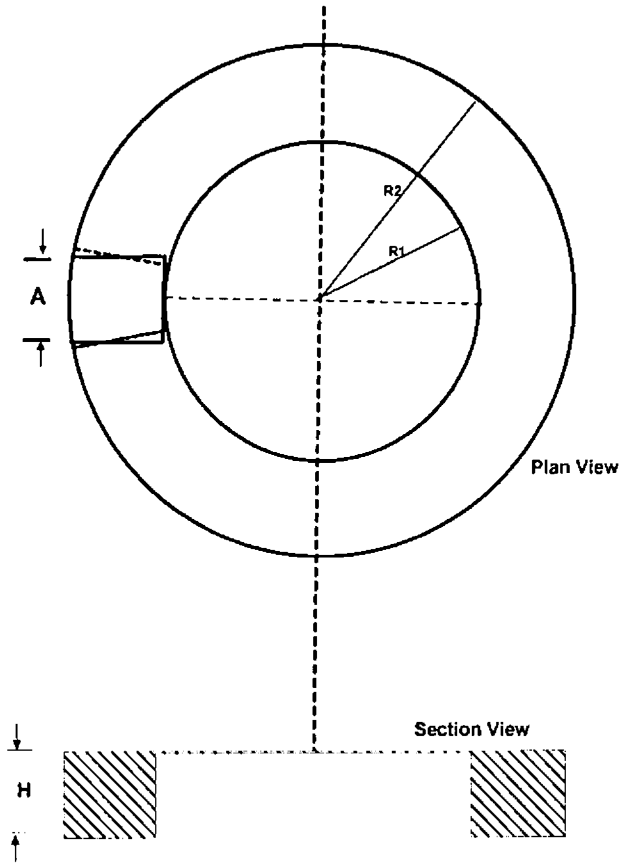

Fig 4.4: Relationship of square to segment of ring both having equal area

The formula (after Ballina, 1990) is

$$g = 2GDA^2 \times \frac{\left[R2 - R1 + \sqrt{R1^2 + H^2} - \sqrt{R2^2 + H^2}\right]}{R2^2 - R1^2} \quad \text{............(4.1)}$$

Where g = gravity attraction

G = gravitational constant

D = density

A = length of the horizontal side of the prism

R1 = inner circular radius of the annular ring

R2 = outer circle radius of the annular ring

H = height of the annular ring of the prism.

RI and R2 may be replaced by (R - C) and (R + C) respectively, where R is the distance from the gravity station to the center of the ring section and C is a constant.

C = 0.63 A

R1 = R - 0.63 A

R2 = R + 0.63 A

Therefore

$$g = GDA\left[1.26A + \sqrt{(R - 0.63A)^2 + H^2} - \sqrt{(R + 0.63A)^2 + H^2}\right] \Big/ 1.26R \quad \text{............(4.2)}$$

The method of computation for the inner zone is concerned with gravitation attraction of a 2 × 2 km area around the gravity station. This area is divided into octants

(Figure 4.5). Each one is assumed to slope continuously from the apex to the outer edge. The octant gravity attraction can be approximated by that of a cylinder with a removed inverted cone (Figure 4.6).represented by the equation given below

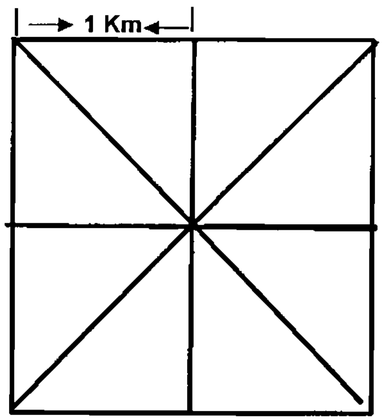

Fig 4.5: Inner zone

The formula is:

$$g = \frac{\Pi G D}{4}\left[R - \sqrt{R^2 + H^2} + H \sin\beta\right] \qquad \text{.............(4.3)}$$

Where
- g = gravity attraction
- G = gravitational constant
- R = cylinder radius
- D = density
- H = cylinder height
- β = angle between the octant surface and a horizontal surface

The total terrain correction is obtained by adding these internal and external corrections.

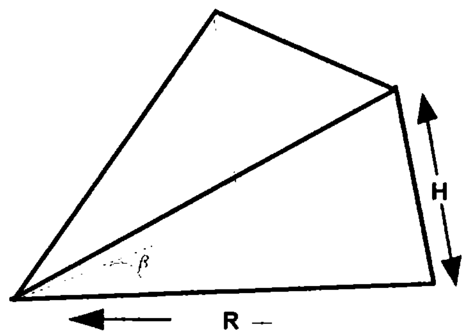

Fig 4.6: Octant

A 1 km x 1 km bathymetric grid was used for this purpose and the terrain correction was computed at every gravity data point. For land areas, the terrain correction is always positive, where as, in marine areas the correction becomes either positive or negative depending on the station elevation with respect to the surrounding topography. For example, when the station elevation is less than the average elevation in a particular zone, the terrain correction applied should be negative. The complete Bouguer anomaly was computed with a reduction density of 1640 kg.m^{-3} from the free air anomaly data and bathymetric relief. Bathymetric relief was modified in order to maintain consistency with the offshore Bouguer anomaly by converting the water load of density 2670 kg.m^{-3} and by adding this rock column to the bathymetric depth giving rise to effective bathymetry (Stark et al. 2003). Both the complete Bouguer anomaly and effective bathymetry data sets were gridded at 5 km interval. The free air anomaly and the complete Bouguer anomaly maps prepared in the study area are shown in Figure 4.7.

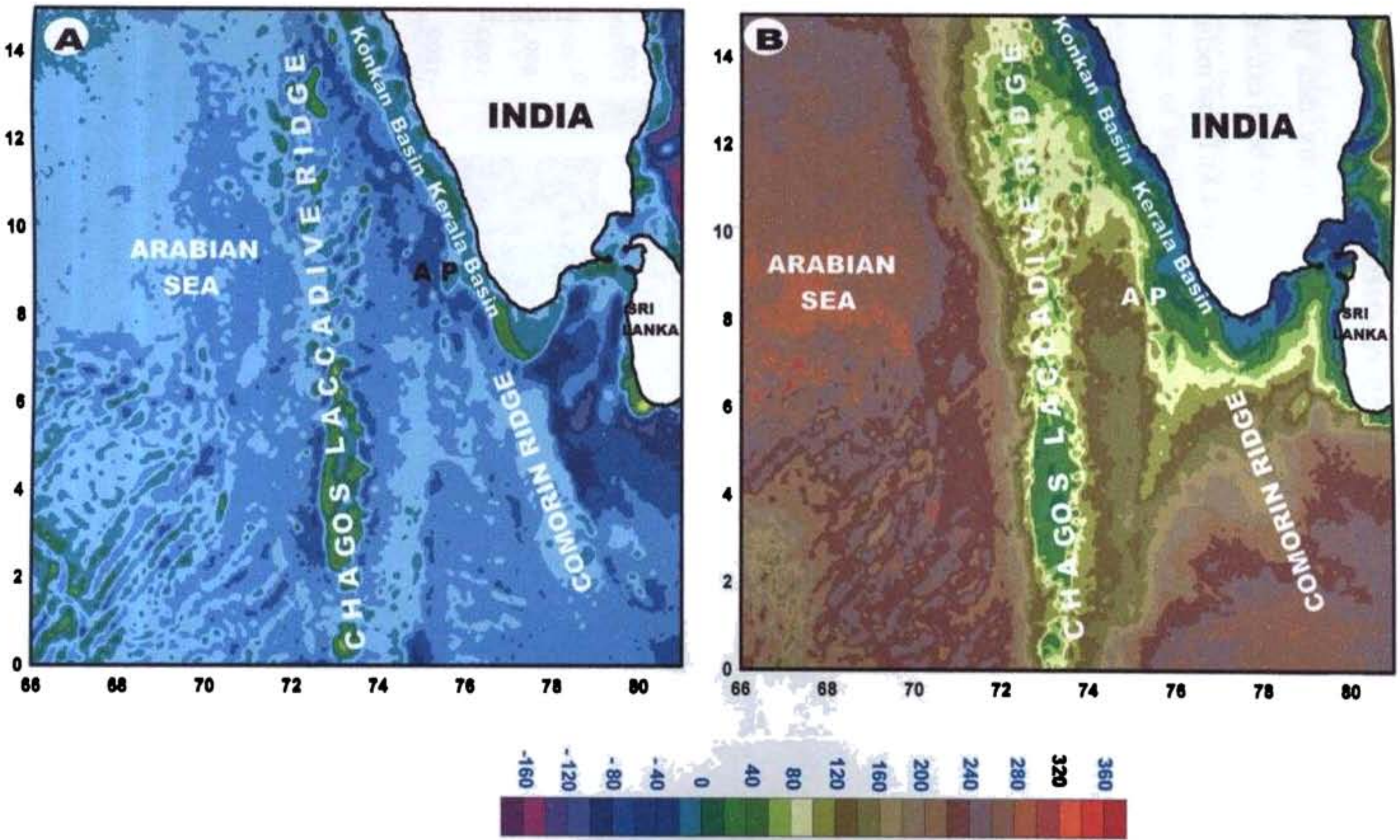

Fig 4.7: Shaded contour maps of a) free air anomaly data of the southwest continental margin of India and the adjoining offshore areas b) complete Bouguer anomaly map obtained from the 1-km gridded bathymetry data of the region. A.P - Alleppey platform. Details are discussed in the text.

4.5 MAXIMUM ENTROPY Te ESTIMATES ALONG THE MARGIN

From the complete Bouguer anomaly and effective bathymetry data grids prepared at 5 km interval in the study region, several data windows have been extracted centered on various geological features/structures of interest (Figure 4.8).These include

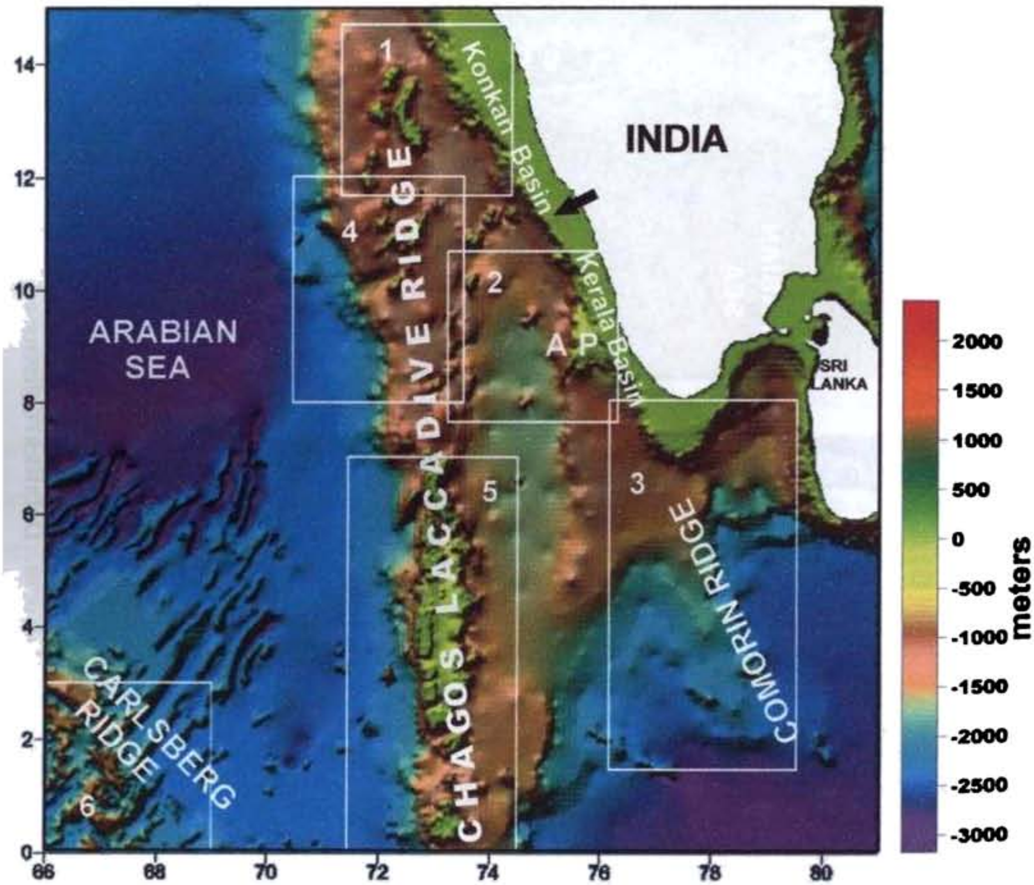

Fig 4.8: Map showing effective bathymetry of the study area. White rectangles numbered indicate data windows considered for the coherence analysis. Thick arrow represents the Tellicherry Arch that separates the Konkan and Kerala basins. A.P- Alleppey Platform.

the Konkan basin, the Kerala basin consisting of Alleppey platform, Comorin Ridge, Chagos Laccadive Ridge (CLR) and the Carlsberg ridge. It is relevant to state here that choosing optimum window size for each of these individual geological features is a key factor for determining the Te value, as larger data windows will give rise to weighted average of the Te in the region and smaller windows will not be able to resolve the coherence in diagnostic waveband (Daly et al. 2004). Advantage of the MESE method is that even data windows over small scale geological features can be analyzed due to high spectral resolution. For the present analysis, a rigorous exercise has been made in order to select optimum window size for each geological feature and finally six windows were selected that gave stable coherence values at transitional wavelength and significantly higher coherence values at longer wavelengths. The observed coherence values have been compared with the theoretical coherence curves for different Te values as a function of wavelength. The theoretical coherence curves were obtained for different Te values considering both surface and subsurface loading based on the method of Forsyth (1985). The value for subsurface to surface loading ratio f is considered as equal to 1. This means that the loading is equal at the surface as well at the subsurface (considered as Moho depth). The best fit theoretical coherence function for a given Te value that gives the least residual error was chosen based on the L1 norm of observed minus theoretical coherence. The plots of different regions showing the observed and best fit theoretical coherence curve as well as the residual error as a function of Te are shown in Figures 4.9 - 4.15. The results are presented below.

4.5.1 Konkan and Kerala Basins

Two windows of ~330 sq km, one, north of the Tellicherry Arch within the Konkan Basin, and, the other, south of Arch in the Kerala Basin covering the Alleppey Platform region have been selected and the coherence between the Bouguer anomaly and the effective bathymetry has been obtained and is shown in figures 4.9 and 4.10.

The plot of residual error as a function on Te shows a Te of 5 km for the Konkan basin (Figure 4.9) and Te of 8 km for the Kerala basin (Figure 4.10).

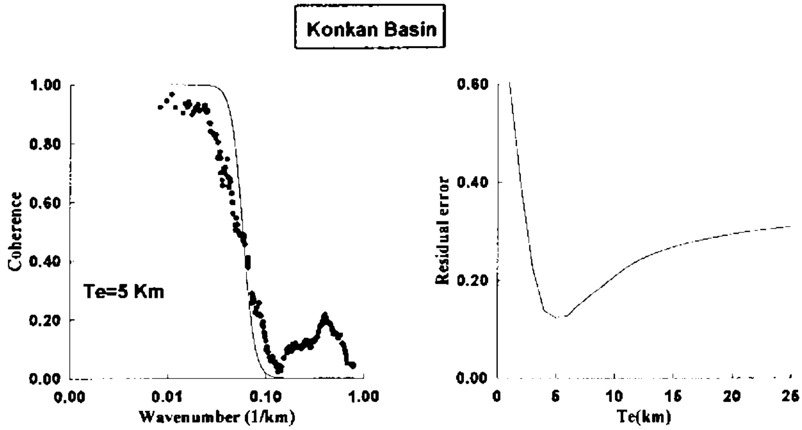

Fig 4.9: Plot showing the maximum entropy coherence as a function of wave number for the Konkan basin. The dot in each plot shows the observed coherence and continuous line represent the best fit theoretical coherence curve. The plot on the right suggest the Te value that gives the minimum residual error based on L1 norm.

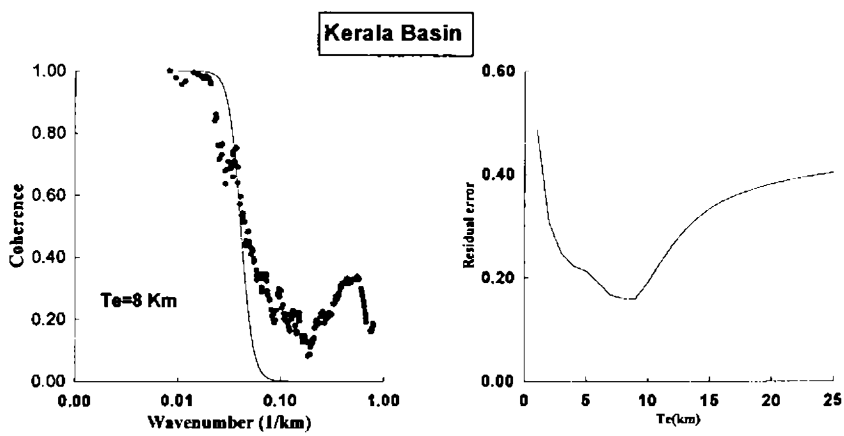

Fig 4.10: Plot showing the maximum entropy coherence as a function of wave number for the Kerala basin. Other details are as in Fig 4.9.

4.5.2 Comorin Ridge

Based on trend and dimension of the ridge, nearly 370 x 720 km window size is required to completely capture the coherence at the transitional wavelength. The coherence plot between the Bouguer anomaly and the effective bathymetry shown in Fig. 4.11 gives rise to a Te value of 10 km for the Comorin Ridge.

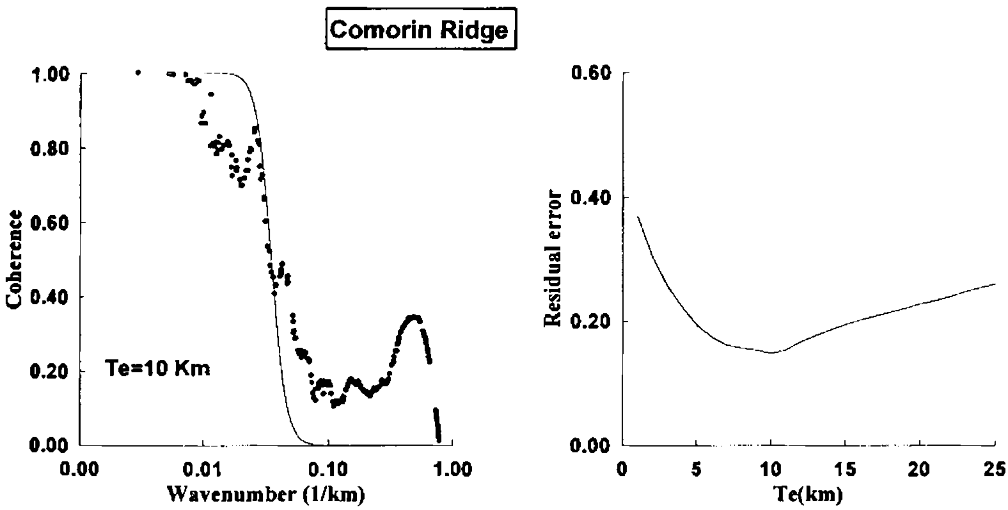

Fig 4.11: Plot showing the maximum entropy coherence as a function of wave number for the Comorin Ridge. Other details are as in Fig 4.9.

4.5.2 Chagos Laccadive Ridge

Mode of emplacement of the CLR is complex and still debated. According to Ben Avraham and Bunce (1977), the ridge is segmented and diverse in origin. They pointed out that the morphological and geophysical characteristics of the ridge between

2° S and 8°N are distinctly different from the ridge further north. North of 8°N, the ridge is wider and beyond 12°N, the ridge becomes indistinguishable from the Pratap Ridge trend and the margin related structures. In view of this, in the present study region, the CLR has been divided into two data windows, one between 0 to 7°N (330 x 770 km) and other between 8° to 12°N (330 x 440 km) and coherence estimate for these two data sets are shown in Fig. 4.12 & 4.13. The plot of residual error for different Te values indicate a Te of 5 km for the northern part (Figure 4.12) and Te of 8 km for the southern part of CLR (Figure 4.13).

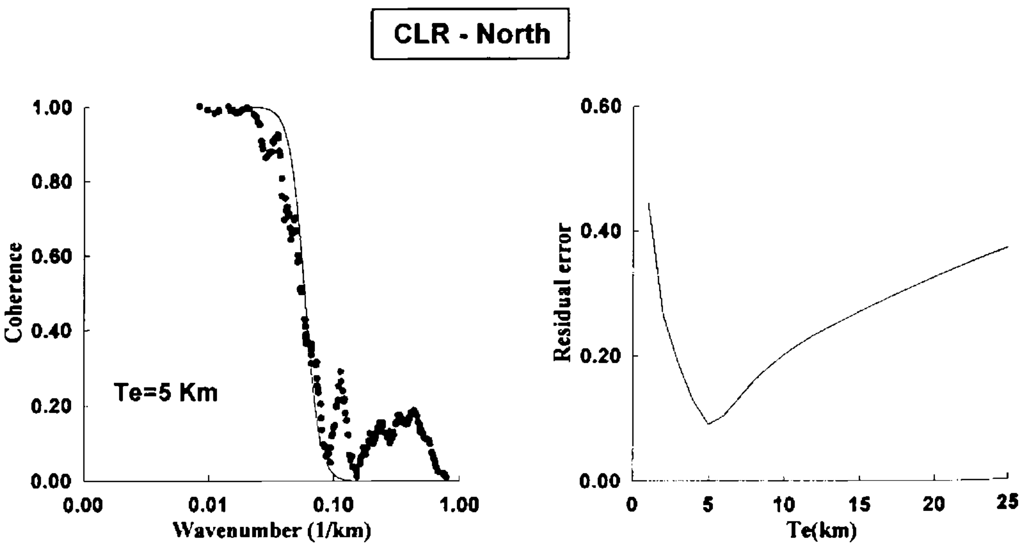

Fig 4.12: Plot showing the maximum entropy coherence as a function of wave number for the Chagos Laccadive Ridge - North. Other details are as in Fig 4.9.

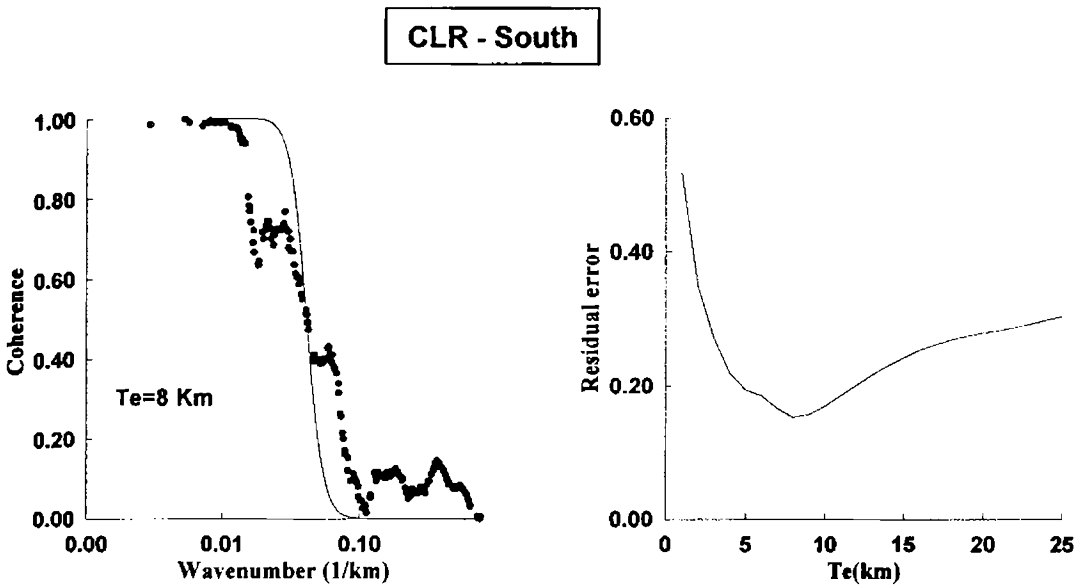

Fig 4.13: Plot showing the maximum entropy coherence as a function of wave number for the Chagos Laccadive Ridge - South. Other details are as in Fig 4.9.

4.5.4 Carlsberg Ridge

Further offshore into the deep oceanic areas, the N-S oriented Central Indian Ridge changes into the NW-SE trending Carlsberg ridge. A window of ~ 330 sq. km is selected in this region and the coherence between the Bouguer anomaly and effective bathymetry has been estimated. The residual error plot shown in the figure suggests a Te value of 7 km for the Carlsberg Ridge (Figure 4.14).

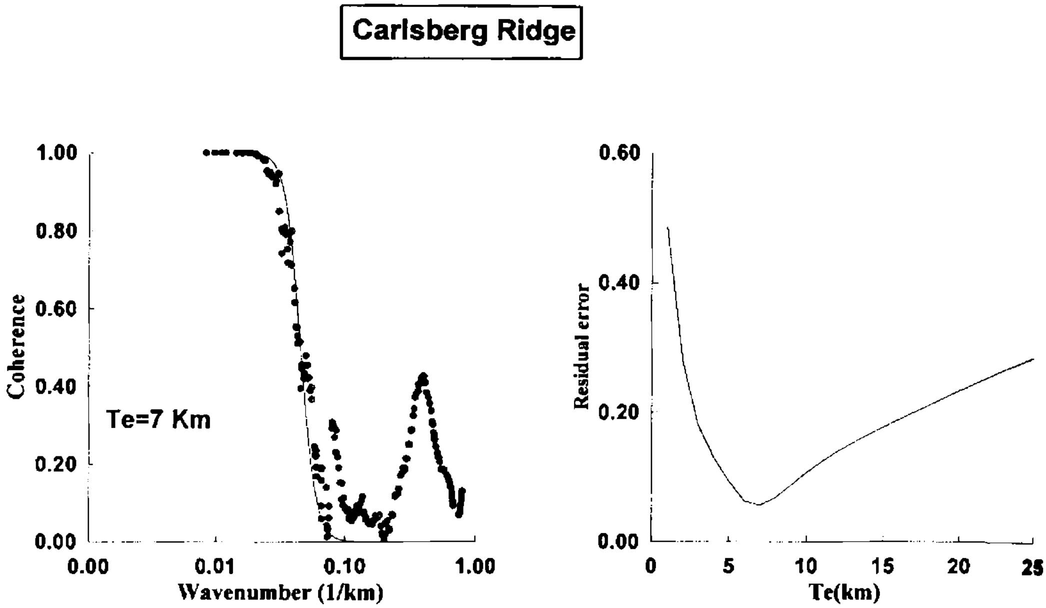

Fig 4.14: Plot showing the maximum entropy coherence as a function of wave number for the Carlsberg Ridge. Other details are as in Fig 4.9.

4.6 SUMMARY OF RESULTS

In the present study, the coherence analysis of gravity and bathymetric data has been carried out using the Maximum Entropy Spectral Estimation (MESE) method to understand the spatial variations in the effective elastic thickness (Te) at the southwest margin of India and the adjoining oceanic areas. For this purpose, the complete Bouguer anomaly and effective bathymetry data grids prepared at 5 km interval in the study region have been used to select several data windows centered on various geological features/structures of interest, which include the Konkan basin, the Kerala basin consisting of Alleppey platform, Comorin Ridge, Chagos Laccadive Ridge (CLR) and the Carlsberg ridge. The study indicates that the Te estimates vary from 5 km – 10 km in the southwest margin of India and increases from north to south. A maximum Te value of 10 km is obtained along the Comorin Ridge. The effective elastic thickness obtained for the selected windows is as follows : Konkan basin – 5 km, Kerala basin – 8 km, Comorin Ridge – 10 km, Chagos Laccadive ridge (North) – 5 km, Chagos Laccadive Ridge (South) – 8 km, Carlsberg Ridge – 7 km.

****

CHAPTER 5 PROCESS ORIENTED APPROACH TO GRAVITY MODELING

5.1 INTRODUCTION

The WCMI mainly consists of five major offshore basins – Kutch, Saurashtra, Bombay, Konkan and Kerala basins. The sedimentation everywhere in these basins is restricted to isolated pockets with thickness not exceeding 2- 3 km, with an exception of Surat depression. In the Surat depression, the thickness of sediments reaches up to 6 km (Biswas and Singh, 1988). While, sediments in the Konkan and Kerala basins have mainly been derived by denudation in the Western Ghats, the other northern basins, the Mumbai, Saurashtra and Kutch have additional sediment source from river Indus. The landward limit of WCMI, is marked by West Coast, Nagar Parkar and East Cambay Faults. The basic framework of the WCMI has been established by the end of Cretaceous. The rifting and drifting episodes in the margin cause initial rift formation and crustal thinning, whereas, the spatio-temporal variations in subsidence and sedimentation pattern shape the basin configuration. Vast amount of seismic as well as well data in the Western offshore basins have clearly defined the basin architecture and its evolution.

In this chapter, the litho-stratigraphic variation of various sedimentary units constructed from available seismic sections as well as the well data in the Konkan and Kerala basins have been used to geophysically model the processes such as lithospheric rifting mechanism, its strength during rifting, flexure and basin configuration, and the evolution of flank uplift topography that led to the present day Western Ghats escarpment.

5.2 GRAVITY AND FLEXURE AT THE PASSIVE CONTINENTAL MARGINS - A REVIEW

Passive continental margins form in response to continental rifting and creation of new ocean basin. Variable amounts of sediments and magmatism, together or individually, explain the diversity of present day passive continental margins. The geometry, style and mechanism of initial rifting would be obscured by these two latter effects (sedimentation or magmatism) at the margin.

The gravity anomaly at a continental margin can be regarded as the result of several processes that have shaped it through time (Watts and Fairhead, 1999). One of the most distinctive geophysical features observed at the passive continental margins is the 'free-air edge effect' anomaly. The anomaly comprises of a bipolar signature, gravity 'high' over the outer shelf and, 'low' associated with slope and rise regions. This distinct anomaly pattern has been attributed to the gravity effect of crustal thinning from continental to oceanic regions by many workers. Worzel (1968) used an Airy model to predict the geometry of crustal thinning and demonstrated the changes that took place in the edge effect anomaly if the Ocean Continent Transition (OCT) was moved landward or seaward of the shelf break. After correcting for the gravity effect of transitional crust from the free-air anomaly, Talwani and Eldholm (1973) observed that many margins are characterised by an outer high, which has a steep gradient landward side and a tail on the ocean ward side. Rabinowitz and LaBrecque (1977) calculated the isostatic anomaly and showed that the outer high persisted even when sediments at the margin were compensated. This characteristic anomaly pattern was interpreted as a criterion for locating Ocean Continent Boundary (OCB) at the margin.

On the other hand, many workers felt that the Airy model, which assumes that, the lithosphere deforms locally rather than regionally to applied loads, may not be applicable at the margins (Walcott, 1972; Cochran, 1973; Watts and Ryan, 1976). According to Watts and Ryan (1976), the sediments at the margin represent a load on the surface of the lithosphere which would flex under their weight. Walcott (1972) and Cochran (1973) modeled the edge effect anomaly using a thin elastic plate and observed that many margins consisting of river deltas are characterised by higher elastic thickness Te of the lithosphere (20-30 km). This observation points towards the significant role of flexure at the rifted margins.

Through spectral analysis of gravity and topography at the margins, Karner and Watts (1982) and Diament et al. (1986) demonstrated the flexure as a better mechanism of compensation to Airy and can explain the outer high observed at the margin. However, they suggested that the Te determined by spectral techniques represents the average response of the crust and the lithosphere to sediment loading during margin evolution. Cochran (1973) observed that the amplitude and wavelength of the gravity anomaly at the margin were sensitive to the elastic thickness (Te).

Studies on Te at different margins world over, in general, show low Te values (Barton and Wood, 1984; Watts, 1988, Fowler and McKenzie, 1989). According to Watts et al. (1982), such low Te values are difficult to reconcile with stratigraphic data and suggested that the rift type basins generally widen with time. However, White and McKenzie (1988) argued that the widening could be explained by low Te if depth dependant stretching model of Royden and Keen (1980) and Rowley and Sahagian (1986), is considered at the margin. On the other hand, some continental rifts such as East African rift (Weissel and Karner, 1989) and the rifted continental margin of New Zealand (Holt and Stern, 1991) are characterised by relatively high Te. Te estimates at the margin also indicate that the passive margins are highly segmented as regards to their long-term strength of the lithosphere (Watts and Stewart, 1998). Watts and Marr (1995) modeled the edge effect anomaly at rifted continental margins in terms of lithospheric response to sediment loading by flexure and observed two types of edge effects at the margin. These are, i) a long-wavelength, high amplitude 'single' associated with high rigidity, strong margin, ii) a short-wavelength, low amplitude 'double' associated with low rigidity, weak margins. Within the second category, they observed onshore and offshore dipping doublets that indicate relatively strong and weak lithosphere respectively.

From the seismic data on crustal and upper mantle structure at the margin, Watts (1988) showed the dependence of Te on age since rifting. The modeling carried out by him is very useful to separate margin evolution as a result of several processes such as rifting, sedimentation, erosion and magmatic underplating and also to estimate the gravity anomaly associated with these processes individually. This method of combining gravity and seismic data to model the lithospheric evolution at the margin is called as 'Process Oriented Approach to Gravity Modeling' by Watts and Fairhead (1999). This method utilizes the flexural backstripping technique and the forward gravity modeling. A detailed description of the method is given in section 3.3.2.

Many previous workers used this method to estimate the spatio-temporal variations in Te at the margin, which strongly indicate that, the passive margins significantly vary in terms of their lithospheric strength, sedimentation and flexure, magmatism etc., and the gravity anomaly pattern is a key indicator in understanding the geological evolution of the margins. Some of these aspects have been dealt in the subsequent sections of this chapter.

5.3 MORPHOTECTONIC HISTORY OF THE WCMI

A ridge graben structural style can be seen in WCMI due to the presence of several linearly extending ridges running parallel to the coast and the presence of sedimentary basins along the coast (Figure 5.1). Major tectonic features as identified by Biswas and Singh (1988) along the WCMI are, shelfal horst graben complex consisting of Kori-Comorin depression, Kori - Comorin ridge, Laxmi - Laccadive depression, Laxmi- Laccadive ridge and Arabian abyssal plain.

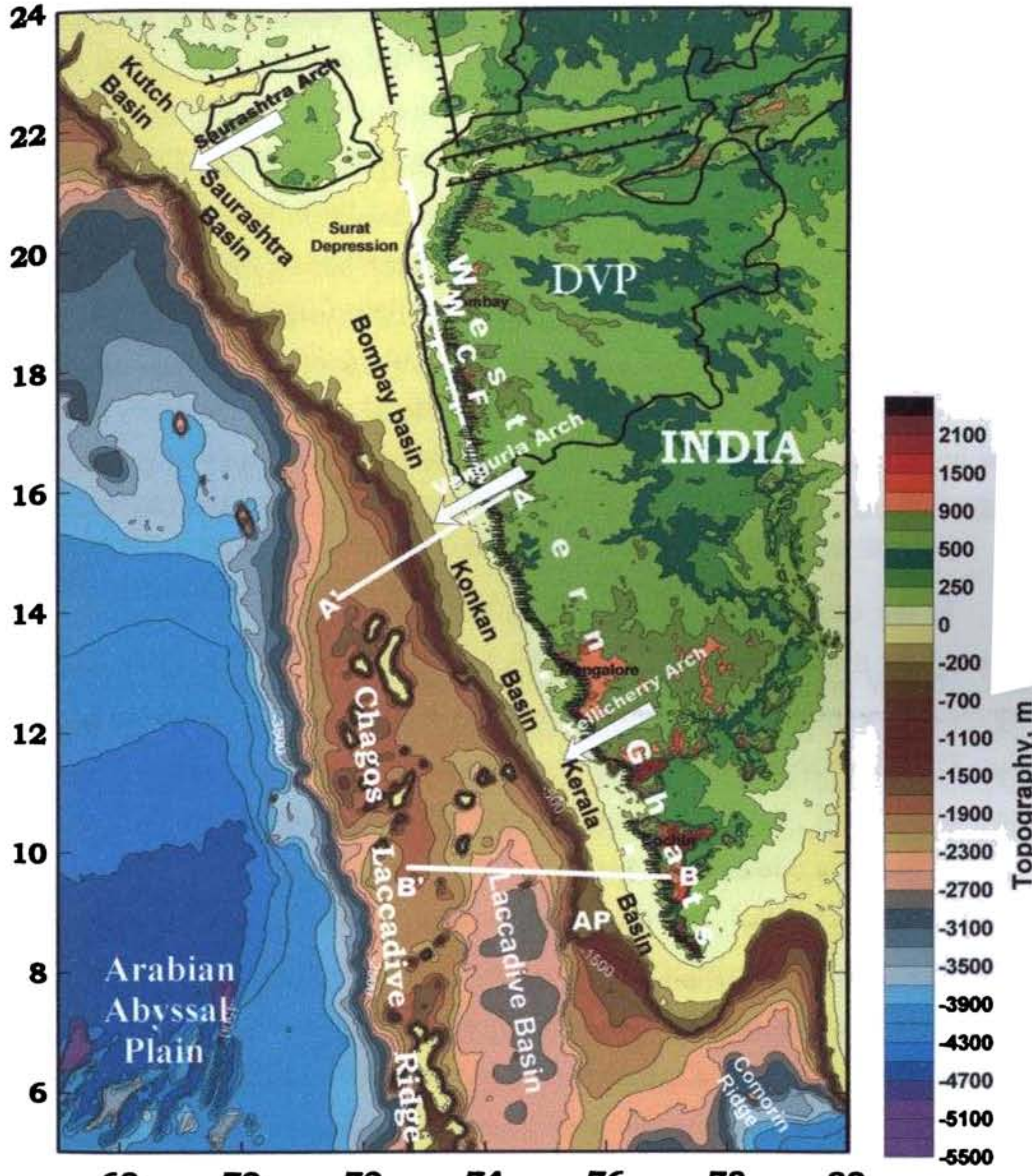

Fig 5.1: Map showing the structural features and location of seismo -geologic sections (AA' – BB') in the WCMI utilized in the present study. WCF- West Coast Fault, DVP – Deccan Volcanic Province. White arrows indicate basement Arches which separate the margin into sub-basins.

The Kori-Comorin ridge is a linear fault bounded structural high which trends NW-SE and traverses the entire length of WCMI. Along the south of Vengurla Arch it becomes a part of continental slope and extends up to Pratap Ridge. The margin is characterised by a wide shelf (> 300 km) with 7-8 km of thick Indus fan sediments in the north, whereas, south of Vengurla Arch, the shelf is narrow (< 100 km) with 3-4 km of sediments concentrated in small localized depressions (Zutshi et al., 1995). The basins came into existence in Late Cretaceous and evolved through Tertiary. It is also relevant to state that the subsurface geology, depositional and tectonic history of these basins has a natural genetic linkage to the denudation and uplift history of the Western Ghats.

In the onshore part of the margin, the most important geomorphological characteristics that can be seen are; an elevated inland plateau, a huge erosionally controlled escarpment, coast parallel monoclinal flexure and the low-lying coastal plains. This remarkable morphological expression along the coast, termed as 'Western Ghats' or 'Sahyadri', has evolved during post-Cretaceous processes of shoulder uplift and scarp recession (Gunnell and Fleitout, 2000). Due to its presence, Gunnell and Fleitout (1998) classified the margin as a high elevated rifted margin. Such geomorphological characteristics have been noticed by Gallagher et al. (1998) at many of the passive margins and at the rifted Continental Flood Basalt provinces such as Parana in Brazil, Karoo of SE Africa and Etendenka of SW Africa. Several previous workers have studied the evolution of such a remarkably consistent morphological expression in terms of coast parallel escarpment. Two basic models of evolution can be seen to develop from these studies, one, the downwarp model (King, 1962; Ollier and Pain, 1997) and the other, scarp retreat model (Gilchrist and Summerfield, 1990; Gilchrist et al., 1994, Kooi and Beaumont, 1994). Also, it is known from the studies that offshore sedimentary record is valuable in understanding the landscape development at the margins, as onshore denudation, sedimentary deposition offshore and the resulting flexural response forms important constraints in generating models on flank-uplift topography (Brown et al., 1990; Rust and Summerfield, 1990; Gilchrist and Summerfield, 1991). This marginal uplift phenomena has been described by many authors as due to; the rift related mechanisms of crustal thinning (Royden and Keen, 1980 ; White and McKenzie, 1988), magmatic underplating (McKenzie, 1984; Watts and Cox,1989), transient thermal effects (Cochran, 1983), secondary convective effects associated with extension (Buck, 1986), and flexural unloading (Weissel and Karner, 1989).

5.4 CONSTRUCTION OF SEISMO-GEOLOGICAL SECTIONS AND LITHO - STRATIGRAPHY OF THE KONKAN AND KERALA OFFSHORE BASINS

The Konkan and Kerala basins form the southern part of the WCMI. The Vengurla Arch, a southwesterly trending basement Arch separates the shelfal horst graben complex of these two basins from that of the Bombay Offshore basin. The Konkan and Kerala basins were divided from each other by another basement Arch called the Tellicherry Arch

A compilation of all available seismic reflection and refraction data, sediment thickness maps, seismo-geological sections and well data published by various previous workers in the Konkan and Kerala basins has been made (Eremenko and Datta, 1968; Rao and Srivastava, 1984; Biswas and Singh, 1988; Singh and Lal, 1993; Zutshi et al., 1995; Thakur et al., 1999; Chaubey et al., 2002). These data are useful in clearly delineating major stratigraphic units of post Tertiary sequence in the Konkan and Kerala offshore. When such clear depiction of sedimentary record is available from seismic data, it can be combined with the gravity data to obtain information from deeper crustal levels and also to understand the attendant tectonic processes that led to the formation of the margin. From these available information, two seismogeologic sections, one, in the Konkan basin, and, the other, in the Kerala basin were constructed for further analysis. The data for these two sections mainly include, the multi-channel seismic profile analysed by Chaubey et al. (2002) for the Konkan basin, and, the seismogeologic section presented by Eremenko and Datta (1968) for the Kerala basin. The lithological and stratigraphic information for these two sections have been obtained by tying the sections to the nearest well data, such as, KR-1-1 in the Konkan basin and the CH-1-1 and K-1-1 in the Kerala basin. From the gridded gravity data, the gravity anomalies have been projected on to these sections (See Fig 5.1 for location of the sections). Some salient aspects on litho-stratigraphy of the Konkan and Kerala basins with reference to the sedimentary sequences along these two seismogeologic sections are presented below:

5.4.1 Konkan Basin

The Konkan basin is a peri-cratonic multi phase rift basin developed in the central part of the WCMI. The N-S trending rift segments have formed as a consequence of focused rifting along the NNW-SSE Dharwar structural trend. The rifts are bordered by major faults and contain arrays of half graben. The rift-drift episodes have been grouped into three major events by Thakur et al.(1999) conforming to three distinct tectono-sedimentary stages. These are pre-rift prior to base Tertiary, syn-rift from Paleocene to Lower Eocene, post rift from Middle Eocene (through Oligocene and Middle Miocene) to Recent. Chaubey et al. (2002) analysed a multi-channel seismic reflection profile across the Konkan offshore and the deeper oceanic areas covering the Laccadive Ridge and the Arabian Sea in order to identify the sedimentary sequences, sedimentation history and the crustal structure in the region. The section consists of six major sedimentary sequences from H1 to H6 ranging in age from Paleocene to Holocene. In the shelf and shelf margin basin, the sequence H1 indicates the beginning of sedimentation since the Paleocene. The sequences H2 and H3 can be correlated with the deposition of Carbonates and Carbonates interspersed with Shales in the shelf and shelf margin basin during Eocene through Middle Miocene, as also reported elsewhere in the shelf region by Rao and Srivastava (1984), Aubert and Droxler (1996). The upper boundary of sequence H3 coincides with the Middle Miocene shelf edge and the top of sequence H2 was identified as Paleo shelf edge during Middle Oligocene (Chaubey et al., 2002). These sequences depict both aggradation and progradation of the sediments at the shelf. Top of sequence H3 has been assigned the age of Middle Miocene. In the post Middle Miocene, as a result of India – Eurasia plate collision and the build up of Himalayas, the onset of intense Indian monsoon resulted in rapid erosion and deposition of terrigenous clastics in the shelf and shelf margin basin which gave rise to termination of carbonate deposition (Rao and Srivastava, 1984; Singh and Lal, 1993; Whiting et al., 1994). The sequences H4, H5 and H6 together indicate a typical sigmoidal reflection pattern suggesting a change in facies of the sediments. While the sequences H4 and H5 correlate with Middle Pliocene and Late Pleistocene, H6 sequence represents the Holocene sediments. These six sedimentary sequences were merged into three major sedimentary units based on the lithological variations and the composite seismo-geologic section is shown in Figure 5.2.

5.4.2 Kerala Basin

The Kerala basin is a major onshore-offshore sedimentary basin observed along the Western Continental Margin of India and is located in its southern most part. The basin covers mostly the southern and central parts of the Kerala coast between 8.5?N – 10.5° N latitudes bounded by the Western Ghats in the east and the Arabian abyssal plain on the west. The major morphological features of the basin are the shelf, shelf margin basin, Alleppey platform in the shelf-slope region, Pratap ridge, Laccadive ridge

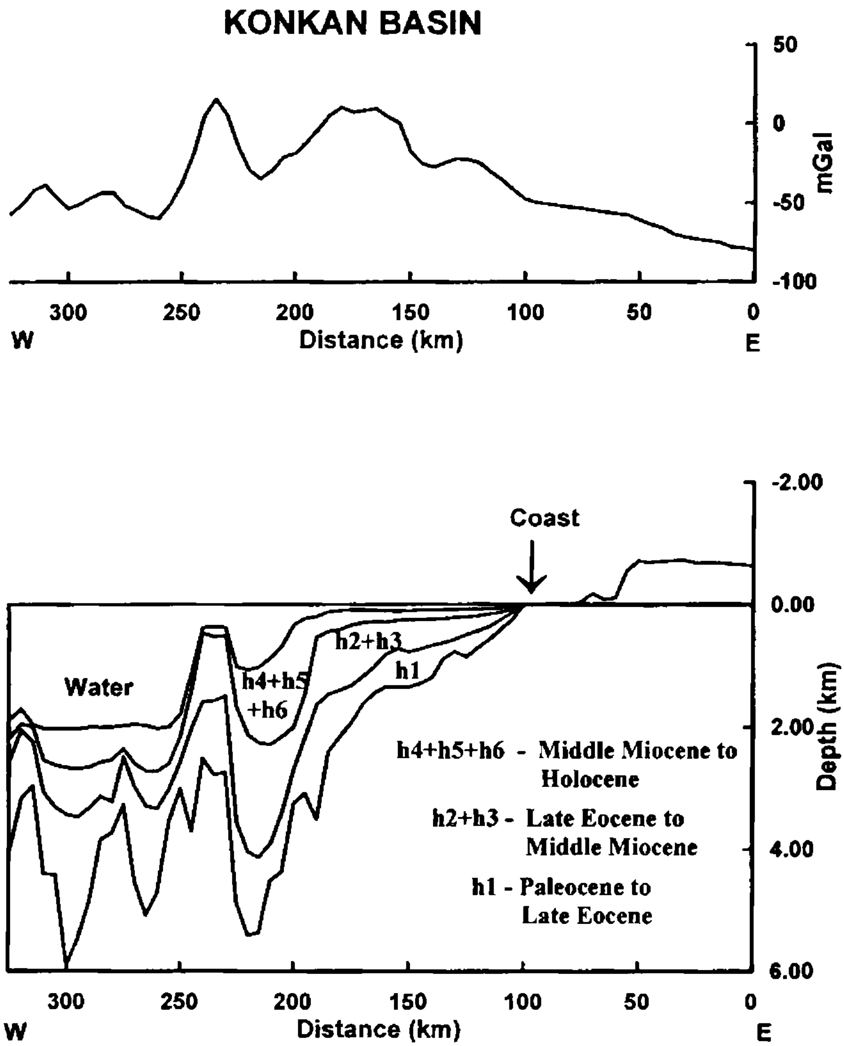

Fig 5.2 : Graph showing the seismogeologic section and projected gravity anomalies in the Konkan basin for further analysis (modified after Chaubey et al., 2002).

and the western Arabian basin. The margin is characterised by complex bathymetry and presence of numerous topographic highs. The horst-graben complex in the shelf region divides the Kerala basin into Cochin depression and Cape Comorin depression. There is marked variation in the trend of the shelf region between Cochin and Quilon, where a wider shelf with a gentle seaward slope is observed and this feature is called the Alleppey Platform by Singh and Lal (1993). The Chagos-Laccadive Ridge acts as a barrier for transport of sediments further west into the Arabian abyssal plain.

The sediment deposition during the early rift phase started with continental environment which changed gradually to paralic and finally to pulsating marine conditions. Most of the rift related regional and local horst- graben structures were covered by sediments. Sediments from the Paleocene to the lower Miocene are coarse and arenaceous. The lithological and stratigraphic information and sedimentation rates in this basin have been reported from few drilled wells (K-1, K-1-1, CH-1-1) as well as from seismic data (Singh and Lal, 1993; Gunnell and Radhakrishna, 2001). Similar to other basins in the north, the terrigenous sequence in the Kerala basin reflects denudation onshore. Gunnell and Radhakrishna (2001) believe that sediment supply during the Paleocene might have been from the Laccadive Ridge or the Mascarene Plateau. The well data indicate that the shelf off Cochin gathered abundant supply of clastics particularly sand derived from granitic terrain. In contrast to the basins in the north, the Kerala basin is characterised by the absence of thick Eo-Oligocene carbonate platform. This change of facies during the Middle Cenozoic was attributed to the predominance of mechanical erosion in Kerala as opposed to geochemical erosion and deep weathering in north during the Paleogene (Gunnell and Radhakrishna, 2001). Sinha Roy (1982) suggested that rifting between Laccadive and the mainland India never reached the stage of sea floor spreading as sediments in the offshore Kerala basin are almost exclusively terrigenous and paralic in nature.

The seismo geologic section across the central part of the Kerala basin constructed from Eremenko and Datta (1968) and the well data consists of five sedimentary sequences The section indicate a thin cover of Mesozoic sediments unconformably overlie the basement. Two thick layers of sediments, one, during the

Paleocene – Eocene period and the other during the Miocene period characterize the sedimentary pattern in the basin. The thin Oligocene sedimentary layer probably marks the regional hiatus in sedimentation. The seismo geologic section is shown in Figure 5.3

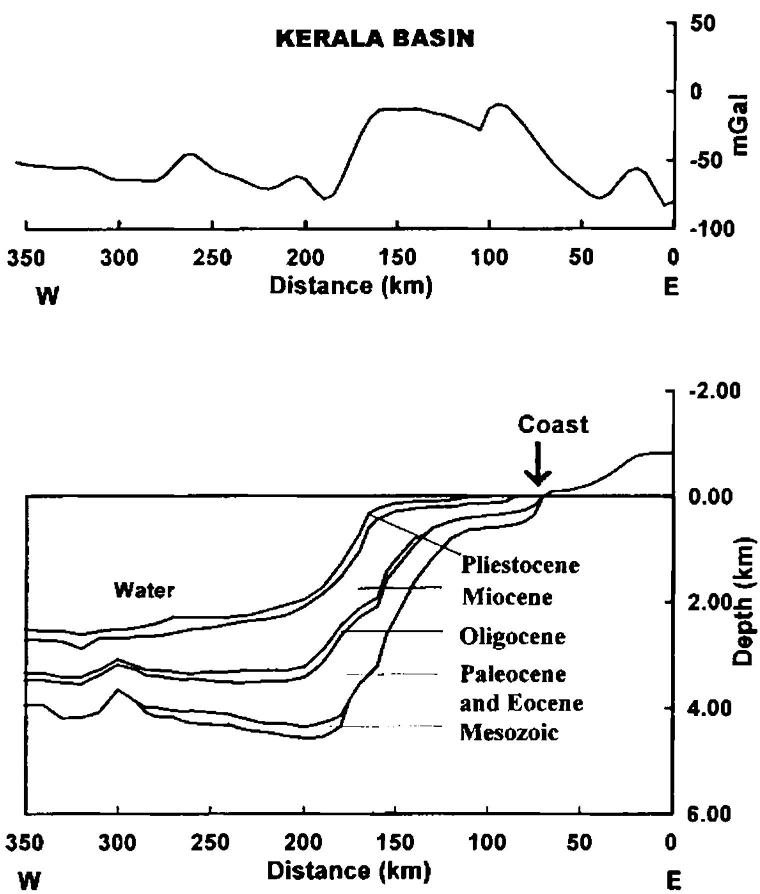

Fig 5.3: Seismogeologic section and the projected gravity anomalies in the Kerala basin considered for further analysis (modified after Eremenko and Datta, 1968).

5.5 LITHOSPHERIC STRENGTH AND MECHANISM OF RIFTING THROUGH PROCESS ORIENTED APPROACH TO GRAVITY MODELING

In the present investigation, the above litho-stratigraphic sections depicting major sedimentary layers in the Konkan and Kerala basins along with the gravity data have been utilized to study the sediment loading, lithospheric flexure and dynamics of rifting at the margin. The lithological parameters for various layers are presented in Table 5.1 and various physical parameters considered in the analysis in Table 5.2. Based on these parameters, the individual sedimentary layers were decompacted and flexurally unloaded for different values of elastic thickness of the lithosphere (Te).

LAYER	LITHOLOGY	SURFACE POROSITY	COMPACTION FACTOR	GRAIN DENSITY
1	Clay and Claystone	0.56	0.39	2.68
2	Dolomitic limestone with shale and Intervening limestone and shales	0.47	0.40	2.7
3	Dolomitic limestone with minor shale	0.51	0.45	2.69
4	Limestone with claystone and Limestone	0.47	0.27	2.6
5	Limestone with claystone	0.44	0.39	2.7
6	Sandstone/siltstone & Limestone/dolomitic	0.36	0.27	2.71
5	Sandstone/silt stone/ shale/ lateritic Clay/ altered basalt	0.63	0.51	2.72

Table 5.1: Lithological parameters used for backstripping the layers in the Konkan and Kerala basins.(Chand S., 2001)

After the layer decompaction, the load due to the layer and hence the flexural deflection it may cause to the basement has been calculated using the finite-difference numerical method (Sawyer et al., 1982). This deflection is subtracted from the basement depths and the remaining layers are decompacted from below. The process is applied for all the layers one by one. The complete flexural unloading of sediments gives rise to the rift stage basement configuration. The flank-uplift topography in the onshore can be reconstructed by backstacking the equivalent volume of sediment at the margin (Brown, 1991). The backstacked topography indicates the rift flank-uplift at the margin.

Density of the crust	2800 kg m^{-1}
Density of the mantle	3300 kg m^{-1}
Average density of sediments	2262 kg m^{-1}
Density of seawater	1030 kg m^{-1}
Young's modulus	100 GPa
Poisson's ratio	0.25
Average gravity	9.81 m s^{-2}
Gravitational constant	6.67 X 10^{-11} m^3 kg^{-1} s^{-2}

Table 5.2: Physical parameters considered in the Process Oriented Approach of gravity modeling. (Chand S., 2001)

According to the 'Process Oriented approach', the sediment loading play an important role in the evolution of the margin and contributes significantly to the edge effect anomaly. At the time of lithospheric breakup, at some margins, the magmatic underplating or depth of necking of the lithosphere may control the geometry of the basin, as well as, explain the process that led to the flank uplift topography at the margin. The rift time topography can be reconstructed through backstacking the eroded sediments (from AFTA studies) back on the present-day scarp (Brown, 1991) with the same Te that was used in backstripping. The rift time morphology is obtained from AFTA studies which will tell about the denudation rate and possible amount of denudation that has taken place. The present day morphology of Western Ghats suggests that the escarpment seems to have gone well inside the original flank uplift and a high denudation took place along the flank causing scarp to retreat. Based on uplift rate of 1.8 cm per 1000 years, Kalaswad et al. (1993) estimated the removal of about 4 km of rift topography from the near coast. From this information, the rift time topography was reconstructed through backstacking. From the rift time basement and rift time topography, the rift anomaly can be calculated. Secondly, the sediment loading can contribute significantly to the edge effect anomaly. The wedge shaped sediment load is associated with central high that is flanked by two lows. The high arises because the sediments are much denser than the water that they displaced and the lows are due to the displacement of high density mantle material with low density crust. These two effects cause the sedimentation anomaly. The third one is erosion anomaly, which is also important though its effect is very less. This anomaly is due to the denudation during the post – rift phase. The calculated anomaly, therefore, is the sum of rift anomaly, sedimentation anomaly and erosion anomaly. An attempt is made here to explain the reconstructed topography by two models such as the lithospheric necking and magmatic underplating (Watts, 1988; Braun and Beaumont, 1989; Kooi et al., 1992; Watts and Stewart, 1998; Watts and Fairhead, 1999). The sum anomaly calculated after incorporating these two models separately will be compared with the observed gravity anomaly at Konkan and Kerala basins, so as to derive the information on rift dynamics, processes led to the flank uplift topography and also the basin evolution.

5.5.1 Necking Model

The necking model assumes strength during Rifting (Braun and Beaumont, 1989). An important modification of the state of flexure can be made by incorporating the 'Depth of Necking'. The Depth of Necking (DON) can be defined as the level in the lithosphere which, in the absence of gravity (or buoyancy forces), would not move vertically during extension (Kooi and Cloetingh, 1992). The DON dictates the amount of Moho and basement topography created by rifting. Depending on the depth of necking (DON), the shape of the basin and the peripheries will vary. A shallow level of necking will result in a basin with depths shallower in comparison to the Moho upwarp, thus leading to a downward flexure (Kooi et al., 1992). In case of a deeper level of necking, the resultant basin will be deeper and results in an upwarp in the basin center and the peripheries (Kooi et al., 1992). According to Braun and Beaumont (1989) and Wiessel and Karner (1989), the DON is related to rheology of the lithosphere and occurs at a level of maximum strength and regarded it as the depth to detachment surface. Using the same Te used in backstripping/backstacking and taking different upwelling scenarios (p values), the Moho upwarp has been determined that creates the rift topography. For a flattened topography i.e., the topography without uplift due to the net upward force, the resultant Moho will be deeper than the Airy Moho. Different p values are used to calculate the net upward force due to the negative buoyancy. If p is 1, it means that there is no net upward force and hence there is Airy isostasy. For larger DON, the mantle upwelling will be less and therefore large upward force. With increasing p value, the net upward force increases because the Moho has not come up enough to balance the subsidence due to rifting and the plate is hence bending upwards. The DON is the median depth between backstripped basement and the upwelled Moho. The Moho configuration so obtained is used to calculate the rift anomaly for that particular Te, which when added to the sedimentation anomaly and erosion anomaly give rise to the total calculated anomaly. The calculated and observed anomalies have been compared for different Te values. For this purpose, Te values of 5 km, 10 km, 15 km, and 20 km were used. At the same time, different amounts of net upward forces obtained for different p values results in crustal geometry corresponding to different DON values. This process is carried out iteratively and the best fit parameters have been considered from RMS difference between the observed and calculated anomaly.

5.5.1.1 Konkan basin

The seismogeologic section shown in figure 5.2 has been analysed using the method described above. The figure 5.4 - 5.7 shows the observed anomaly and calculated anomalies for different Te values and for different 'p' values. The best fit values are obtained from the RMS difference and the crustal model for the best fit parameter is shown in Figure 5.8.

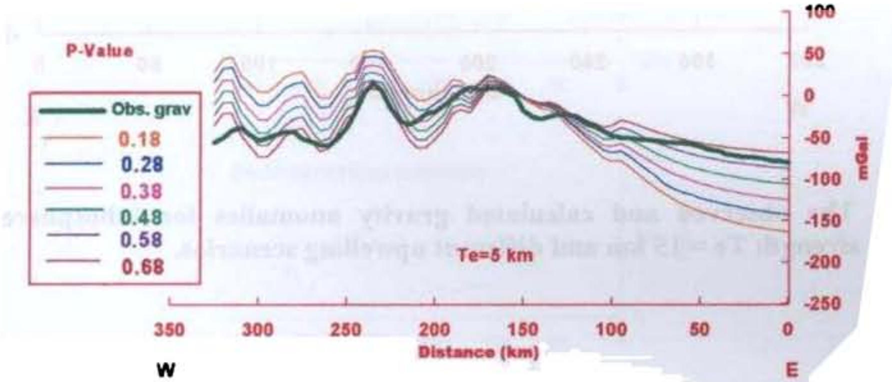

Fig 5.4: The observed and calculated gravity anomalies for lithosphere strength Te = 5 km and different upwelling scenarios. Details are discussed in the text.

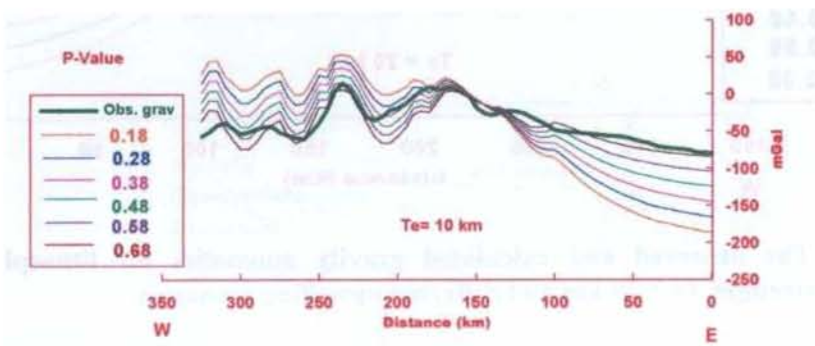

Fig 5.5: The observed and calculated gravity anomalies for lithosphere strength Te = 10 km and different upwelling scenarios.

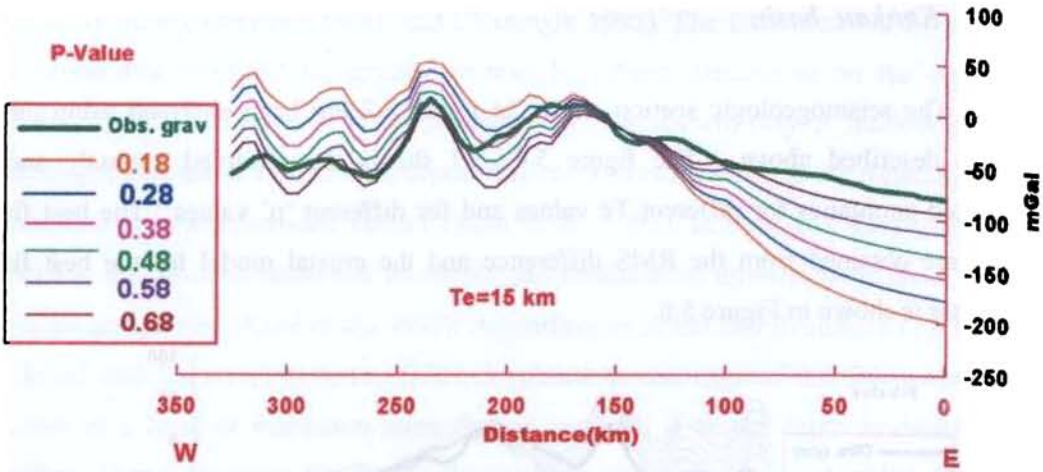

Fig 5.6: The observed and calculated gravity anomalies for lithosphere strength Te = 15 km and different upwelling scenarios.

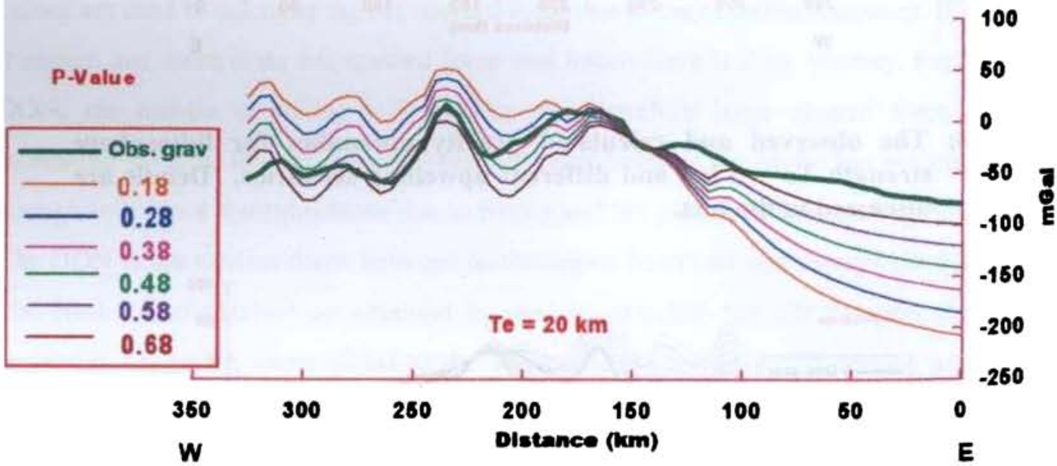

Fig 5.7: The observed and calculated gravity anomalies for lithosphere strength Te = 20 km and different upwelling scenarios.

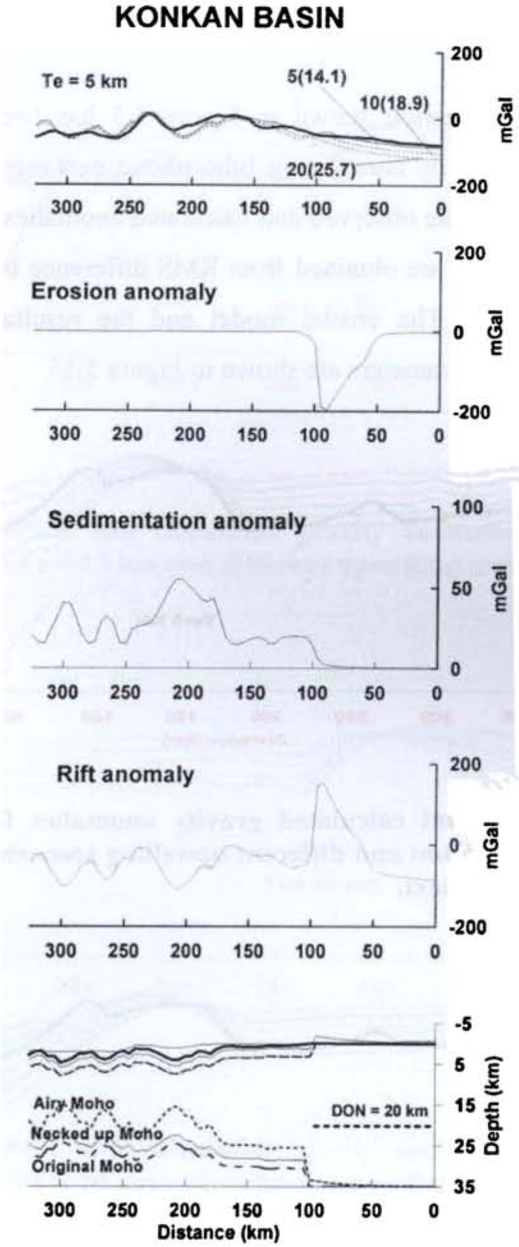

Fig 5.8: Process oriented gravity modeling for lithospheric necking model considering the best fit parameters from Fig. 5.4 - 5.7 (Te = 5 km, p = 0.58 and DON = 20 km) for the Konkan basin. The thick line on the top-most curve shows observed anomaly and the thin line calculated anomaly.

5.5.1.2 Kerala basin.

The seismogeologic section shown in Figure 5.3 has been analysed through process based approach and by considering lithospheric necking as described above. The Figures 5.9-5.12 shows the observed and calculated anomalies for different Te and p values. The best fit values are obtained from RMS difference between the observed and calculated anomalies. The crustal model and the resultant gravity anomaly components for the best fit parameters are shown in Figure 5.13

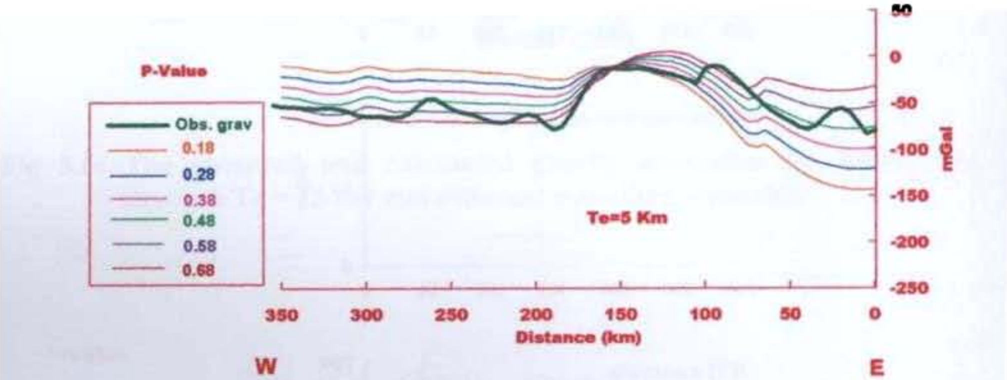

Fig 5.9: The observed and calculated gravity anomalies for lithosphere strength Te = 5 km and different upwelling scenarios. Details are discussed in the text.

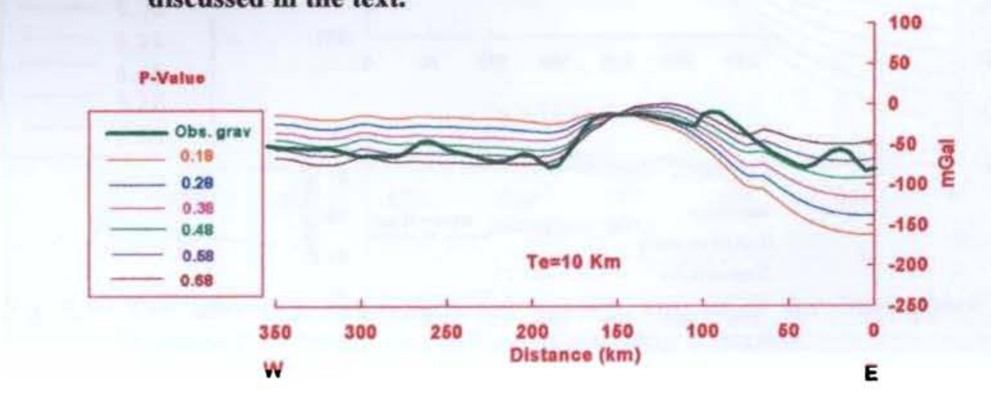

Fig 5.10: The observed and calculated gravity anomalies for lithosphere strength Te = 10 km and different upwelling scenarios.

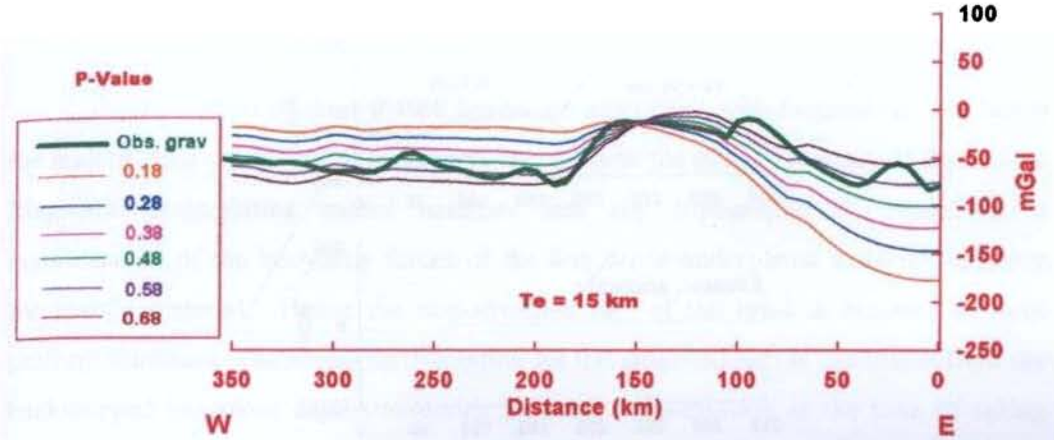

Fig 5.11: The observed and calculated gravity anomalies for lithosphere strength Te = 15 km and different upwelling scenarios.

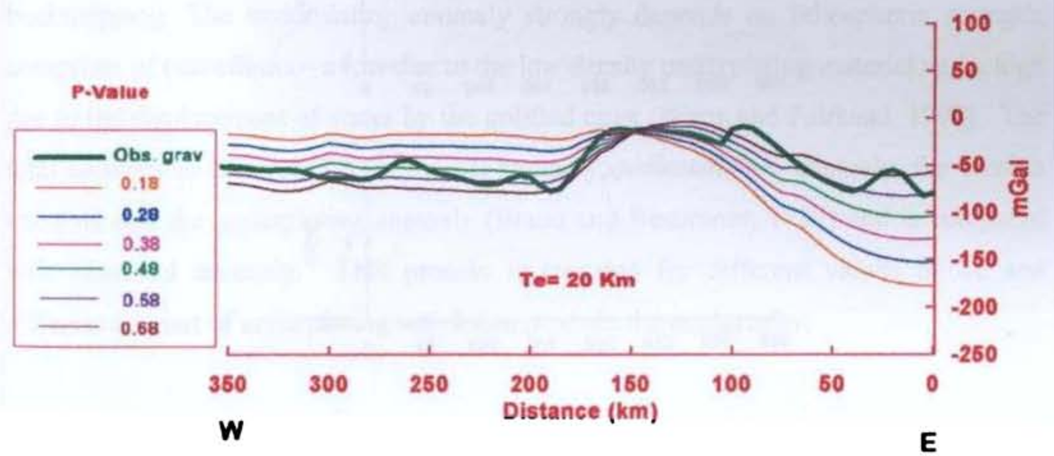

Fig 5.12: The observed and calculated gravity anomalies for lithosphere strength Te = 20 km and different upwelling scenarios.

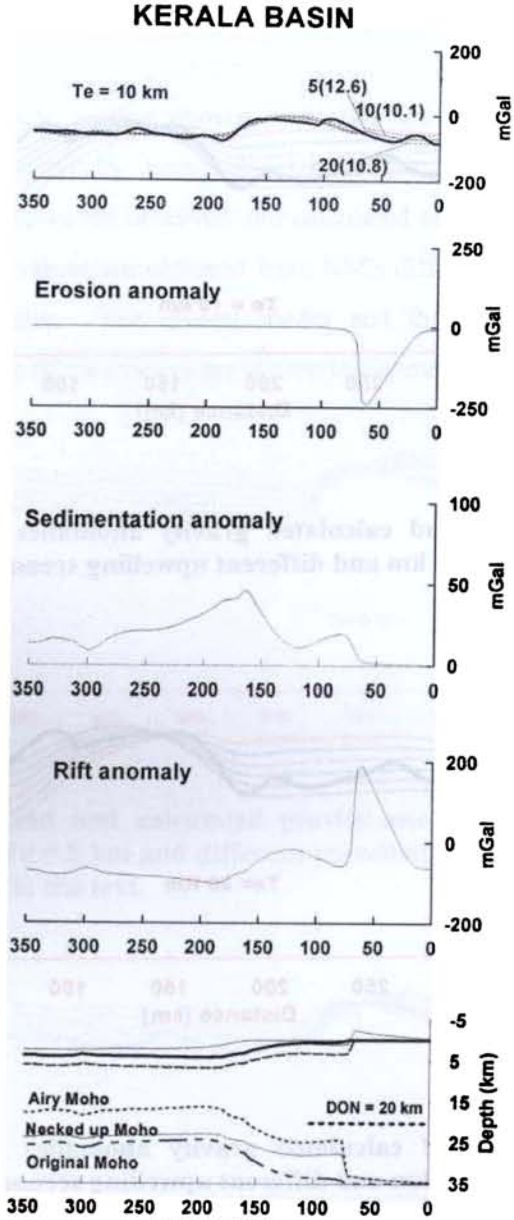

Fig 5.13: Process oriented gravity modeling for lithospheric necking model considering the best fit parameters from Figures 5.9-5.12 (Te = 10 km, p = 0.58 and DON = 20 km) for Kerala basin. Thick line on the top-most curve shows the observed anomaly and the thin line calculated anomaly.

5.5.2 Magmatic underplating model

Most of the rift type basins are associated with magmatism and hence the underplating occurs and this underplating disturbs the state of isostasy of the region. Magmatic underplating model assumes that any topography is created as a manifestation of the buoyancy forces of the less dense underplated material replacing the mantle material. Hence the non-stretched part of the crust is assumed to have uniform thickness. The Moho configuration for the stretched part is calculated from the backstripped basement depths assuming an Airy compensation at the time of rifting (Watts, 1988). Since the possible cause of underplating is a later event, we assume that the crust attained its elastic thickness during underplating and hence the rift time topography using backstacking is calculated using the same Te used for calculating the backstripping. The underplating anomaly strongly depends on lithospheric strength, comprises of two effects – a low due to the low density underplating material and a high due to the displacement of water by the uplifted crust (Watts and Fairhead, 1999). The total anomaly is calculated from the rift anomaly, sedimentation anomaly, the erosion anomaly and the underplating anomaly (Braun and Beaumont, 1989) and is compared with observed anomaly. This process is repeated for different values of Te and different amount of underplating which can produce the topography.

5.5.2.1 Konkan basin

Using the sections shown in Fig 5.2, the backstripped/ backstacked basements are forward modeled with underplating method with different Te values and are shown in Figure 5.14. The best fit values are obtained from RMS difference between the observed and calculated anomalies and the Te values obtained is 5 km and is shown in Figure 5.15.

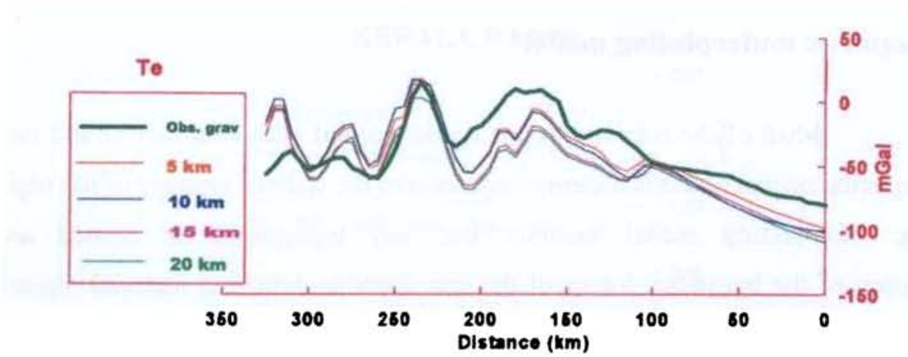

Fig 5.14: Graph showing the observed and calculated anomalies for different lithospheric strength (Te) and taking into account of underplating.

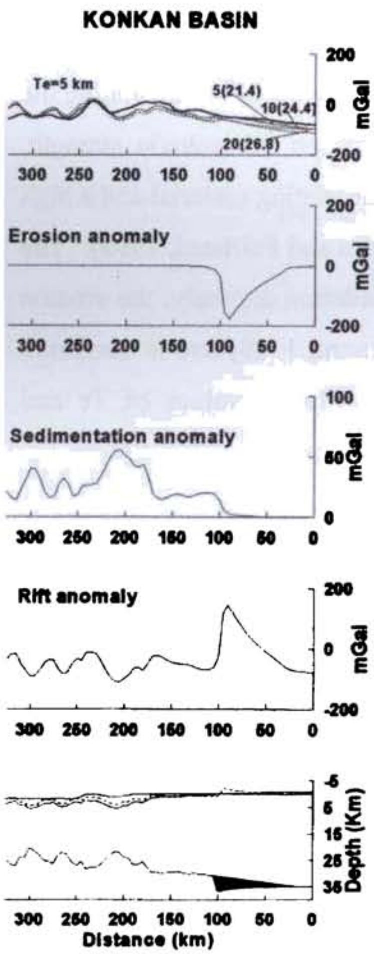

Fig 5.15: Process oriented approach to gravity modeling for the underplating model for the best fit Te= 5 km. The shaded portion shows the underplated material.

5.5.2.2 Kerala basin

The seismogeologic section shown in figure 5.3 is flexurally unloaded and the backstripped and backstacked basements are obtained for different Te values of 5 km, 10 km, 15 km, and 20 km. These basements are modeled with underplating and the results are shown in figure 5.16. Using the RMS error method the best fit ... considered to be of Te value 10 km (Figure 5.17).

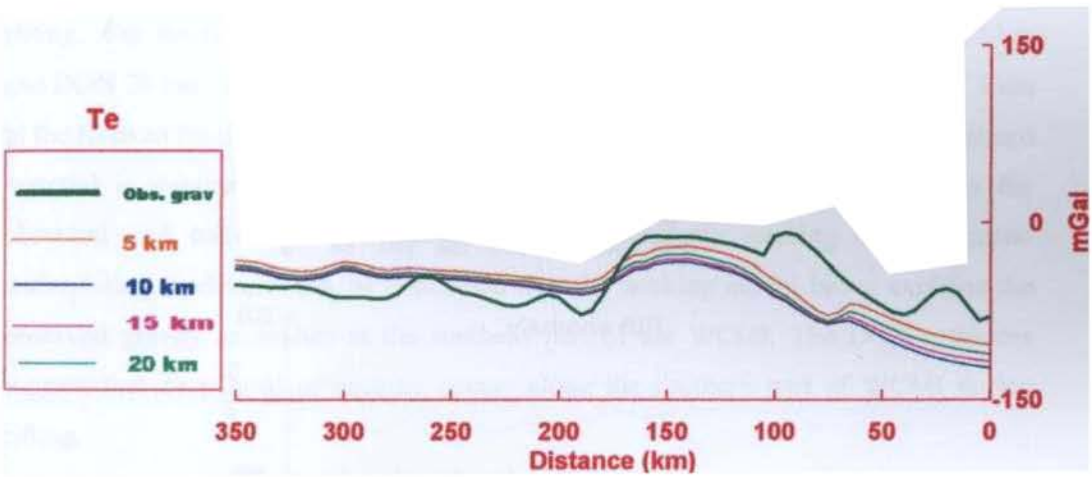

Fig 5.16: Graph showing the observed and calculated anomalies for different lithospheric strength (Te) and taking into account of underplating.

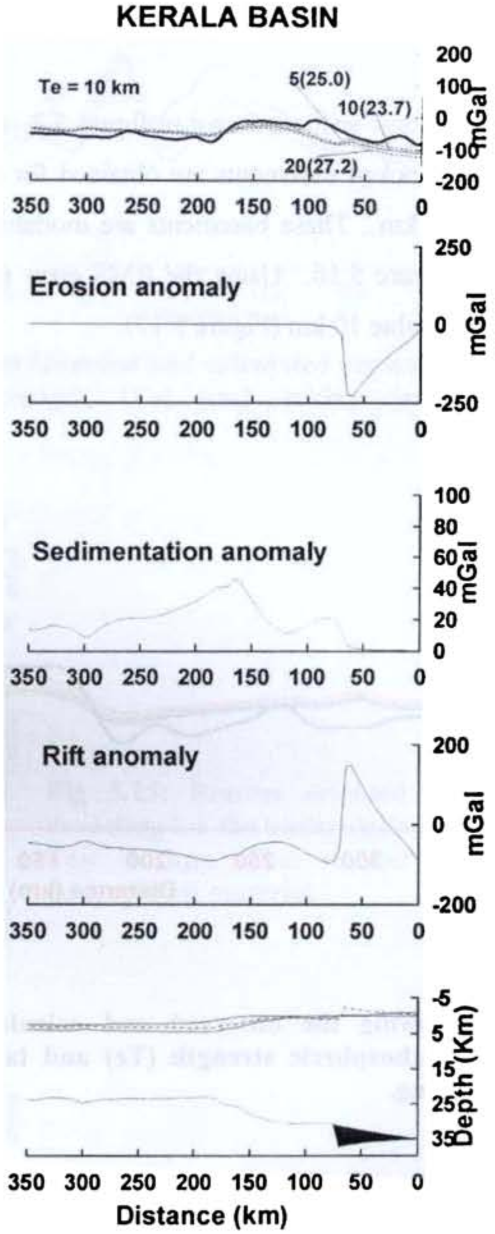

Fig 5.17: Process oriented approach to gravity modeling for the crustal underplating model for best fit Te = 10 km. The shaded portion shows the underplated material

5.6 SUMMARY OF THE RESULTS

The sediment loading and flexural characteristics of the lithosphere have been carried out along two seismo-geologic sections compiled from the available seismic data in the Konkan and Kerala basins in the present study. Based on the process-oriented approach, two lithospheric models – lithospheric necking model and magmatic underplating - were tested and the results are summarised as follows. The result obtained for the lithospheric necking model along the Konkan basin suggests a lithospheric strength of 5 km and the depth of necking (DON) of 20 km at the time of rifting. For the Kerala basin, the analysis brings out a lithospheric strength of 10 km and DON 20 km. For the magmatic under plating model, the results show a Te of 5 km in the Konkan basin and Te of 10 km in the Kerala basin. Nearly, 5-6 km of underplated material is required to explain the rift-flank topography at the margin. From the observed and calculated anomalies for both lithospheric necking and magmatic underplating models, it can be concluded that the necking model better explains the observed gravity anomalies at the southern part of the WCMI. The DON estimates suggest that deep level of necking occurs along the southern part of WCMI during rifting.

****

CHAPTER 6 GEODYNAMIC IMPLICATIONS

The southwest continental margin of India has evolved due to rifting between India and Madagascar at 88 Ma and subsequent seafloor spreading. During this period, several major ridges and horst-graben structures were formed at the margin. In the southern most part, the Comorin Ridge aligned along the margin, is another topographic feature believed to be related to the earliest phase of margin evolution. In the present study, two different approaches, such as, the coherence analysis of gravity and bathymetry and the process oriented approach to gravity modeling have been used to estimate effective elastic thickness (Te) at the southwest margin of India. The coherence analysis brings out effective elastic thickness (Te) values of 5-10 km along the Konkan and Kerala basins, and the Comorin Ridge at the margin and 5-8 km along the Chagos Laccadive Ridge north of the equator. The elastic thickness values increase southward and maximum Te value of 10 km is observed below the Comorin Ridge. The process oriented approach to gravity modeling gives a Te value of 5 km at Konkan basin and 10 km at the Kerala basin. Though both these results indicate a general increase in the lithospheric strength towards south, the physical meaning of these values must be clearly distinguished. While, the coherence or admittance based methods give rise to integrated mechanical strength of the lithosphere at present, the process oriented approach brings out the lithospheric strength at the margin at the time of rifting. However, both these results can be cleverly combined and together analysed to understand the regional geodynamic processes, flexural characteristics, rift-flank topography and basin evolution.

Effective elastic thickness Te along the continental margins depend on the age of the margin, rifting and sedimentation (Karner and Watts, 1982; Diament et al., 1986; Lavier and Steckler, 1997), rift-shear tectonics along the margin (Verhoef and Jackson, 1991; Chand et al., 2001) and proximity to mantle plume source or plume lithosphere interactions during rifting and breakup (Tamsett, 1984; Courtillot et al., 1999). Effective elastic thickness is related to flexural rigidity of the lithosphere and therefore the flank uplift topography at the margin can be modeled. Through such models the topographic evolution of the Western Ghats can be understood. The Te estimates obtained in the present study have been analyzed from the point of view of above aspects relevant to WCMI to understand the geodynamics of the margin.

6.1 INDIA AND MADAGASCAR BREAKUP – ROLE OF MARION MANTLE PLUME

Plate reconstruction models unequivocally place India – Madagascar fit during the Gondwana times (Katz and Premoli, 1979; Agarwal et al., 1992). While first break between them appear to have taken place during 140 Ma (Besse and Courtillot, 1988), actual rifting started at 88 Ma (Storey et al., 1995). The role of Marion mantle plume during the rifting and breakup of India and Madagascar is critical to our understanding of geodynamics of the margin. Cretaceous flood basalts of Madagascar which show a mean age of 88 Ma emplaced over no more than 6 My have been related to the Marion mantle plume (Storey et al., 1995). Anil Kumar et al. (2001) suggested that the mafic dyke activity in Karnataka and Kerala-Tamil Nadu (Radhakrishna et al., 1994) and volcanic lavas of St. Mary islands at the southwest coast of India (Valsangkar et al., 1981) are co-eval and compositionally similar to the magmatism at the eastern-rifted margin of Madagascar. However, compared to the east coast of Madagascar, where, the magmatism was wide spread and outcropped along ~1500 km (Storey et al., 1997), the plume related igneous activity is less along the southwest coast of India. As the plate reconstruction models indicate the location of the Marion plume 100 km south of Madagascar at the time of continental breakup (Muller et al., 1993; Storey, 1995; Storey et al., 1995), it is unlikely that the plume has generated substantial magmatism associated with the break up of WCMI. Generally, active plume interaction at the time of break up generates either large-scale sub aerial volcanism in terms of flood basalt province or volcanic margins. While the former is absent, gravity models in the southern Indian shield and the adjoining offshore (Radhakrishna et al., 2002; Arts et al., 2003) do not indicate the presence of large-scale crustal underplating or thicker magmatic crust generally observed along the volcanic margins. The Te estimates at the margin obtained in the present study range between 5 – 10 km and increase southward with a maximum Te of 10 km in the Comorin Ridge region. It is expected that active plume interaction weakens the lithosphere mechanically and generally give rise to very low Te values, which is not so here. We therefore tend to suggest that the Marion mantle plume having its focal point in the southern part of Madagascar that erupted thick lava pile at the volcan de l'Androy (Storey et al., 1995) played a limited role at the WCMI in the south unlike the wide spread Deccan large igneous province emplaced by the Reunion mantle plume in the north. However, crustal seismic data from multi-channel seismic reflection and refraction surveys at the southwest margin is required to resolve some of these issues related to Gondwanaland breakup.

6.2 ISOSTASY AND MECHANISM OF RIFTING AT THE SOUTHWEST MARGIN OF INDIA

The observed Te values for the Konkan (Te = 5 km) and Kerala (Te= 8 km) basins obtained from coherence analysis are found to be lower than the Te estimates of 8-15 km obtained by Chand and Subrahmanyam (2003) for WCMI based on admittance analysis. This discrepancy could be because they considered very long profiles covering deep oceanic areas that are regionally distributed all along the WCMI. While, their Te estimates represent average strength of the lithosphere along WCMI, the Te values obtained in the present study refer to basin-wide lithospheric strength at the margin. Further, it is found that Te values increase southward with maximum value observed below the Comorin Ridge. Further west, along the Chagos Laccadive Ridge (CLR), the Te value (Te= 4 km) obtained by Ashalatha et al. (1991) is different from Te estimates for CLR (5-8 km) in the present study. Based on the geophysical data, Ben Avraham and Bunce (1977) observed that the CLR is segmented from south to north in terms of crustal thickness, nature of crust and extent of volcanism. According to them, in the present study region, the ridge north of 8°N has been emplaced volcanically, while, between 8°N - 0° it is a continental fragment. Our estimates show Te values of 5 km and 8 km in the north and south respectively. However, the coherence plot (Fig 4.13) for the southern part of the ridge (0° - 7°N) shows slightly lower coherence values at longer wavelengths which may indicate hidden loads (Verhoef and Jackson, 1991).

Chand and Subrahmanyam (2003) carried out process oriented gravity modeling along a profile located in the central part of the Konkan basin (off Mangalore which is mid-way to profiles AA' and BB' shown in Fig 5.1). The best fit parameters obtained by them give rise to Te of 15 km and the depth of necking (DON) of 20 km. The results obtained in the present study using the same approach along two seismic sections (AA' and BB' referred above) indicate Te value of 5 km in the Konkan basin and Te of 10 km in the Kerala basin with DON = 20 km. These results suggest deep level of necking occurred at the WCMI during rifting and lateral variations in the lithospheric strength, though not very significant, exists from north to south along the margin. As the data windows considered in the Konkan and Kerala basins cover the region between the coast and CLR, the observed elastic thickness (5-8 km) represents in fact an average value across the margin within the extended continental/transitional crustal domain. All Te estimates referred above indicate that the lithospheric strength at the southwest margin is everywhere less than 15 km. The low elastic strength observed in the extended part of the shield crust (below Konkan and Kerala basins) is consistent with the low Te values (11-16 km) for the South Indian shield crust reported by Stephen et al. (2003) based on multitaper coherence method. It must be pointed out that the Te values < 15 km generally applicable in the case of oceanic lithosphere that is less than 30 M.y. old or a continental crust with a surface heat flow > 80 $mW.m^{-2}$ (Daly et al., 2004). Both these situations do not exist in the present study region. In response to the rifting, a series of horsts and grabens have formed in the basin along the dominant basement tectonic trends. By the end of early rift stage, these horsts and grabens were covered by sediments, while post-rift phase witnessed subsidence of the margin and tilting of depositional surface due to thermo tectonic adjustments (Singh and Lal, 1993). Karner (1991) and Lavier and Steckler (1997) argued that low Te values at the margin result from thermal blanketing and loading of large amount of sediments. On the contrary, Fowler and McKenzie (1989) suggested that sediments may not significantly affect the initial elastic strength at the margin. A comparison of Te estimates obtained in the present study from both process oriented approach and coherence analysis, also support the observation made by Fowler and McKenzie (1989) as no significant change in the lithospheric strength was observed since rifting. Based on the mechanism of Courtney and Beaumont (1983), Daly et al. (2004) suggested that low Te values of < 15 km at the passive margins could be the consequence of loads emplaced during continental breakup under extremely high temperature gradients. This could be a possible cause, as the southwest coast and adjoining shelf region are characterized by the presence of several localized gravity highs, which are believed to be due to basic intrusives or thinning of the crust (Chandrasekharam, 1985).

6.3 LITHOSPHERIC STRENGTH AND EVOLUTION OF THE WESTERN GHATS

The Western Ghats extending over a distance of 1500 km parallel to the coast has characteristics of rift flank uplift topographic similar to those observed along many other rifted continental margins. It runs through varied lithologies and Dikshit (1981) observed contrastingly different morphology for Western Ghats north and south of 16° N. As the present study region falls south of 16° N, the results would provide valuable input in understanding evolution of the non-volcanic segment of the Western Ghats.

Several mechanisms of formation of flank – uplift topography at the passive margins are available from many previous studies (McKenzie, 1978; Royden and Keen, 1980; Cochran, 1983; Buck, 1986; Wiessel and Karner, 1989; among others). However, these models failed explain the process by which topography was retained over geological times. Gilchrist and Summerfield (1990) and Gallagher et al., 1995) highlighted the significance of onshore denudational history to explain the present day topography at the margin and suggested that margins not only remain elevated but also sometimes undergo uplift. Gilchrist and Summerfield (1990) suggested that the Western Ghats topography has evolved as a consequence of differential denudation and flexural isostasy. Many later workers analysed this problem using onshore erosional history (Widdowson and Cox, 1996, Widdowson, 1997), Apatite Fission Track Analysis (Kalaswad et al., 1993; Gunnell et al., 2003), and post – rift onshore denudation and offshore sedimentation (Gunnell and Fleitout, 1998; Gunnell and Radhakrishna; 2001; Chand and Subrahmanyam, 2003).

It is now well known that flexural strength of the lithosphere (Te) is important in model studies related to flank uplift topography to estimate upward deflection (or rebound) due to denudational unloading in the onshore or downward deflection (or subsidence) due to sediment loading in the offshore. Elastic thickness estimates for the lithosphere in the region, as discussed above, indicate low strength with Te values 5-15 Km at the southwest margin and 11-16 km for the Indian shield. If these values represent the long-term strength of the lithosphere, it is indicative of a weaker lithosphere since rifting in both onshore as well as offshore areas of the southwest margin. This observation is in contrast to the Te values obtained through denudation driven flexural modeling by Gunnell and Fleitout (1998), where Te values are much higher of the order of 70 km in the case of broken plate model and 35 km in the case of continuous plate model. It must be pointed out that one must consider the flexural effects of loss of material due to erosion of rift flank and its deposition offshore while attempting to reconstruct the rift flank uplift topography. The gravity based analysis through combined backstripping and backstacking presented in the previous chapter ruled out the magmatic underplating as a mechanism for flank uplift during rifting and suggested that a Te of 5- 10 km and deep level of necking (Depth of Necking 20 km) can explain the topography of the Western Ghats. Similar observation made by Chand and Subrahmanyam (2003) for Western Ghats topographic evolution further strengthens the above result. Also, observations in other margins (Buck, 1991; Kooi et al., 1992; Hopper and Buck, 1996), where rifting took place in an old craton point to the necking phenomenon acting as the cause for rift-flank uplift.

6.4 GEOPHYSICAL CHARACTERISTICS AND PROBABLE MODE OF EMPLACEMENT OF COMORIN RIDGE

Marine geophysical studies in the region of Comorin Ridge indicate that, the ridge is a structural feature marking the boundary between the continental and oceanic crust (Kahle et al., 1981), or, it is a transform ridge formed during early phase of opening of Indian Ocean (Desa et al., 2006). From the existing knowledge, it is not clear whether the ridge had formed during India- Madagascar break up or during an earlier break up of Gondwanaland at the southwest margin of Sri Lanka. Geomagnetic induction models reveal the presence of an anomalous conductive structure below the Comorin ridge (Thakur et al., 1986; Mareschel et al., 1987; Agarwal and Weaver, 1989). Arora et al. (2003) referred to this conductive structure as South India Offshore Conductive Anomaly (SIOCA). They noticed that SIOCA spatially correlates with other broad wavelength geophysical signatures observed south of India such as low velocity region, low magnetization anomaly and the Indian Ocean Geoid low. As SIOCA requires large amount of partial melt at depth, Arora et al. (2003) inferred that active interaction of Marion mantle plume at the margin during break up resulted in large-scale volcanism and substantial partial melt. Though such an inference can convincingly explain the SIOCA, still the mode of emplacement of the Comorin ridge at the Ocean continent boundary (OCB) is not known. As we believe that the Marion mantle plume did not play an active role at the Indian margin during break up, the presence of large partial melt zone in the region of Comorin ridge as well as its emplacement at OCB may have to be explained by a mechanism other than the Marion plume. However, in support of active Marion plume interaction, it can be argued that the thermal effect due to the plume died out, while mechanical strength is regained and partial melts persist in the region. Fluids can persist for longer geological time; say 100my, only if the crust remains stable thermally and mechanically (Bailey, 1990). Our observation of Te 10 km in the Comorin ridge region do not indicate a very weak plume affected lithosphere, therefore, the partial melt zone has little to do with the abnormal thermal activity arising from the plume. In such a situation, the convective partial melting model proposed by Mutter et al. (1988) is useful to explain the presence of partial melt zone. The mechanism of convective partial melting does not require hot mantle and a large amount of mantle material is propelled through the melting zone that results in large melt volumes. This process can produce more than three times of melt than the passive rifting and spreading becomes normal within few million years after its inception (Hinz et al., 1987). We consider this alternative scheme because it not only explains the presence of partial melts but also, provides a mechanism of emplacement of the Comorin Ridge.

Similar to the Comorin Ridge, many continental margins have revealed the presence of topographic and basement highs or ridges. Based on their geophysical signatures, such features have been inferred as structural highs formed at the OCB (Scrutton and Du Plessis,1973; Talwani and Eldholm, 1973, 1977; Rabinowitz and La Brecque, 1977; Eldholm and Sundvor, 1980; Mauffret and Montadert, 1987; among others). These marginal topographic highs or ridge like features may represent uplifted continental crustal blocks formed as outer high during late rift stage (Schuepbach and Vail, 1980), emplacement of the mantle rocks (Peridotite) bounding the thinned continental crust at the OCB just before initiation of oceanic crustal accretion (Mauffret and Montadert,1987; Boillot et al., 1988), oceanic basement highs when the oceanic material is injected at higher elevations (Rabinowitz and La Brecque,1977), initial high rate of basaltic intrusion at the onset of normal seafloor spreading or faulting in the newly formed oceanic crust (Eldholm and Sundvor,1980). The mechanisms of emplacement of marginal topographic highs discussed above involve passive rifting and normal sea floor spreading, and therefore, do not give rise to large amounts of partial melt that was inferred below the Comorin Ridge. The location of OCB along the eastern edge of the Comorin Ridge (Kahle et al., 1981) indicated that the ridge is made up of oceanic crust formed at the onset of seafloor spreading. Rapid initial seafloor spreading generated excess volcanism through strong convection which had emplaced the ridge as an oceanic basement high. It should be noted that large scale volcanism may blur the crustal transition and therefore, may not produce a sharp boundary between the continental and oceanic crust (Hinz et al., 1987). Such crustal contamination and absence of sharp OCB may be possible for the Comorin Ridge, as no clear magnetic edge effect anomaly or diagnostic magnetic signature is seen associated with the isostatic gradient at the eastern edge of the ridge (Kahle et al., 1981).

****

CHAPTER 7 SUMMARY AND CONCLUSIONS

The Continental Margins of India, evolved due to rift-drift events of the Indian subcontinent, is an extensive Atlantic type passive continental margin. It extends on either side of the Indian Peninsular shield and is generally referred as Eastern Continental Margin of India (ECMI) and Western Continental Margin of India (WCMI). The WCMI has evolved through rifting and subsequent seafloor spreading between India and Madagascar at 88 Ma. The margin comprises of several surface/sub-surface structural features that include the Chagos-Laccadive Ridge (CLR), Laxmi Ridge (LR), Pratap Ridge (PR) and a belt of numerous horst graben structures in the sediment filled basins bordering the West Coast of India. The WCMI comprises of five major sedimentary basins. These are Kutch, Saurashtra, Bombay, Konkan and Kerala basins and are separated by southwesterly trending structures namely, the Saurashtra Arch, Surat depression, Vengurla Arch and Tellicherry Arch respectively. The juxtaposition of WCMI and Eastern Continental Margin of Madagascar (ECMM) is consistent with Precambrian trends, lithologies and age provinces.

The continental breakup in Gondwanaland is believed to have resulted from the interaction of series of hotspots or mantle plumes. Approximately around 88 Ma, the combined India - Madagascar - Seychelles block came over the location of the Marion mantle plume. As a result, the separation of Madagascar from Seychelles-India block occurred. The separation of Seychelles and India took place during the Paleocene. The widespread volcanism over the Indian landmass due to Re Union mantle plume at K-T boundary (~65 Ma) led to the formation of Deccan Continental Flood Basalt Province. As India moved further north, the influence of this hotspot created Chagos-Laccadive Ridge and reorganization of nearby spreading centers in the oceanic areas. Major morpho-tectonic features in the Arabian Sea are believed to have been inherited from the breakup history of Madagascar and Seychelles from India. Six contiguous tectonic elements running north-south in the shelf and deep oceanic areas of the

Arabian Sea have been identified along the WCMI. These are shelfal horst-graben complex, Kori-Comorin ridge, Laxmi-Laccadive depression, Laxmi-Laccadive ridge and Arabian abyssal plain. The Western offshore contains several deep water sedimentary basins extending from Kutch in the north to Cape-Comorin in the south. The formation of these basins occurred because of the thermo-mechanical evolution of the continental margin since the breakup of Madagascar around 88 Ma.

The offshore area between the Vengurla Arch in the north and Tellicherry Arch in the south along the central part of the west cost of India is known as the Konkan basin. Several structural features such as the Pratap Ridge complex, the shelf-margin basin, the mid shelf basement ridge and inner shelf graben are delineated in the Konkan Offshore. The Kerala offshore basin located south of Tellicherry Arch was formed during Middle to late Cretaceous as a result of an early phase of rifting between India and Madagascar. Alleppey platform is the major tectono-morphological element in the shelfal horst - graben complex. The shelfal horst-graben complex consists of two major depressions called Cochin depression and Cape - Comorin depression.

The WCMI is bordered by coastal region of low elevation with an average width of 50 km. The coastal region rises in small steps and there is a drastic change in altitude, which reaches even up to 1500 m that runs parallel to the coast along its entire length. This precipitous terrain which is well known as Western Ghats is having highly varied lithologies like peninsular gneisses, granulites and Deccan basalts. This feature has been considered to be formed as a result of differential denudation and flexural isostasy. Apatite Fission Track Analysis (AFTA) indicates that the escarpments formed due to uplift during rifting followed by a lateral scarp retreat.

In the present study, the southern part of WCMI outside the Deccan Volcanic Province (DVP) has been considered for detailed geophysical data analysis. A systematic gravity data analysis and interpretation integrated with available seismic data has been carried out in order to estimate the effective elastic thickness (Te) at selected segments of the margin and analyse spatial variations in elastic strength during rifting and flexure due to sedimentation, and model the flank uplift topography during rifting and subsequent evolution of Western Ghats.

The study region consists of Konkan and Kerala offshore basins, and the deep oceanic parts of the Arabian Sea covering the Chagos Laccadive and Carlsberg Ridges. South of the WCMI and Southwest of Sri Lanka, the distinct topographic expression of the Comorin Ridge can be seen aligned along the margin. In view of its significance, the Comorin Ridge is also considered in the present study. The study area lies between 63° E to 80° E longitude, 0 to 16° N latitude.

The strength of the lithosphere is an important factor that determines the amount of bending and the degree to which the compensation approaches the prediction of local models. It is well known that the lithosphere responds to long term geological loads not locally, as Airy and Pratt models would predict, but regionally by flexure. Significant information has been derived from the studies on elastic thickness of the lithosphere regarding the long-term mechanical properties of the lithosphere and the relationship to plate and load age. The amplitude and wavelength of the gravity anomalies at the continental margin are sensitive to the value of effective elastic thickness (Te). The gravity anomaly at the continental margins can be considered as a result of several processes that include rifting, sedimentation, erosion and magmatic underplating operating through time. This distinctive gravity field at the margin called 'edge effect anomaly', a gravity high over the outer shelf, and low associated with the slope and rise regions, has been modeled by several workers to understand the crustal processes and geodynamics of the passive continental margins. Two different approaches are available to model this edge effect gravity anomaly of the margin, one, is through isostatic response estimates using admittance/coherence to model the isostasy in terms of flexural isostatic compensation mechanisms, the other is through process oriented approach in which detailed crustal seismic information on initial crustal structure (from seismic reflection and refraction data) is incorporated to model the gravity edge effect anomaly by clubbing the gravity contributions from different processes such as rifting, sedimentation, erosion and underplating.

In the present thesis, these two approaches are dealt in detail along the southern part of WCMI to understand the geodynamic evolution of the margin. The basic geophysical data required for such a study is the gravity and topographic data in the margin. As the available ship-borne bathymetry data is sparse in the region, the 1-minute grid digital GEBCO bathymetry in the offshore areas has been used throughout the study. Though vast amount of ship-borne gravity data have been acquired by several national and international agencies along the WCMI and the adjoining oceanic areas, still large data gaps exists and the coverage was not uniform. The satellite derived GEOSAT free air gravity data gives a uniform coverage of 2-minute interval in the offshore areas. A comparison of the satellite derived GEOSAT gravity and GEBCO bathymetry with the shipboard gravity and bathymetry reveal that both data sets match well along the Indian offshore regions. These two data sets were essentially used to carry out analysis of gravity and topography at the southwest margin of India.

The free air anomaly is in general smaller and approaches to zero at longer wavelengths. On the other hand, the Bouguer anomaly strongly correlates with the topography at longer wavelengths. In general, the correlation of the Bouguer anomaly to topography is wavelength dependent. This wavelength dependency is useful in evaluating the isostatic compensation over topographic features. In addition, the wavelength range at which the transition from compensated to uncompensated topography occurs is diagnostic of the lithospheric rigidity. As the simple Bouguer anomaly contains errors due to strong lateral topographic variations, terrain correction was applied to the data to obtain Complete Bouguer anomaly. In the present study, the coherence analysis of gravity and bathymetric data has been carried out using the Maximum Entropy Spectral Estimation (MESE) method to understand the spatial variations in the effective elastic thickness (Te) at the southwest margin of India and the adjoining oceanic areas. For this purpose, from the complete Bouguer anomaly and effective bathymetry data grids prepared at 5 km interval in the study region, several data windows have been extracted centered on various geological features/structures of interest. The study indicates that the Te estimates vary from 5 km – 10 km in the southwest margin of India and increases from north to south. A maximum Te value of 10 km is obtained along the Comorin Ridge. The effective elastic thickness obtained for the selected windows is as follows : Konkan basin – 5 km, Kerala basin – 8 km, Comorin Ridge – 10 km, Chagos Laccadive ridge (North) – 5 km, Chagos Laccadive Ridge (South) – 8 km, Carlsberg Ridge – 7 km.

From all available seismic information, two seismogeologic sections, one, in the Konkan basin, and, the other, in the Kerala basin were constructed for further analysis. The lithological and stratigraphic information for these two sections have been obtained by tying the sections to the nearest well data, such as, KR-1-1 in the Konkan basin and the CH-1-1 and K-1-1 in the Kerala basin. From the gridded gravity data, the gravity anomalies have been projected on to these sections. In the present investigation, the above litho-stratigraphic sections depicting major sedimentary layers in the Konkan and Kerala basins along with the gravity data have been utilized to study the sediment loading, lithospheric flexure and dynamics of rifting at the margin. The result obtained for the lithospheric necking model along the Konkan basin suggests a lithospheric strength of 5 km and the depth of necking (DON) of 20 km at the time of rifting. For the Kerala basin, the analysis brings out a lithospheric strength of 10 km and DON 20 km. For the magmatic underplating model, the results show a Te of 5 km in the

Konkan basin and Te of 10 km in the Kerala basin. Nearly, 5-6 km of underplated material is required to explain the rift-flank topography at the margin. From the observed and calculated anomalies for both lithospheric necking and magmatic underplating models, it can be concluded that the necking model better explains the observed gravity anomalies at the southern part of the WCMI. The DON estimates suggest that deep level of necking occurs along the southern part of WCMI during rifting.

Analysis of gravity and bathymetry data along the southwest continental margin of India and the adjoining oceanic areas give rise to effective elastic thickness Te estimates ranging between 5-10 km for the Konkan and Kerala basins and the Comorin Ridge along the margin. The elastic thickness increase southward and maximum Te of 10 km is observed below the Comorin Ridge. The Chagos Laccadive Ridge shows on elastic strength of 5 – 8 km along part of the ridge north of equator. These results, when compared with the Te values obtained from process oriented gravity modeling, indicate low elastic strength < 15 km at the southwest margin but not as low as that observed below active plume affected margins. Other geological factors also support the limited role played by the Marion mantle plume during the rifting and breakup of India and Madagascar. The presence of substantial partial melt zone in the Comorin Ridge region, as observed by the geomagnetic induction models can be alternatively explained, if we invoke the convective partial melting model. The Comorin Ridge might have been emplaced as an oceanic basement high due to large scale volcanism during the onset of seafloor spreading. Due to the strong lateral variations in terms of rifting style, strength, sedimentation along different segments in a continental margin setting, the invoked model could be relevant only in the region of the Comorin Ridge. The gravity based analysis through combined backstripping and backstacking method ruled out the magmatic underplating as a mechanism for flank uplift during rifting and suggested that a Te of 5 – 10 km and deep level of necking (DON $= 20$ km) can explain the topography of Western Ghats. However, detailed seismic data at the southwest margin is required to understand the nature of crust and processes during rifting and breakup of Gondwanaland. Recognizing various tectonic, magmatic and the related structural factors along with their geophysical characteristics is the key to understand the evolutionary history in different segments of the margin.

****

REFERENCES

Agarwal, A.K. and Weaver, J.T. (1989), Regional electromagnetic induction around the Indian Peninsula and Sri Lanka: A three-dimensional numerical model study using the thin sheet approximation. Phys. Earth Planet. Inter. v.54, pp. 320-331.

Agarwal, P. K., Pandey, O. P. and Negi, J. G. (1992). Madagascar : a continental fragment of the paleo super Dharwar craton of India. Geology, v. 20, pp. 543-546.

Anil Kumar, Pande, K., Venkatesan, T.R. And Bhaskar Rao, Y.J. (2001). The Karnataka Late Cretaceous dykes as products of the Marion hotspot at the Madagascar-India breakup event: evidence from 40Ar-39Ar geochronology and geochemistry. Geophys. Res. Lett., v. 28, pp. 2715-2718.

Arora, B.R., Subba Rao, P.B.V. and Nagar, V. (2003). Electrical conductivity signatures of plume - lithosphere interactions in the Indian Ocean. Mem. Geol. Soc. India, v.53, pp. 393-418.

Arts, K.P., Radhakrishna, M., Murthy, B.V.S, Arora, S.K. and Nambiar, C.G. (2003). Gravity anomalies, structure and tectonics of the Kerala Basin, Southwest Continental Margin of India. Mem. Geol. Soc. India., v.54, pp. 203-216.

Ashalatha, B., Subrahmanyam, C. and Singh RN (1991) Origin and emplacement of Chagos – Laccadive ridge, Indian Ocean, from admittance analysis of gravity and bathymetry data. Earth Planet Sci. Lett. v.105, pp. 47 – 54.

Aubert O, Droxler AW (1996) Seismic stratigraphy and depositional signatures of the Maldive carbonate system (Indian Ocean). Mar Petrol Geol., v.13,pp. 503–536.

Babenko, K. M., Panayev, V. A. and Svistunov, Y. I. (1980). Structure of the sedimentary layer of the Arabian Sea. Dokl. Akad. Nauk. SSSR, v. 237, pp. 60-63 (English Translation).

Bachman, R. T. and Hamilton, E. L. (1980). Sediment sound velocities from sonobuoys: Arabian Fan. Jour. Geophys. Res., v. 85, pp. 849-852.

Bailey, R.C. (1990). Trapping Of Aqueous Fluids In The Deep Crust. Geophysical Research Letters, v.17 pp.1129-1132.

Ballina, L.H.R. (1990). Fortran Program For Automatic Terrain Correction Of Gravity Measurements. Computers and Geosciences, v.16, pp. 237-244.

Barton, P. J. and Wood, R. J. (1984). Tectonic evolution of the North Sea basin: crustal stretching and subsidence. Geophys. J. R. astr. Soc., v.79, pp. 987–1022.

Bechtel, T. D., (1989).Mechanisms of isostatic compensation in East Africa and North America, Ph.D. thesis, Brown Univ., Providence, R. I.

Bechtel, T.D.., D.W.Forsyth, and C.J. Swain (1987), Mechanisms of isostatic compensiaton in the vicinity of the East African Rift, Kenya, Geophy. J. R.Aston. Soc. v. 90, pp 445-465.

Ben Avraham, Z. and Bunce, E.T (1977) Geophysical Study of the Chagos-Laccadive Ridge, Indian Ocean. J. Geophys. Res, v.82, pp.1295-1305.

Bendat, J. S., and A. G. Piersol, (1993).Engineering Applications of correlation and spectral analysis, 2nd ed., John Wiley, New York.

Bendat, J. S., and Piersol, A. G., (1986). Random data: Analysis and measurement procedures: John Wiley and Sons, New York, pp.566.

Besse, J. and Courtillot, V. (1988). Paleogeographic maps of the continents bordering the Indian Ocean since the early Jurassic. Jour. Geophys. Res., v. 93, pp. 11791-11808.

Bhattacharya, G. C., Chaubey, A. K., Murthy, G. P. S., Srinivas, K., Sarma, K. V. L. N. S., Subrahmanyam, V. and Krishna, K. S. (1994), Evidence for sea floor spreading in the Laxmi basin, northeastern Arabian Sea. Earth Planet. Sci. Lett., v. 125, pp. 211 – 220.

Bhattacharya, G. C., G. P. S. Murty, K. Srinivas, A. K. Chaubey, T. Sudhakar, and R. R. Nair (1994b), Swath bathymetric investigation of the seamounts located in the Laxmi Basin, eastern Arabian Sea, Mar. Geod., v.17, pp.169 – 182.

Biswas, S. K. (1982). Rift basins in western margin of India and their hydrocarbon prospects with special reference to Kutch basin. Am. Assoc. Pet. Geol. Bull., v. 64, pp. 209 – 220.

Biswas, S. K. (1987). Regional tectonic framework, structure and evolution of the western marginal basins of India. Tectonophysics, v. 135, pp. 307 – 327.

Biswas, S. K. (1988). Structure of the western continental margin of India and related igneous activity. Geol. Surv. Ind., Mem., v.10, pp. 371-390.

Biswas, S. K. and Singh, N. K. (1988). Western continental margin of India and hydrocarbon potential of deep sea basins. 7th offshore south Asia conference, Singapore. pp. 170-181.

Biswas, S. K. (2001). Structure of the western continental margin of India and related igneous activity. Memoir, Geological Society of India, v. 47, pp. 349-364.

Boillot, G., Girardeau, J. And Kornprobst, J. (1988) Rifting of the Galicia margin: crustal thinning and emplacement of mantle rocks on the seafloor. Proc. ODP sci. results, v.103, pp. 741-755.

Bott, M.H.P. and Kusznir, N. (1979) Stress distributions associated with compensated plateau uplift structures with application to the continental splitting mechanism. Geophys. J. R. Astron. Soc., 56, 451–459.

Braun, J. and Beaumont, C., (1989). A physical explanation of the relation between flank uplifts and the breakup unconformity at rifted continental margins. Geology, v.17, pp. 760-764.

Brown, R.W. (1991) Backstacking apatite fission-track 'stratigraphy': a method for resolving the erosional and isostatic rebound components of tectonic uplift histories.,Geology, v.19, pp. 74-77.

Brown, R.W., Rust, D.J., Summerfield, M.A., Gleadow, A.J. and Dewitt, M.C.J. (1990) An Early Cretaceous phase of accelerated erosion on the south-western margin of Africa: evidence from apatite fission track analysis and the offshore sedimentary record., Nuclear Tracks Radiation Measurement , v. 17, pp. 339–350.

Buck W.R. (1986). Small-scale convection induced by passive rifting: The cause for uplift of rift shoulders. Earth Planet. Sci. Lett., v.77, pp. 362-372.

Buck, W. R. (1991). Modes of continental lithospheric. Extension. J. of Geophys. Res., v. 96, pp. 20161–20178.

Burg J.P. (1975), Maximum entropy spectral analysis, Ph.D. dissertation, Stanford University. Standford, Calif.

Chand, S and Subrahmanyam, C. (2003). Rifting between India and Madagascar – mechanism and Isostasy. Earth Planet Sci. Lett., v.210, pp. 317–332.

Chand, S., Radhakrishna, M. and Subrahmanyam, C. (2001). India - East Antartica conjugate margins: Gravity and isostasy. Earth Planet Sci. Lett. v.185, pp. 225-237

Chand, S., 2001. Subsidence analysis along the continental margins of India. PhD thesis, Osmania University.

Chandrasekharam, D. (1985) Structure and evolution of the western continental margin of India deduced from gravity, seismic, geomagnetic and geochronological studies. Phy. Earth Planet Interiors, v. 41, pp. 186-198.

Chaubey, A. K., Bhattacharya, G. C. and Gopala Rao, D. (1995). Sea floor spreading magnetic anomalies in the southeastern Arabian Sea, Marine Geology, v. 128, pp. 105 – 114.

Chaubey, A. K., Bhattacharya, G. C., Murthy, G. P. S. and Desa, M. (1993). Spreading history of the Arabian Sea: some new constraints. Marine Geology, v. 112, pp. 343-352.

Chaubey, A. K., Bhattacharya, G. C., Murty,G. P. S., Srinivas, K., Ramprasad, T and Gopala Rao, D. (1998). Early Tertiary seafloor spreading magnetic anomalies and paleo-propagators in the northern Arabian Sea. Earth Planet. Sci. Lett., v. 154, pp. 41-52.

Chaubey, A. K., Gopala Rao, D., Srinivas, K., Ramprasad, T., Ramana, M. V. and Subrahmanyam, V. (2002). Analysis of multichannel seismic reflection, gravity and magnetic data along a regional profile across the central-western continental margin of India. Marine Geology, v. 182, pp. 303-323.

Chave, A.D., D.J. Thomson, and M.E. Ander, (1987). On the robust estimation of power spectra, coherences, and transfer functions. J. Geophys. Res., v. 92,pp. 633-648.

Closs, H., Bungenstock, H. and Hinz, K. (1969). Results of seismic refraction measurements in the northern Arabian Sea. A contribution to the International Indian Ocean Expedition. Meteor.Res.Results, v. (3), pp. 1-28.

Cochran, J.R. (1983). Effects of finite extension times on the development of sedimentary basins. Earth Planet. Sci. Lett., v. 66, pp. 289-302.

Cochran, M.D. (1973), Seismic signal detection using sign-bits, Geophysics, v. 36, pp. 1042–1052.

Coffin, M. F. and Rabinowitz, P. D., (1987). Reconstruction of Madagascar and Africa: Evidence from the Davie Fracture zone and western Somali basin. Jour. Geophys. Res., v.92, pp. 9385-9406.

Courtillot, V, Feraud G, Maluski H, Vandamme D, Moreau, M G and Besse J, (1988) Deccan flood basalts and the Cretaceous/Tertiary boundary; Nature v.333, pp. 843–846.

Courtillot, V., Besse, J., Vandamme, D., Montigny, R., Jaeger, J. J. and Cappetta, H. (1986). Deccan flood basalts at the Cretaceous/Tertiary boundary? Earth Planet. Sci. Lett., v.80, pp. 361-374.

Courtillot, V., Jaupart, C., Manighetti, I., Tapponnier, P. and Besse, J. (1999). On causal links between flood basalts and continental break up. Earth Planet. Sci. Lett., v.166, pp. 177-195.

Courtney, R. C and Beaumont, C. (1983). Thermally-activated creep and flexure of the oceanic lithosphere. Nature , v. 305,pp. 201–204.

Cox, K. G. (1989). The role of mantle plumes in the development of continental drainage patterns. Nature, v.342, pp. 873-877.

Crawford, A. R. J. (1978). Narmada/Son lineament of India traced in to Madagascar. J. Geol. Soc. of India, v. 19, pp. 144-153.

Daly, E., Brown, C., Stark, C.P. and Ebinger, C.J. (2004). Wavelet and multitaper coherence methods for assessing the elastic thickness of the Irish Atlantic margin. Geophys. J. Int., v.159, pp. 445-459.

Desa, M., Ramana, M.V.And Ramprasad, T. (2006). Seafloor spreading magnetic anomalies south off Sri Lanka. Marine Geology, v.229 , pp. 227-240.

Devey, C.W. and Stephens, W.E., (1991). Tholeiitic dykes in the Seychelles and original spatial extent of the Deccan. J. Geol. Soc. Lond., v.148, pp. 979–983.

Dewey, J.F. and Burke, K. (1974). Hotspots and continental break-up: implications for collisional orogeny. Geology v.2, pp.57-60.

Diament, M., Sibuet, J.C. and Hadaoui, A. (1986). Isostasy of the Northern Bay of Biscay Continental Margin. Geophys. J. R. Astr. Soc., v. 86, pp. 893-907.

Dikshit, K.R. (1981) The Western Ghats : A Geomorphic Overview. New Perspectives In Geography .

Dirghangi, R. S., Kothari, V., Waraich, R. S., Baruah, R. M., Lal N. K. and Zutshi P. L. (2000). 3rd Conference and Exposition on Petroleum Geophysics, New Delhi, India, pp. 278-283.

Dorman, L.M., Lewis, B.T. (1970). Experimental isostasy, 1, Theory of the determination of the earth's isostatic response to a concentrated load. J. Geophys. Res., v. 75, pp. 3357-3366.

Duncan, R. A and D.G.Pyle (1988) Rapid eruption of the Deccan flood basalts at the Cretaceous/Tertiary boundary, Nature, 333, 841–843.

Duncan, R. A., (1990). The volcanic record of the Reunion hot spot. Proc. Ocean. Drill. Prog. Results, v. 5, pp. 3-10.

Einsele, G., (1992) Sedimentary basins : Evolution, facies and sediment budget, Springer Verlag Publishers, pp. 628.

Eldholm, O. and Sundvor, E. (1980). The Continental Margin of the Norwegian-Greenland Sea: recent results and outstanding problems. Phil.Trans.R. Soc.Lond., v.A 294, pp. 77-86.

Embleton, B. J. J. and McElhinney, M. W. (1975). The palaeo position of Madagascar: Palaeomagnetic evidence from the Isalo group. Earth. Planet. Sci. Lett., v. 27, pp. 329-341.

Eremenko, N. A. and Datta, A. K. (1968). Bull. Oil and Natural Gas Comm. v. 5(1), pp. 29-40.

Ewing, M., Eittreim, S. L., Truchan, M. and Ewing, J. (1969). Sediment distribution in the Indian Ocean. Deep-sea Res., v. 16, pp. 231-248.

Forsyth, D.W. (1985). Subsurface loading and estimates of the flexural rigidity of Continental Lithosphere. J. Geophys. Res., v 90., pp. 12623– 12632.

Fowler, S. and Mckenzie, D.P. (1989). Gravity studies of the Rockall and Exmouth plateau using SEASAT altimetry. Basin Research, v.1 , pp. 27-34.

Fowler, S. R., White, R. S., Spence, G. D. & Westbrook, G. K. (1989). The Hatton Bank continental margin II. Deep structure from two-ship expanding spread seismic profiles. Geophysical Journal, v. 96, pp. 295–309.

Gallagher ,K.C., Hawkesworth and Mantovani, M. (1995) Denudation fission track analysis and the long term evolution of passive margin topography: Application to the SE Brazilian margin, J. South.am.Earth.Sci.,v.8, pp. 65-77.

Gallagher, K. and Brown R. (1997) The onshore record of passive margin evolution., J. Geol. Soc. Lond., v.154, pp. 451 457.

Gallagher, K., Brown, R. and Johnson, C. (1998). Fission track analysis and its applications to geological problems. Annu. Rev. Earth. Planet. Sci., v. 26, pp. 519-572.

Gallagher, K., Hawkesworth, C.J. and Mantovani, M.S.M.,(1994), The denudation history of the onshore continental margin of SE Brazil inferred from apatite fission track data. J. Geophys. Res., v. 99, no. B9, pp.18.117-18.145.

Ghosh, B. N., Zutshi, P. L., (1989), Indian west coast shelf break tectonic features, Geol. Surv. Ind. Spl. Pub. v.24, pp. 309 – 318.

Gilchrist, A. R. and Summerfield, M. A. (1990). Differential denudation and flexural isostasy in the formation of rifted margin upwarps. Nature, v. 346, pp. 739-742.

Gilchrist, A. R. and Summerfield, M. A. (1991). Denudation, isostasy and landscape evolution. Earth Surface Processes and Landforms, v. 16, pp. 555 - 562.

Gilchrist, A. R., H. Kooi, and C. Beaumont (1994). The post-Gondwana geomorphic evolution of southwestern Africa: Implications for the controls on landscape development from observations and numerical experiments. J. Geophys. Res., v. 99, pp. 12211– 12228.

Gopala Rao, D. (1990). Magnetic studies of basement off the coast of Bombay, west India. Tectonophysics, v. 174, pp. 1-18.

Gordon, R. G. and DeMets, C. (1989). Present-day motion along the Owen Fracture Zone and Dalrymple Trough in the Arabian Sea. J. Geophys. Res., v. 94, pp. 5560-5570.

Green, A. G. (1972). Seafloor spreading in the Mozambique channel. Nature, Physical Science, v. 236, pp. 19-21.

Gunnell, Y., Fleitout L.(2000) Morphotectonic Evolution Of the Western Ghats, India, In M. A. Summerfield (Eds), Geomorphology and Global Tectonics:John Wiley & Sons, Chichester ; New York, pp. 321-338.

Gunnell, Y., and Fleitout, L. (1998) Shoulder uplift of the Western Ghats Passive margin, India: A denudational model. Earth surface processes and landforms, v.23, pp 391-404.

Gunnell, Y., and Radhakrishna B.P., (2001). Sahyadri, the great escarpment of the Indian subcontinent. Mem. Geol. Soc. of India, v. 47(1), pp. 717.

Gunnell, Y., Gallagher, K., Carter, A., Widdowson, M., and Hurford, A.J.(2003). Denudation history of the continental margin of western peninsular India since the early Mesozoic – Reconciling apatite fission – track data with geomorphology: Earth and Planet. Sci. Lett., v 2., pp 187-201.

Harbinson, R. N. and Bassinger, B. C. (1973). Marine Geophysical study of western India. Jour. Geophys. Res., v. 78, pp. 432 – 440.

Hinz, K., Mutter, J.C., Zehnder, C.M. and The NGT Study Group (1987) symmetric conjugation of continent-ocean boundary structures along the Norwegian and east Greenland Margins. Mar. Pet. Geol., v.166, pp. 165-187.

Holt, W.E. and Stern, T.A. (1991). Sediment loading on the western margin of the New Zealand Continent: implications for the strength of young continental lithosphere. Earth and Planetary Science Letters, v. 107, pp.523-538.

Hooper P. R., (1990). The timing of crustal extension and the eruption of continental flood basalts. Nature v.345, pp. 246-249.

Hopper, J. R. ; Buck, W. R. (1996). The effect of lower crustal flow on continental extension and passive margin formation. J. Geophys. Res., v. 101 , No. B9 , pp. 20,175

Horsfield S. J., R. B. Whitmarsh, R. S. White, and J. C. Sibuet, (1993) .Crustal structure of the Goban Spur rifted continental margin NE Atlantic, Geo- phys. J. Int., v. 119,pp. 1–19,

Jaeger, J.J., Courtillot, V. and Taponnier P., (1989). Paleontological view of the ages of the Deccan Traps, the Cretaceous/Tertiary boundary, and the India-Asia collision. Geology, v. 17, pp. 316–319.

Johnson B. D., Powell, C. M., Veevers, J. J. (1976). Spreading history of the Eastern Indian Ocean and Greater India's flight from Antarctica and Australia, Geol. Soc. Am. Bull. v. 87, 1560-1566.

Kahle, H-G., Naini, B.R., Talwani, M. and Eldholm, O (1981) Marine geophysical study of the Comorin Ridge, North Central Indian Basin. J. Geophys. Res. v. 86, pp. 3807-3814.

Kalaswad, S., Roden, M.K., Miller D.S., and Morisawa, M. (1993). Evolution of the continental margin of Western India - New evidence from Apatite Fission track dating. Journal of Geology, v.101, pp. 667-673.

Kane, M.F. (1962). A comprehensive system of terrain corrections using a digital computer. Geophysics, v.27, No 4, pp. 455–462.

Karasik, A. M., Merkur'yev, S. A., Mitin, L. I., Sochevanova, N. A. and Yanovskiy, V. N. (1986). Main features in the history of opening of the Arabian Sea, according to data of a systematic magnetic survey. Doklady Akademii Nauk. SSSR, v. 286, pp. 933-938.

Karner, G.D. (1991) Sediment blanketing and the flexural strength of extended continental lithosphere. Basin Res. v.3, pp. 177–185.

Karner, G.D. and Watts, A.B. (1982) On isostasy at Atlantic - type continental margins. J. Geophys. Res. v. 87, pp. 2923-2948.

Katz, M.B. And Premoli, C. (1979). India and Madagascar in Gondwanaland based on matching Precambrian lineaments. Nature, v. 279, pp. 312-315.

Kay, S. M, (1988). Modern Spectral Estimation. Prentice-Hall, Englewood Cliffs, N. J.

Kay, S. M., and S. L. Marple, (1981).Spectrum analysis: A modern perspective. Proc. IEEE, v.69, 1380– 1419.

Kent, R. W, Storey M and Saunders A D , (1992) Large igneous provinces: sites of plume impact or plume incubation; Geology, v. 20 , pp. 891–894.

Kent, R. (1991). Lithospheric uplift in Eastern Gondwana : Evidence for a long-lived mantle plume system. Geology, v. 19, pp. 19-23.

Khain, V.Yu., (1992). The role of rifting in the evolution of the Earth's crust. Tectonophysics v.215, 1-7.

King, L. C. (1962) The Morphology of the Earth.Edinburgh: Oliver & Boyd (2nd. ed., 1967).

Kolla, V. And Coumes, F. (1990) Extension of structural and tectonic transform from the Indian subcontinent into the eastern Arabian Sea. Mar. and Pet. Geol. v. 7, pp. 188-196.

Kolla, V. and Coumes, F.(1987). Morphology, internal structure, seismic stratigraphy and sedimentation of the Indus Fan, Am. Assoc. Petrol. Geol. Bull., v. 71, pp. 650-677.

Kooi, H. and C. Beaumont (1994). Escarpment evolution on high-elevation rifted margins; Insights derived from a surface-processes model that combines diffusion, advection and reaction. J. Geoph. Res., v. 99, pp 12191- 12209.

Kooi, H. and S. Cloetingh (1992). Lithospheric necking and regional isostasy at extensional basins 2. Stress-induced vertical motions and relative sea level changes. J. Geoph. Res. v. 97, pp. 17573-17591.

Kooi, H. Cloetingh, S. Burrus, J.(1992) Lithospheric necking and regional isostasy at extensional basins 1. Subsidence and gravity modeling with an application to the Gulf of Lions margin (SE France), J. Geophys. Res. v 97 pp. 17553-17571.

Krishna et al., (2006), Nature of the crust in the Laxmi Basin (14°–20°N), western continental margin of India, Tectonics, v. 25, TC1006, Doi: 10.1029/2004TC001747.

Lavier, L.L. and Steckler, M.S. (1997) The Effect Of Sedimentary Cover On The Flexural Strength Of The Continental Lithosphere. Nature, v.389, pp. 476-489.

Lawver, L. A., Royer, J. Y., Sandwell, D. T. and Scotese, C. R. (1991). Crustal development : Gondwana break-up. In : Thomson, M. R. A., Crame, J. A., Thomson, J. W. (Eds), Geological Evolution of Antarctica, Cambridge Univ. Press, Cambridge, pp. 533-539.

Le Pichon, X., and J. C. Sibuet, (1981) . Passive margins: a model of formation. Journal of Geophysical Research, v. 86, pp. 3708-3720.

Lim, J.S. and Malik, N.A. (1981). A new algorithm for two dimensional maximum entropy power estimation. IEEE Trans. Acoust. Speech Signal Process, v. ASSP, v.30, pp. 788-797.

Lowry, A. R., and R. B. Smith .(1994). Flexural rigidity of the Basin and Range – Colorado Plateau –Rocky Mountain transition from coherence analysis of gravity and topography. J. Geophys. Res , v. 99, pp. 20123– 20140.

Malod, J. A., Droz, L., Mustafa Kemal, B., and Patriat, P. (1997), Early spreading and continent to oceanic basement transition beneath the Indus deep sea fan : northeastern Arabian Sea. Marine Geology, v. 141, pp. 221 – 235.

Mareschal, M., Vasseur, V.G., Srivastava, B.J. and Singh, R.N. (1987). Induction models of Southern India and effect of offshore Geology. Phys. Earth Planet Inter., v. 45, pp.137-148.

Masson, D. G. (1984), Evolution of the Mascarene basin, western Indian Ocean, and the significance of the Amirante arc. Mar. Geophys. Res. v. 6, pp. 365 – 382.

Mathur, R. B. and Nair, K. R., (1993). Exploration of Bombay offshore basin. In: Proc. second seminar on petroleum basins of India. KDMIPE and ONGC, Indian Petroluem Publishers, Dehra Dun, v.2, pp. 365-396.

Mauffret, A. and Montadert, L. (1987). Rift Tectonics on the passive continental margin off Galicia (Spain). Mar. Pet. Geol., v. 4, pp. 49-69.

McElhinney, M. W., Embleton, B. J., Daly, L. and Pozzi, J. P. (1976). Palaeomagnetic evidence for the location of Madagascar in Gondwana land. Geology, v. 4, pp. 455-457.

McKenzie, D. P. and Bickle, M.J.(1989). The volume and composition of melt generated by extension of the Lithosphere. Journal of Petrology, v.29, pp. 625–679.

McKenzie, D. P. and Sclater, J. G. (1971). The evolution of the Indian Ocean since the Late Cretaceous. Geophy. Jour. Roy. Astr. Soc. v. 25, pp. 437 – 528.

McKenzie, D. P., (1984). A possible mechanism for epeirogenic uplift. Nature, v. 307, pp. 616–618.

McKenzie, D. P., and Bowin, C. (1976).The relationship between bathymetry and gravity in the Atlantic Ocean. Jour. Geophys. Res., v. 81, pp. 1903–1915.

McKenzie, D. P., and Fairhead, J. D.(1997). Estimates of the effective elastic thickness of the continental lithosphere from Bouguer and free air gravity anomalies. J. Geophys. Res., v. 102, pp. 27,523– 27,552.

McKenzie, D.P., (1978). Some remarks on the development of sedimentary basins. Earth Planet. Sci. Lett. 40, pp. 25-32.

McWilliams, M.O., (1981). Palaeomagnatism and Precambrian tectonic evolution of Gondwana. In: Kröner, A. (Ed.), Precambrian Plate Tectonics. Amsterdam, Elsevier, pp. 649–687.

Miles, P. R., and Roest, W. R. (1993). Earliest sea floor spreading anomalies in the north Arabian Sea and the ocean-continent transition. Geophy. Jour. Int. v. 115, pp. 1025 – 1031.

Miles, P. R., Munschy, M. and Segoufin, J. (1998). Structure and early evolution of the Arabian Sea and East Somali basin. Geophys. Jour. Int. v. 134, pp. 876 – 888.

Mishra, D.C ; Laxman, G. and Arora, K., (2004) Large-wavelength gravity anomalies over the Indian continent: Indicators of lithospheric flexure and uplift and subsidence of Indian Peninsular Shield related to isostasy, Current Science, v. 86, No. 6, pp 861-867.

Molnar, P., Pardo – casaa, F. and Stock, J. (1988). The Cenozoic and late Cretaceous evolution of the Indian Ocean basin: Uncertainties in the reconstructed position of the Indian, African and Antarctic plates. Basin Res., v. 1, pp. 23-40.

Morgan, J.V., Barton, P.J. and White, R.S., (1989), The Hatton Bank continental margin - III. Structure from wide-angle OBS and multichannel seismic refraction profiles, Geophys. J. Int., 98, pp. 367-384.

Morgan, W. J. (1981). Hot spot tracks and the opening of the Atlantic and Indian Ocean. In : Emiliani, E.(Ed), The Sea, v. 7, pp. 443-475, Wiley Intersciences, New York.

Muller, R.D., Royer, J.Y. and Lawver, L.A. (1993), Revised plate motions relative to the hotspots from combined Atlantic and Indian Ocean hotspot tracks. Geology v. 21, pp. 275-278.

Mutter, J.C. (1993), Margins declassified. Nature, v. 364, pp. 393-394.

Mutter, J.C., Buck, W.R. and Zehnder, C.M. (1988). Convective partial melting I : A model for the development of thick igneous crust during the initiation of spreading. J. Geophys. Res., v. 93, pp. 1031-1048.

Naini, B. R. and Talwani, M. (1982). Structural framework and evolutionary history of the continental margin of western India, In : Studies in continental margin geology (Eds. J. S. Watkins and C. L. Drake) Am. Assoc. Pet. Geol. Mem., v. 34, pp. 167 – 191.

Naini. B. R. and Kolla, V. (1982). Acoustic character and thickness of sediments of the Indus fan and the continental margin of western India. Marine Geology, v. 47, pp. 181 – 195.

Nair, K.M., Singh, N.K. Ram, J.. Gavershetty, C.P and Muraleekrishnan, B. (1992). Stratigraphy and Sedimentation of Bombay offshore basin, India, Geological Society of India Bulletin, v. 40, p. 415-442.

Narain, H., Kaila, K. L. and Verma, R. K., (1968). Continental margins of India. Can.J.Earth Sci., v.5, pp.1051-1065.

Neprochnov, Y. P., (1961). Sediment thickness of the Arabian Sea-Basin. Dokl. Akad. Nauk. SSSR, v.139, pp. 177-179 (in Russian).

Norton, I. O. and Sclater, J. G., (1979). A model for the evolution of the Indian Ocean and the breakup of the Gondwnana Land. Jour. Geophys. Res., v.84, pp. 6803-6830.

Ollier C.D, Pain C.F., (1997). Equating the basal unconformity with the palaeoplain: a model for passive margins. Geomorphology, v 19, pp. 1–15.

Pande, K., Venkatesan, T.R., Goplan, K., Krishnamurthy, P., and MacDougall, J.D., (1988), 40Ar-39Ar ages of alkali basalts from Kutch, Deccan volcanic province, India, in Workshop on Deccan Flood Basalts, p. 145-150, Geological Society of India, Bangalore.

Pandey, O. P., Agrawal, P. K. and Negi, J. G. (1995). Lithosphere structure beneath Laxmi ridge and Late Cretaceous geodynamic events. Geo Marine Lett. v. 15, pp. 85 – 91.

Pandey, O. P., Agrawal, P. K. and Negi, J. G. (1996). Evidence of low-density sub crustal underplating beneath western continental margin of India and adjacent Arabian Sea : geodynamical considerations. J. Geodynamics v. 21, pp. 365 – 377.

Percival, D. B., and Walden, A. T. (1993). Spectral analysis for physical applications, Multitaper and conventional Univariate techniques. Cambridge Univ. Press, New York.

Powar, K. B. (1987). Evolution of the Deccan volcanic province. Presidential Address, Proc. Seventy – fourth Indian Sci. Congr., Bangalore. pp. 1-30.

Powell, C. McA., Roots, S. R. and Veevers, J. J. (1988). Pre – breakup continental extension in East Gondwanaland and the early opening of the eastern Indian ocean. Tectonophysics, v. 155, pp. 261-283.

Rabinowitz, P.D. and La Brecque, J.L. (1977), The isostatic gravity anomaly: Key to the evolution of the Ocean-Continent boundary at passive continental margins. Earth Planet. Sci. Lett., v. 35, pp. 145-150.

Radhakrishna, M., Verma, R.K. and Arts, K.P. (2002) Lithospheric structure below the eastern Arabian Sea and adjoining West Coast of India based on integrated analysis of gravity and seismic data. Mar. Geophys. Res., v. 23, pp. 25-42.

Radhakrishna, T., Dalimeyer, R.D. and Joseph, M. (1994), Paleomagnetism and 36Ar/40Ar Vs 39Ar/40Ar isotope correlation ages of dyke swarms in central Kerala, India: tectonic implications. Earth Planet. Sci. Lett. 21: 213-226.

Rai, D. and Ramaswamy, V. (2000) Basement configuration of western offshore, Konkan-Kerala basin. Journal of geophysics, v. 21, pp 85-90.

Ramana, M. V., Ramprasad, T., Desa, M., (2001). Seafloor spreading magnetic anomalies in the Enderby basin, East Antarctica, Earth Planet. Sci. Lett. v. 191, pp. 241-255.

Rao, P.R. and Srivastava, D.C. (1984). Regional Seismic facies analysis of western offshore India: Bulletin of ONGC, v.21, pp. 83-96.

Rao, R. P. and Talukdar, S. N. (1980). Petroleum geology of Bombay High field, India. In : Halbouty, M. T. (Ed.), Giant Oil and Gas Fields of the Decade 1968-1978. Am. Assoc. Pet. Geol. Mem., v. 30, pp. 487-506.

Rao, T. C. S., (1970). Seismic and magnetic surveys over the continental shelf off Konkan coast. Proc. 2nd Symposium on Upper Mantle Project, Hyderabad, India, pp.59-71.

Richards, M. A., Duncan, R. A. and Courtillot, V. E., (1989). Flood basalts and hot spot tracks : plume heads and tails. Science, v. 246, pp. 103-107.

Rowley, D.B., and D.L. Sahagian, (1986). Depth-dependent stretching: a different approach. Geology, v.14, pp. 32-35.

Royden, L., Keen, C.E., (1980). Rifting process and thermal evolution of the continental margin of eastern Canada determined from subsidence curves. Earth Planet. Sci. Lett. 51, 343-361.

Royer, J. Y., Sclater, J. G., and Sandwell, D. T. (1989). A preliminary tectonic fabric chart for the Indian Ocean, Proceedings of the Indian Academy of Sciences (EPS), v. 98, pp. 7-24.

Rust, R.J. and Summerfield, M.A. (1990). Isopach and borehole data as indicators of rifted margin evolution in southwestern Africa. Marine and Petroleum Geology, v.7, pp.277-287 .

Sandwell, D.T. And Smith, W.H.F. (1997) Marine Gravity anomaly from GEOSAT and ERS-1 Satellite Altimetry. Jour. Geophys. Res., v. 102, pp. 10039-10054.

Sastri, V. V., Sinha, R. N., Gurcharan Singh, and Murti, K.V.S., (1973). Stratigraphy and tectonics of sedimentary basins on east coast of Peninsular India. AAPG Bull., v. 57., pp. 655-678.

Sawyer, D.S. (1985). Total tectonic subsidence: A Parameter for distinguishing crust type at the U.S. Atlantic continental margin. Jour. Geophys. Res., v 90., pp 7751-7769.

Sawyer, D.S. Toksoz, M.N.. Sclater, J.G. Swift B.A. (1982). Thermal evolution of the Baltimore Canyon trough and Georges Bank Basin, in: J.S. Watkins, C.L. Drake, (Eds.), Studies in Continental Margin Geology. AAPG Mem. v. 34,pp. 167-191.

Schlich, R., (1982). The Indian Ocean: aseismic ridges, spreading centres and basins, in the Ocean Basins and Margins: The Indian Ocean, 6, edited by A.E.Naim, and F.G.Stehli, pp. 51-147, Plenum Press, New York.

Schuepbach, M.A. and Vail, P.R. (1980) Evolution of outer highs on divergent continental margins. In: Continental tectonics. National Acad. Sci., Washington, DC., pp. 50-61.

Scrutton, R.A. And Du Plessis, A. (1973) Possible marginal ridge south of South Africa. Nature, v. 242, pp. 180-182.

Simons, F.J., Zuber, M.T. And Korenaga, J. (2000). Isostatic response of the Australian lithosphere: Estimation of effective elastic thickness and anisotropy using multitaper spectral analysis. J. Geophys. Res. v. 105 (B8), pp. 19163– 19184.

Singh, A. P., (1999), The deep crustal accretion beneath the Laxmi ridge in the northeastern Arabian Sea : the plume model again, Jour. Geodynamics, v. 27, pp. 609 – 622.

Singh, N. K. and Lal, N. K., (1993). Geology and petroleum prospects of Konkan-Kerala Basin. In: Proc. 2nd Seminar on Petrluem Basins of India. KDMIPE and ONGC, India Petroluem Publishers, Dehra Dun, v.2, pp.461-469.

Sinha Roy S. (1982).Himalayan Main Central Thrust and its implication for Himalayan inverted metamorphism. Tectonophysics, v. 84, pp. 197-224.

Sleep N.H. (1971). Thermal effects of the formation of Atlantic continental margins by continental breakup. Geophysi. J.R.Astr. Soc., v. 24, pp 325-350.

Slepian, D. (1978). Prolate spheroidal wave functions, Fourier analysis and uncertainty, The discrete case.Bell Syst. Tech. J., v. 57, 1371– 1429, Spohn and Schubert, (1982). Modes of mantle convection and the Removal of heat from the Earth's interior, Jour. of Geophys. Res. v. 87 (Nb6)., pp. 4682-4696.

Stark, C.P., Stewart, J. And Ebinger, C.J. (2003). Wavelet transform mapping of effective elastic thickness and plate loading: Validation using synthetic data and application to the study of Southern African tectonics. J. Geophys. Res., v.108 (B12), doi :10.1029/2001JB000609.

Steckler, M.S. and Watts, A.B. (1978). Subsidence of the Atlantic-type continental margin of NewYork. Earth planet. Sci. Lett., v. 41, pp. 1-13.

Stephen, J., Singh, S.B. and Yedekar (2003) Elastic thickness and isostatic coherence anisotropy in the South Indian Peninsular Shield and its implications. Geophysical Res.Let., v. 30, doi : 10.1029/2003gl017686.

Stokes, W. L. (1965). Essentials of earth history : New Delhi. Prentice Hall of India (private) Ltd., pp. 502.

Storey, B.C. (1995). The role of mantle plumes in continental break up. Nature, v.37, pp. 301-308.

Storey, M., Mahoney, J. J., Saunders, A D., Duncan, R. A., Kelley, S P., Coffin, M F. (1995), Timing of hot spot related volcanism and the break up of Madagascar from India. Science, v. 267, pp. 852 – 855.

Storey, M., Mahoney, J.J. and Saunders, A.D. (1997), Cretaceous basalts in Madagascar and the transition between plume and continental lithosphere mantle sources. In: J.J.Mahoney, M.F.Coffin (Eds) Large Igneous Provinces- Continental, Oceanic and Planetary flood volcanism, AGU monograph, v.100, pp. 95-122.

Subba Raju, L. V., Kamesh Raju, K. A., Subrahmanyam, V., Gopala Rao, D. (1990). Regional gravity and magnetic studies over the continental margin of the central west coast of India. Geo Marine Letters., v.10, pp. 31 – 36.

Subba Rao, K. V. and Sukheswala, R. N. (1981). Deccan volcanism and related basalt provinces in other parts of the world. Geological Society of India, Memoir. v. 3, pp. 474.

Subrahmanya, K. R. (1998). Tectono-Magmatic evolution of the West Coast of India. Gond. Res., v. 1, Nos 3 / 4, pp. 319-327.

Subrahmanyam, C., Gireesh, R. and Gahalaut, V. (2005). Continental slope characteristics along the tsunami-affected areas of eastern offshore of India and Sri Lanka. J. Geol. Soc. India, v.65, pp. 778–780.

Subrahmanyam, V., Gopala Rao, D., Ramana, M.V., Krishna, K.S., Murthy, G.P.S. And Gangadhar Rao, M. (1995) Structure and tectonics of the Southwestern Continental Margin of India. Tectonophysics , v. 249, pp. 267-282.

Subrahmanyam, V., Krishna, K. S., Murthy, G. P. S. Gopala Rao, D., Ramana, M. V. and Gangadhara Rao, M. (1994). Structural interpretations of the Konkan basin, southwestern continental margin of India based on magnetic and bathymetric data. Geo Marine Lett., v. 14, pp. 10-18.

Subrahmanyam, V., Ramana, M. V. and Gopala Rao, D. (1993). Reactivation of Precambrian faults on the southwestern continental margin of India : evidence from gravity anomalies. Tectonophysics, v. 219, pp. 327 – 339.

Talwani, M. and Eldholm, O. (1973). Boundary between continental and oceanic crust at the margin of rifted continents. Nature, v. 241, pp. 325–330.

Talwani, M. and Eldholm, O. (1977), Evolution of the Norwegian-Greenland Sea. Geol. Soc.Am. Bull. v.88, pp 969-999.

Talwani, M. and Reif, C., (1998). Laxmi ridge – A continental sliver in the Arabian Sea, Mar. Geophys. Res., v. 20, pp. 259 – 271.

Tamsett, D. (1984). An application of the response function technique to profiles of bathymetry and gravity in the Gulf of Aden. Geophys. J.R.Astr. Soc. v.78, pp: 349-369.

Tapley B. and M.C. Kim (2001). Applications To Geodesy, In "Satellite Altimetry And Earth Sciences", L.L Fu and A. Cazenave (Eds), Academic Press.

Thakur, N.K., Mahashabde, M.V., Arora, B.R., Singh, B.P., Srivastava, B.J. and Prasad, S.N. (1986), Geomagnetic variation anomalies in Peninsular India. Geophys. J.R. Astr. Soc. v. 86: 839-854.

Thakur, S. S., Arasu, R. T., Subrahmanyam, V. S. R., Srivastava, A. K. and Murthy, A. V. S. (1999). Basin configuration in Konkan deep waters, Western Indian offshore. Jour. Geol. Soc. India, v.53, pp.79-88.

Thompson, T. L. (1976). Plate tectonics in oil and gas exploration of the continental margin. Am. Assoc. Pet. Geol. Bull., v. 60, pp. 1463-1501.

Thomson, D. J. (1982). Spectrum estimation and harmonic analysis. Proc. IEEE, v.70, pp. 1055–1096.

Todal, A. and Eldholm, O., (1998). Continental margin off western India and Deccan Large Igneous Province, Mar. Geophys. Res., v.20, pp. 273 – 291.

Touzi, R., A. Lopes, J. Bruniquel, and Vachon, P. (1999). Coherence estimation for SAR imagery. IEEE Trans. Geosci. Remote Sens., v. 37, pp. 135–149,

Touzi, R., Lopes, A. and Vachon, P. (1996). Estimation of the coherence function for interferometric SAR applications. paper presented at European Conference on Synthetic Aperture Radar 1996, EUSAR, Ko¨nigswinter, Germany,

Tukey, J. W. (1967). "An introduction to the calculations of numerical spectrum analysis," in Spectral Analysis of Time Series, B. Harris, editor, pp. 25-46, J.Wiley and Sons.

Unrug R., (1996). The assembly of Gondwanaland, Episodes, v. 19, pp. 11–20.

Valsangkar, A.B., Radhakrishnamurty, C., Subbarao, K.V., Beckinsale, R.D. (1981) Palaeomagnetism and potassium–argon age studies of acid igneous rocks from the St. Mary Islands. In: Subbarao, K.V., Sukheswala, R.N. (Eds.), Deccan Volcanism. Mem. Geol. Soc. Ind. v.3, pp. 265–276.

Vandamme, D. V., Courtillot, Besse, J. and Montigny, R. (1991). Palaeomagnetism and age determination of the Deccan traps (India) results of Nagpur – Bombay traverse and review of earlier work. Rev. Geophys., v. 29, pp. 259-290.

Veevers, J. J., Powell, C. M. A. and Johnson, B. D. (1980). Sea – floor constraints on the reconstruction of Gondwanaland. Earth and Planet. Sci. Lett., v. 51, pp. 435-444.

Venkatesan, T. R., Pande, K. and Gopalan, K. (1993). Did Deccan volcanism pre – date the Cretaceous transition. Earth. Planet. Sci. Lett., v. 119, pp. 181-190.

Verhoef, J. And Jackson, H.R. (1991) Admittance signatures of rifted and transform margins : examples from Eastern Canada. Geophys. J. Int. v. 105, pp. 229-239.

Walcott, R.I. (1972). Gravity, flexure and the growth of sedimentary basins at the continental edge. Geol. Soc. Am. Bull., v. 83, pp. 1845-1848.

Watts , A. B. (1978). An analysis of isostasy in the world's oceans, 1, Hawaiian-Emperor seamount chain. J. Geophys. Res., v.83, pp. 5989-6004.

Watts, A.B. (1988) Gravity anomalies, crustal structure and flexure of the lithosphere at the Baltimore Canyon Trough, Earth. Planet. Sci. Lett. v 89, pp. 221-238.

Watts A.B. (2001). Isostasy and flexure of the lithosphere, Cambridge University Press. pp 472.

Watts A. B and Fairhead,(1999), A process-oriented approach to modeling the gravity signature of continental margins, The Leading Edge February 1999, pp. 258-263.

Watts A.B. and Stewart J., (1998) Gravity anomalies and the segmentation of the continental margin offshore West Africa, Earth planet. Sci. Lett., v.156, pp. 239–252.

Watts, A.B. and Cox K.G. (1989). The Deccan Traps: An interpretation in terms of progressive lithospheric flexure in response to a migrating load, Earth and Planet Sci. Lettrs., v. 93, pp. 85-97.

Watts, A. B., and C. Marr. (1995). Gravity anomalies and the thermal and mechanical structure of rifted continental margins, in Rifted Ocean-ContinentBoundaries. ed: E. Banda, Kluwer Acad., Norwell,Mass., pp. 65– 94

Watts, A. B., and E. Burov (2003). Lithospheric strength and its relationship to the elastic and seismogenic layer thickness. Earth Planet. Sci. Lett., v.213, pp. 113 –131.

Watts, A.B and Ryan, W.B.F. (1976). Flexure of the lithosphere and continental margin basins. Tectonophysics., v.36., pp. 25–44.

Watts, A.B., G.D. Karner and M.S. Steckler. (1982). Lithospheric flexure and the evolution of sedimentary basins, in: The Evolution of Sedimentary Basins, (ed.) P. Kent, M.H.P. Bott, D.P. McKenzie and C.A. Williams, Phil. Trans, Roy. Soc. Lond., v. 305A, pp. 249-281,

Weissel, J.K., Karner, G.D. (1989). Flexural uplift of rift flanks due to mechanical unloading of the lithosphere during extension. J. Geophys. Res. v. 94, pp 13919-13950.

Welch, P. D. (1967). "The Use of the Fast Fourier Transform for the Estimation of Spectra" A Method Based on time averaging over short, modified Periodograms. IEEE Trans. Acoust. Electroacoustics v. AU - 15, v. 2, pp.70-73.

White R.S. and McKenzie D, (1995). Mantle plumes and flood basalts. Jour. of Geophys. Res , v. 100, pp. 17543-17585;

White, N., McKenzie D., (1988). Formation of the "steer's head" geometry of sedimentary basins by differential stretching of the crust and mantle. Geology v.16, pp. 250-253.

White, R. S., and McKenzie, D. P., (1989). Magmatism at rift zones : the generation of volcanic continental margins and flood basalts. J. Geophys.Res., v. 94, pp. 7685-7729.

White, R.S. (1992) Magmatism during and after continental break up. In : Storey, B.C., Alabaster, T. and Pankshurst, R.J. (Eds.) Magmatism and the causes of continental break up. Geol. Soc. Lond Spl. Pub. v.68, pp. 1-16.

Whiting, B.M., Karner, G.D. and Driscoll, N.W., (1994). Flexural and stratigraphic development of the west Indian continental margin. J. Geophys. Res., v.99, pp. 13791–13811.

Whitmarsh, R. B., (1974). Some aspects of plate tectonics in the Arabian Sea, Init. Rep. DSDP., v.23, pp. 527-535.

Widdowson, M and Cox, K.G. (1996). Uplift and Erosional history of the Deccan traps, India: Evidence from laterites and drainage patterns of the Western Ghats and Konkan Coast. Earth. Planet. Sci. Lett., v.137, pp. 57-69.

Widdowson, M. (1997). Tertiary paleosurfaces of the SW Deccan, Western India implications for passive margin uplift, in: M. Widdowson (Ed.), Paleosurfaces: Recognition, Reconstruction and Palaeoenviromental Interpretation, Geol. Soc. London Spec. Publ. v.120,pp. 221-248.

Windley, B.F., Razafiniparany, A., Razakamanana, T., Ackermand, D. (1994). Tectonic framework of the Precambrian of Madagascar and its Gondwana connections. Geologische Rundschau, v.83, pp. 642-659.

Worzel, J.L. (1968). Advances in marine geophysical research of continental margins. Canadian Journal of Earth Sciences, v 5., pp. 963–983.

Yatheesh, V., Bhattacharya, G.C. and Mahender, K. (2006). The terrace like feature in the mid-continental slope region off Trivandrum and a plausible model for India Madagascar juxtaposition in immediate pre-drift scenario. Gondwana research, v.10, pp. 179-185.

Yoshida, J., Nagashima, H., and Ma, Wen-Ju (1987). A double diffusive lock-exchangeflow with small density difference. Fluid Dynamics Research, v.2, pp. 205-215.

Yoshida, M., Rajesh, H.M., Santosh, M. (1999). Juxtaposition of India and Madagascar: a perspective. Gondwana Research, v.2, 449-462.

Zutshi, P.L., Jain M. M., Tarun S., Swathi M., (1995). Geology and Hydrocarbon resources of the Indian offshore region, Oil Asia, OCT-DEC, pp. 11-21.

****